Merrill, Christine Lee. Molecular mechanisms of etomoxir-induced toxicity. (Under the direction of Kevin T. Morgan and Talmage T. Brown).

Etomoxir (ET) is a member of a family of substituted 2-oxirane-carboxylic acids that inhibit mitochondrial long-chain fatty acid β-oxidation (FAO), ketogenesis and gluconeogenesis. Once converted to its CoA ester, ET irreversibly binds to the CPT-1 catalytic site and prevents long chain fatty acids from entering the mitochondrion. Along with this inhibition of FAO, ET causes a shift in energy substrate utilization from fatty acids to glucose, leading to systemic hypoglycemia, hypoketonemia, and hypotriglyceridemia (Wolf, 1992). These effects make ET potentially useful in the treatment of non-insulin-dependent diabetes mellitus (NIDDM). The compound has been shown to induce cardiac and hepatic hypertrophy in animals and, therefore, has not been fully developed as an antidiabetic agent to date. It is well established that ET activates the peroxisome proliferator activated receptor-alpha (PPARα) which can cause both oxidative stress and dysregulation of the cell cycle control gene program. The goal of this research was to evaluate the ET-induced alterations in gene expression profiles in hepatocytes to elucidate the possible role of cell growth dysregulation and/or oxidative stress in ET-induced hepatic toxicity. In HepG2 cells treated with a high dose of ET, gene expression strongly suggestive of oxidative stress was observed and this was supported by decreased levels of reduced glutathione, reduced/oxidized glutathione ratio (GSH/GSSG), concurrent increase in oxidized glutathione (GSSG) and superoxide generation. A significant

decrease in mitochondrial membrane potential and ATP levels implicated impairment of mitochondrial energy metabolism. Other gene expression findings suggested activation of p53, DNA repair and cell cycle arrest. In rats, ET induced a strong mitogenic response in the livers of rats 24 h after administration of one 25 mg/kg dose, that was consistent with the cell proliferation caused by peroxisome proliferators. This finding was coincident with a predominance of cell proliferation/growth-related gene expression alterations. Oxidative stress genes were down regulated; suggesting that this is not a viable etiologic mechanism for induction of ET-induced hepatic hypertrophy. PPARα appears to play a role in ET-induced hepatic hypertrophy, as shown by the early cell proliferation followed by increased level of PPARA mRNA, peroxisome proliferation and increase of PPARα-related genes.

Molecular mechanisms of etomoxir-induced toxicity

By

Christine Lee Merrill

A dissertation submitted to the Graduate Faculty of

North Carolina State University

In partial fulfillment of the Degree of

Doctor of Philosophy

COMPARATIVE BIOMEDICAL SCIENCES

Raleigh

2002

APPROVED BY:

Talmage T. Brown Co-chair of Advisory Committee	**Kevin T. Morgan** Co-chair of Advisory Committee
Richard T. Miller	Philip L. Sannes
Tony R. Fox	

BIOGRAPHY

Christine (Chris) Lee Merrill was born August 23, 1956 in Mount Clemens, Michigan to Carol and Fred Merrill. She graduated from Murphy High School, Mobile, Alabama in 1974. In 1978, Chris graduated from Auburn University with a Bachelor of Science degree in Secondary Science Education and a minor in German Language. She taught 7th grade biology for two years in Smyrna, Georgia. After two years of the hardest work in her life, Chris left teaching and returned to school to complete pre-requisite courses needed to apply to veterinary school. In 1988, she graduated from the College of Veterinary Medicine at North Carolina State University with a Doctor of Veterinary Medicine degree. Chris worked 7 years in toxicology at Becton Dickinson and Company, Research Triangle Park, NC, managing an experimental studies group which evaluated prototype medical devices for safety and efficacy. An opportunity to expand her education and realm of experience presented itself in 1995 and Chris rejoined North Carolina State University-College of Veterinary Medicine for 2 years more as a resident in anatomic pathology. After completion of the residency, she entered a Ph.D. program at NCSU in pathology during which time she successfully completed her boards in Veterinary Anatomic Pathology and became a member of the American College of Veterinary pathologists. She joined GlaxoSmithKline pharmaceutical company as a Director of Regulatory and Discovery Pathology in February of 2002.

ACKNOWLEDGEMENTS

I would like to thank Drs. Ron Tyler, Ruth Lightfoot and Henry Wall and GlaxoSmithKline for tremendous support that I received during my Ph.D. program. I could not have done it without them and I do intend to pay it forward. My thanks also go out to Dr. Kevin Morgan for his brilliant mind, original view of the world and persistent reminders to “get it done”. I appreciate the strong background in pathology that I received under the tutelage of Drs. Talmage Brown, John Cullen, Rich Miller, Don Meuten, and John Barnes at NCSU. A big thank you goes to the members of my Ph.D. committee who are not already thanked above, Drs. Tony Fox and Phil Sannes.

On a personal note, I would like to thank my parents, Fred and Carol Merrill, who always stressed the importance of education and who helped support me, financially and otherwise, throughout the many years that I have been in school. I very much want to thank Gail Hafley, from the bottom of my heart, for the tremendous support and compassion that she has afforded me during this long journey – I really couldn’t have done it without her.

TABLE OF CONTENTS

LIST OF TABLES vi

LIST OF FIGURES vii

LIST OF ABBREVIATIONS ix

GENERAL INTRODUCTION

Body 1

References 21

MANUSCRIPT I 31

Abstract 32

Introduction 33

Materials and Methods 35

Results 42

Discussion 46

References 53

Tables and Figures 59

MANUSCRIPT II 70

Abstract 71

Introduction 72

Materials and Methods 75

Results 81

Discussion 91

References 98

Tables and Figures 104

GENERAL SUMMARY AND CONCLUSIONS..... 116

LIST OF TABLES

MANUSCRIPT I

Table 1.1: Cell Counts, Mitotic Index, Apoptotic/Necrotic Index 59

Table 1.2: ET-induced mRNA expression changes 60

MANUSCRIPT II

Table 2.1: Day 2 Cell Proliferation Gene Changes 104

Table 2.2: Energy Metabolism Gene Expression 105

LIST OF FIGURES

GENERAL INTRODUCTION

Figure 0.1: The structural formula of etomoxir 2

MANUSCRIPT I

Captions for Manuscript I Figures 61

Figure 1.1: Morphologic changes in control vs. 1 mM ET-treated HepG2 cells 63

Figure 1.2: Microarray platform gene expression changes confirmed by RT-PCR 64

Figure 1.3: RT-PCR analysis of 7 stress genes in timecourse study 65

Figure 1.4: Depletion of GSH, decrease in GSH:GSSG ratio, increase in GSSG 66

Figure 1.5: Superoxide radical generation 67

Figure 1.6: ATP assay 68

Figure 1.7: Dose-dependent reduction in mitochondrial membrane potential 69

MANUSCRIPT II

Figure 2.1: Serum triglyceride changes 106

Figure 2.2: Increase in mitotic figures (photomicrograph) 107

Figure 2.3: Increase in mitotic figures (bar chart) 108

Figure 2.4: Day 2 Growth-related gene expression changes 109

Figure 2.5: Platform comparison: cell proliferation gene expression changes 110

Figure 2.6: Day 11 Growth-related gene expression changes 111

Figure 2.7: Day 43 Growth-related gene expression changes 112

Figure 2.8: Day 85 Growth-related gene expression changes 113

Figure 2.9: Platform comparison of oxidative stress genes 114

Figure 2.10: PPARα-target gene expression changes 115

List of Abbreviations

ACC, acetyl-CoA carboxylase

ACLY, ATP citrate-lyase

ADP, adenosine diphosphate

ADCY, adenylyl cyclase

cAMP, cyclic adenosine monophosphate

AMP, adenosine monophosphate

ANOVA, analysis of variance

ANT, adenine nucleotide translocase

AOX, acyl-CoA oxidase

APC, adenomatous polyposis coli

ATP, adenosine triphosphate

CACT, carnitine-acylcarnitine translocase CCNC, cyclin C

CCND3, cyclin D3

CCNE, cyclin E

CDC20, cell division cycle 20 homolog – aka p55cdc

CDC25B, cell division cycle 25B

CDK1, cyclin dependent kinase 1

CDK2B, cyclin dependent kinase –2 beta

CDK5, cyclin dependent kinase 5 – aka cdc2-related protein kinase

CDKN1A, cyclin-dependent kinase inhibitor 1A

CDKN1B, cyclin-dependent kinase inhibitor 1B - aka p27

CL-6, delayed-early insulin-induced gene CL-6

COT, carnitine octanoyl transferase

CPT1A, carnitine palmitoyltransferase 1-A (liver isoform)

CPT1B, carnitine palmitoyltransferase 1-B (muscle isoform)

CPT-2, carnitine palmitoyltransferase-2

CYP1A1, cytochrome P450 1A1

CYP4A, cytochrome P450 4A family

EB, ethidium bromide

ECI, δ3, δ2-enoyl-CoA isomerase

EDN1, endothelin-1

EGR1, early growth response 1

ERK1, extracellular signal-regulated kinase 1

ET, etomoxir

FAO, fatty acid oxidation

FAS, fatty acid synthase

FAT, fatty acid translocase – aka CD36

FATP, fatty acid transport protein

FOS, c-fos mRNA

G-6-P, glucose-6-phosphate

GADD153, DNA damage-inducible gene 153

GADD45, DNA damage-inducible gene 45

GAP, GTPase activating protein

GCLM, γ-glutamate-cysteine ligase modifier subunit

GHRH, growth hormone releasing hormone

GHRHR, growth hormone releasing hormone receptor

GIP, glucose-dependent insulinotropic peptide

GLUT, glucose transporter

GMFB, glia maturation factor beta

GRP78, glucose-regulated protein 78-kD

GPAM, glycerol-3-phosphate acyltransferase

GPD2, glycerol-3-phosphate dehydrogenase

GSH, reduced glutathione

GSH/GSSG, reduced/oxidized glutathione ratio

GSR, glutathione reductase

GSSG, oxidized glutathione

HE, hydroethidine

H&E, hematoxylin and eosin

HKII, hexokinase II

HMGCR, 3-hydroxy-3-methylglutaryl coenzyme A reductase

HMGCS, 3-hydroxy-3-methylglutaryl coenzyme A synthase

HO1, heme oxygenase 1

HSPA1A, heat shock 70kD protein 1

HSP40, heat shock protein 40 homolog

IGF1R, insulin-like growth factor 1 receptor

IGFBP1, insulin-like growth factor binding protein 1

IMM, inner mitochondrial membrane

JUN, c-jun

3KACT, peroxisomal 3-ketoacyl-CoA thiolase

LCAD, long-chain acyl-CoA dehydrogenase

LDH, lactate dehydrogenase

LEP, leptin

LEPR, leptin receptor

LCFA-CoA, long-chain fatty acyl-Coenzyme A

LCFA-CoA/LCFA-carn, long-chain fatty acyl-CoA/long-chain acylcarnitine ratio

LIF, leukemia inhibitory factor

LIPE, hormone sensitive lipase

MAPK14, mitogen-activated protein kinase 14 – aka MAP kinase p38

MDM2, mouse double minute 2 homolog

ME1, malic enzyme 1

MMP, mitochondrial membrane potential

mRNA, messenger ribonucleic acid

MYC, c-myc

NADH, nicotinamide adenine dinucleotide

NEFA, non-esterified fatty acids

NF2, neurofibromatosis 2

NIDDM, non-insulin-dependent diabetes mellitus

NR1D1, nuclear receptor subfamily 1, group D, member 1 – aka Rev-ERBA-alpha and thyroid hormone receptor

OGG1, 8-oxoguanine DNA glycosylase 1

OMM, outer mitochondrial membrane

OSC, oxidosqualene lanosterol-cyclase

PAI2A, plasminogen activator inhibitor 2 type A

PBS, phosphate buffered saline

PCNA, proliferating cell nuclear antigen

PDE, cAMP phosphodiesterase

PDK, pyruvate dehydrogenase kinase

PDH, pyruvate dehydrogenase

PEPCK, phosphoenolpyruvate carboxykinase

PDP, pyruvate dehydrogenase phosphatase

PFK-1, phosphofructokinase-1

PFKFB1, 6-phosphofructo-2-kinase/fructose-2, 6-bisphosphatase

POCA, clomoxir

PPARα, peroxisome proliferator activated receptor-alpha

PPRE, peroxisome proliferator response element

PRPS2, phosphoribosylpyrophosphate synthetase subunit 2

RBC, red blood cell

RAD23A, UV excision repair protein

ROS, reactive oxygen species

RT-PCR, real time-polymerase chain reaction

SCD2, stearoyl-CoA desaturase

SOD2, Mn+ superoxide dismutase

SPAT, serine pyruvate aminotransferase

SQLE, squalene epoxidase

TCA, tricarboxylic acid cycle

TDGA, tetradecylglycidic acid

TG, triglycerides

TGFBR1, transforming growth factor-beta 1 receptor

TGFBR2, transforming growth factor-beta 2 receptor

TNFA, tumor necrosis factor alpha

TOP2A, topoisomerase Iiα

TP53, tumor protein p53

TXNRD1, thioredoxin reductase

VEGFD, vascular endothelial growth factor D

VLCAD, very long chain acyl-CoA dehydrogenase

VLDL, very low density lipid cholesterol

WBC, white blood cell.

General Introduction

Etomoxir (ET) is a member of a family of substituted 2-oxirane-carboxylic acids that inhibits mitochondrial long-chain fatty acid β-oxidation (FAO) by irreversibly binding to the catalytic site of carnitine palmitoyltransferase-1 (CPT-1). CPT-1 is considered the rate-limiting step in the transportation of long-chain fatty acids from the cytosol into the mitochondrial matrix. Secondary to inhibition of FAO, ET causes a shift in energy substrate utilization from fatty acids to glucose, leading to systemic hypoglycemia, hypoketonemia, and hypotriglyceridemia (Wolf 1992). These effects make ET potentially useful in the treatment of non-insulin-dependent diabetes mellitus (NIDDM). However, the compound has been shown to induce both cardiac and hepatic hypertrophy in animals and, therefore, has not been fully developed as an antidiabetic agent to date (Rupp and Jacob 1992; Vetter *et al.* 1995; Yotsumoto *et al.* 2000). The mechanism(s) of the respective hypertrophies have not yet been worked out, but are shown to be different from those involved in hyperthyroidism and hypertension (Rupp and Jacob 1992; Vetter *et al.* 1995). ET activates PPARα, and PPARα-agonists have been shown to cause hepatic hypertrophy in rodents, but it has not been demonstrated that ET causes hepatic hypertrophy via activation of PPARα. There are numerous reports in the literature linking the switch of energy substrate from fatty acids to glucose with cardiac hypertrophy, but the effects on liver weight are unclear. It is not yet known whether ET exerts the hypertrophic effects on the liver by activation of PPARα, energy substrate conversion or by some, as yet, unknown pathogenic mechanism.

Figure 0.1: The structural formula of etomoxir

Etomoxir (ethyl-2-[6-(4-chlorphenoxy)hexyl]oxirane-2-carboxylate) is arguably the best known and most published member of the oxirane-carboxylate family; other members include tetradecylglycidic acid (TDGA or palmoxirate) and clomoxir (POCA) (sodium-2-[5-(4-chlorophenyl)-pentyl]-oxirane-2-carboxylate). All of these compounds are characterized by their ability to specifically inhibit CPT-1 (EC2.3.1.21). This specificity is attributable to the fact that the inhibitors are not the compounds themselves, but are the corresponding coenzyme A esters of the (R)-(+)-isomers which are formed in the cell by the action of acyl-CoA synthetase (Anderson 1998; Eistetter and Wolf 1986; Schudt and Simon 1984; Wolf 1990). The inhibition of CPT-1 by ET is irreversible due to the covalent binding of the epoxide moiety (Fig. 1) to the substrate binding site of CPT-1 (Declercq *et al.* 1987; Murthy and Pande 1990; Wolf 1990).

Esters of oxirane-carboxylates are colorless, water-insoluble, oily liquids or low melting point solids that are stable for at least 5 years at room temperature. The sodium salts are crystals with melting points >90º C, water-soluble and stable in the solid form for at least 2 years. In aqueous solutions at a pH between 3.7 and 7, these compounds slowly decompose as the oxirane ring opens. At pH > 8 and due to the action of esterases, the ester linkage is hydrolyzed forming the free acids or the corresponding salts. When in the blood, these substances in this

biochemical form mimic fatty acids and are subject to the same transport and transformation reactions, e.g. albumin and fatty acid binding protein binding and intracellular esterification with coenzyme A (Wolf 1990).

CPT-1 is the gatekeeper controlling the entry of long-chain fatty acids into the mitochondrial matrix, thereby controlling rates of mitochondrial FAO. Long-chain fatty acids cannot cross the inner mitochondrial membrane into the matrix without the participation of CPT-1. This enzyme, situated on the inner face of the outer mitochondrial membrane, binds activated fatty acids (fatty acyl-CoA esters) and catalyzes their conversion to acyl-carnitines, releasing coenzyme A to the cytosol in the process. CPT-1 exists as two isoforms encoded by separate genes. Liver-type CPT-1 (L-CPT-1 or CPT-1A) is expressed primarily in liver but is also expressed at a lower level in all other tissues examined to date. Muscle-type CPT-1 (M-CPT-1 or CPT-1B) is expressed abundantly in the heart, skeletal muscle and brown adipose tissue (Brandt *et al.* 1998). Another enzyme, the carnitine:acyl carnitine translocase (CACT) positioned within the inner mitochondrial membrane (IMM), shuttles acyl carnitine through the IMM in exchange for carnitine. Then a second CPT (CPT-2), located on the inner face of the IMM, catalyzes the reverse reaction of CPT-1 forming acyl-CoA in the matrix and releasing carnitine to be shuttled out of the mitochondrion by CACT (Anderson 1998; Brandt *et al.* 1998; Kashfi and Cook 1999). Once inside the mitochondrial matrix, the long-chain acyl CoA is available for FAO.

When a choice is available, most tissues will use fatty acids as fuels before ketone bodies, and both before glucose (Moran and Scrimgeour 1994). The glucose-fatty acid cycle (Randall Cycle) describes how the preference for a particular energy substrate is determined by metabolic conditions. When blood glucose is low, the production of both glucagon and epinephrine is high which stimulates adenylyl cyclase (converts ATP to cyclic adenosine monophosphate, a.k.a. cAMP) increasing the levels of cAMP. High levels of cAMP trigger activation of protein kinase A which, in turn, triggers activation of hormone-sensitive lipase in the adipocyte causing release of non-esterified fatty acids (NEFA). NEFA are taken up by tissues and metabolized by beta oxidation and the citric acid cycle to yield reducing power that can generate ATP via electron transport chain and oxidative phosphorylation. Beta oxidation produces increased levels of citrate, acetyl CoA and NADH which then inhibit glucose oxidation: citrate inhibits phosphofructokinase-1 (PFK-1) and acetyl CoA and NADH inhibit pyruvate dehydrogenase complex by stimulating pyruvate dehydrogenase kinase (PDK). Therefore, the products of beta-oxidation not only provide a readily available source of reducing equivalents to the cell, but also inhibit glucose utilization.

The catabolic state is reversed by ingestion of food leading to high blood glucose levels and subsequent increase in insulin concentration. Insulin causes inhibition of adenylyl cyclase and stimulation of cAMP phosphodiesterase, both of which decrease levels of cAMP. Insulin also stimulates lipase phosphatase, which

dephosphorylates hormone-sensitive lipase to the inactive form. The net effect of insulin in this scenario is to inhibit release of NEFA (Moran and Scrimgeour 1994; Murray *et al.* 2000). Insulin is pivotal in controlling energy metabolism by stimulating glucose uptake, glycogen synthesis, glycolysis, fatty acid synthesis and esterification and protein synthesis. Inhibitory effects of insulin are associated with glycogenolysis, fatty acid oxidation, ketogenesis, gluconeogenesis and proteolysis.

In the fed state, when glucose is abundant and insulin is present, the preferred energy substrate (fatty acid) is prevented from leaving its storage site, forcing the tissues to utilize glucose. The body stores the energy in this excess glucose for later use via formation of glycogen and fatty acids/triglycerides. During fatty acid synthesis, futile cycling (concurrent FAO) is prevented through inhibition of CPT-1 by malonyl-CoA. In rat liver mitochondria, the IC_{50} (concentration causing 50% inhibition) of ET for CPT-1 is several hundred times less than that of malonyl-CoA, most likely due the reversibility of the inhibition by malonyl-CoA (Wolf 1990). Another possible explanation for the large difference in IC_{50} between ET and malonyl-CoA may be due to the separate binding sites for the two CPT-1 inhibitors (Kashfi and Cook 1999). However, this “separate binding site” theory has been disputed using competitive binding studies with rat liver mitochondria (Morillas *et al.* 2000).

Inhibition of CPT-1 causes a shift away from FAO and toward glycolysis, with insulin and glucagon playing major roles in flipping this metabolic switch. A study by Park et al. (1995) showed that the V_{max} for CPT-1 in the outer mitochondrial membrane from the livers of both starved and diabetic rats increased 2- and 3-fold respectively over fed control values with no change in Km values for substrates. Regulation of malonyl-CoA sensitivity of CPT-1 in isolated mitochondrial outer membranes was indicated by an 8-fold increase in Ki during starvation and by a 50-fold increase in Ki in the diabetic state. CPT-1 mRNA was 7.5 fold greater in livers of 48-h-starved rats and 14.6 times greater in livers of insulin-dependent diabetic rats compared with livers of fed rats. In rat H4IIE cells, insulin increased CPT-1 sensitivity to inhibition by malonyl-CoA in 4 h, and sensitivity continued to increase up to 24 h after insulin addition. CPT-1 mRNA levels in H4IIE cells were decreased by insulin after 4 h and continued to decrease so that at 24 h there was a 10-fold difference. These results suggest that the presence of insulin, directly or indirectly, inhibits transcription of the CPT-1 gene (Park *et al.* 1995).

In order to understand how the inhibition of FAO could increase the level of glycolysis, we must first review the relevant aspects of intermediary metabolism to better understand effects of ET on the cell and the body as a whole. After a meal, the presence of food in the intestinal lumen causes the secretion of gastrointestinal hormones, such as gastric inhibitory polypeptide and cholecystokinin, which trigger insulin release from the beta cells of the pancreas.

The increase in blood glucose concentration following absorption of dietary glucose causes the beta cells to release even more insulin (Moran and Scrimgeour 1994). In mammals, sugars are taken into cells by glucose transporters (GLUT), that vary by tissue type and insulin responsiveness. Although genes for 11 GLUT isoforms have been identified in the human genome, only GLUTs 1-5, 8, and 9 have been shown to transport sugars. GLUT1 is highly expressed in endothelial cells lining the blood vessels of the brain, although it is expressed to some degree in most tissues. GLUT3 is expressed primarily in neurons and together, GLUT1 and GLUT3 allow glucose to cross the blood-brain barrier and enter neurons. GLUT2 is a low affinity (high K_m) glucose transporter present in liver, intestine, kidney and pancreatic beta cells, which mediates bi-directional transport of glucose in the hepatocyte. This transporter functions as part of the glucose sensor system in beta cells and in the absorption of glucose by intestinal epithelial cells. GLUT4 is expressed primarily in muscle and adipose tissue and is the major insulin-responsive glucose transporter isoform. GLUT5 is a fructose transporter highly expressed in the intestine, and the recently identified GLUTs 8 and 9 appear to function in blastocyst development (GLUT8) or in the brain and leukocytes (GLUT9). Since GLUT4 is the insulin-responsive isoform, it has drawn most of the attention of workers in the field of diabetes research (Watson and Pessin 2001).

Once inside the cell, glucose is phosphorylated to glucose-6-phosphate (G-6-P) by hexokinase, the first of 3 regulated reactions in glycolysis. In most tissues,

high levels of G-6-P allosterically inhibit hexokinase, thus controlling rate of entry of glucose into the glycolytic pathway. However, hexokinase isoenzyme IV (glucokinase) which predominates in the liver and pancreas is free of the G-6-P allosteric control. The free-flow of glucose into the liver via GLUT2 and the rapid conversion to G-6-P enables the liver to store excess glucose in the form of glycogen in times of “feast”. In times of “famine”, GLUT2 is a bi-directional glucose transporter capable of exporting glucose generated via glycogenolysis and gluconeogenesis to the systemic circulation.

The next regulated enzymatic reaction of glycolysis is catalyzed by phosphofrucokinase-1 (PFK-1) which converts fructose-6-phosphate to fructose 1, 6-bisphosphate. The regulation of PFK-1 is more complex than that of hexokinase, with several different entities serving as inhibitors or activators. ATP wears 2 hats, acting as both a substrate of PFK-1 and as an allosteric inhibitor. This nucleotide decreases the affinity of PFK-1 for its glycolytic substrate fructose-6-phosphate. AMP is an allosteric activator of PFK-1 that acts by relieving the inhibition caused by ATP. ATP concentrations are greater than ADP or AMP concentrations, and relatively minor changes in ATP concentration may cause large changes in its hydrolysis products. Therefore, [AMP] tends to have a greater effect on the regulation of PFK-1 than does [ATP]. As the concentration of citrate, an intermediate of the glycolytic pathway, increases it inhibits the activity of PFK-1 which then reduces the flow of substrate entering the pathway. Fructose 2,6-bisphosphate is a strong activator of PFK-1. When glucose levels

are high, the enzyme phosphofructokinase-2 (PFK-2) actively converts fructose-6-phosphate to fructose 2,6-bisphosphate, which then stimulates the activity of PFK-1. However, when glucose is low, glucagon activates adenylate cyclase in hepatocytes, forming cAMP which then activates protein kinase A. The active protein kinase A phosphorylates a serine residue in PFK-2 which inhibits the kinase site and activates the separate phosphorylase site of the same (bifunctional) enzyme. The phosphorylase removes one of the phosphate groups from fructose 2,6-bisphosphate, converting it to fructose-6-phosphate and, thus, removing the stimulus for PFK-1 activation. High levels of citrate also inhibit PFK-2 (Moran and Scrimgeour 1994; Murray *et al.* 2000).

The third enzyme involved in the regulation of glycolysis is pyruvate kinase, which converts phosphoenolpyruvate to pyruvate. This enzyme is stimulated by fructose 1,6-bisphosphate in a “feed- forward” form of activation and is inhibited by glucagon-activated protein kinase A. When ATP is needed (i.e. during exercise), AMP levels are high, which removes the inhibition of PFK-1 by ATP. The associated increase in inorganic phosphate within the cell stimulates PFK-2 which increases fructose 2,6-bisphosphate, also removing the inhibition of PFK-1 by ATP. More fructose 1,6-bisphosphate is produced which then increases the activity of pyruvate kinase. Once the ATP supply has been adequately replenished, an accumulation of glycolytic and TCA intermediates such as G-6-P and citrate, respectively, will provide negative feedback. In other words, the presence of substrate and the need for ATP production will lead to increased

glycolysis, while the over-abundance of glycolytic intermediates, the presence of ATP, and/or the influence of glucagon (in hepatocytes) will dampen glycolytic activity.

Poised at the interface between the glycolytic pathway and the TCA cycle, pyruvate is a versatile intermediate. The metabolic and oxidative condition of the cell will determine the fate of pyruvate. For example, if the cell is in oxygen deficit (as in muscle during prolonged contraction), then pyruvate can be converted to lactate by lactate dehydrogenase. This reaction also helps to allow continuance of oxygen-independent glycolysis by providing the oxidized NAD^+ required to convert glyceraldehyde-3-phosphate to 1,3 bisphosphoglycerate in the presence of glyceraldehyde-3-phosphate dehydrogenase (GPD2). If the cell is in a state of anabolism, and citrate is being shuttled to the cytosol to synthesize fatty acids, then pyruvate can be carboxylated to form oxaloacetate (anaplerosis), replenishing TCA intermediates. Also, when acetyl-CoA accumulates due to a shortage of TCA intermediates, acetyl-CoA directly stimulates the activity of pyruvate carboxylase resulting in increased formation of oxaloacetate. The most common fate of pyruvate is to be decarboxylated to acetyl-CoA which may then undergo complete oxidation to provide ATP, or which may be used to form fatty acids, cholesterol, and ketones. The conversion of pyruvate to acetyl-CoA is driven by the phosphorylation state of pyruvate dehydrogenase (PDH), which is controlled by two enzymes, PDK and pyruvate dehydrogenase phosphatase (PDP). Phosphorylated PDH is the less active form of the enzyme. PDK activity

is stimulated by NADH, acetyl-CoA, and ATP, and is inhibited by high levels of pyruvate, ADP and Ca^{2+}. PDP is stimulated by Ca^{2+} and, in adipose tissue, by insulin.

Three non-equilibrium enzymatic reactions within the TCA cycle are considered to be points of regulation: citrate synthase, isocitrate dehydrogenase, and α-ketoglutarate dehydrogenase. All three of these reactions are stimulated by Ca^{2+}, which is high in muscle during contraction. ATP and long chain fatty acyl-CoA inhibit citrate synthase. The presence of oxidized dehydrogenase cofactors (e.g. NAD^{+}) is required for the isocitrate dehydrogenase and α-ketoglutarate dehydrogenase steps. In general, the TCA cycle is enhanced by low ATP/ADP and NADH/NAD ratios and stimulated by the inverse ratios.

Electron transport and oxidative phosphorylation are the final steps down the pathway to generate ATP from energy substrate. Because neither oxidized nor reduced NAD(H) can diffuse through the inner mitochondrial membrane, shuttle systems are in place to transfer reducing power from the cytosol to the mitochondrial matrix. There are 2 shuttle systems involved in this energy transfer: the malate-aspartate shuttle (more active in the liver) and the glycerol-phosphate shuttle. In both shuttles, NADH, the reduced co-enzyme generated during glycolysis, must pass its reducing power to a metabolite that is transported into the mitochondrion. The reducing power is passed back to another NAD^{+} in the matrix and the metabolite is then transported back to the cytosol. Once inside the

mitochondrial matrix, the NADH is then oxidized by Complex I of the electron transport chain, which then passes the electrons to Q to form QH_2. As part of the TCA cycle, succinate is oxidized to fumarate by Complex II (succinate dehydrogenase complex) which then donates 2 electrons to Q. The electrons are transferred from QH_2 to Complex III, to cytochrome c to Complex IV and then to the final electron acceptor, oxygen. This overall transfer of electrons is down an energetically favorable gradient, which provides the needed impetus to move protons from the matrix to the intermembrane space, creating the chemical and electrical energy gradient that drives the formation of ATP. Complex V uses the influx of protons (proton-motive force) through its channel to drive the conversion of ADP to ATP. The concept of a proton-motive force driving the formation of ATP, was formulated by Peter Mitchell in the early 1960's and is referred to as the chemiosmotic theory. In order to provide the substrate needed for this reaction, both ADP and inorganic phosphate (P_i) must be transported into the matrix. The adenine nucleotide translocase (ANT) exchanges ATP from the matrix for cytosolic ADP and the hydrogen-phosphate symporter transports both hydrogen ions (H^+) and P_i into the matrix. Control of oxidative phosphorylation is based on substrate availability (NADH, O_2, and P_i) and need for ATP.

Now that we have reviewed the relevant aspects of intermediary metabolism, the effects of ET on the cell and the body as a whole can be examined more thoroughly. Clinico-pathological changes associated with dosing of ET vary depending on the dose, duration and metabolic state of the patient. For example,

in diabetic and fasted animals and humans, ET is associated with a decrease in serum glucose, triglycerides, NEFA, cholesterol, and ketones (Anderson 1998; Eistetter and Wolf 1986; Spurway *et al.* 1997; Wolf 1990, 1992). Researchers disagree whether or not blood glucose decreases in ET-dosed, healthy, fed subjects. In one 8 day study of healthy, fed rats dosed with 18 mg/kg/day ET, serum glucose dropped 27% (Schmitz *et al.* 1995). This contrasts with another study in which healthy, fed rats were dosed with 8 mg/kg/day ET for 4 weeks with no significant change in serum glucose (Rupp and Jacob 1992). Here the difference may be attributable to the dose (the lower dose showing no change in glucose) or to the duration of dosing (the longer duration providing more time for the body to become tolerant to the drug). The effects of ET on lipid metabolism vary depending on the duration of dosing. The acute effect consists of a time and dose-dependent increase in NEFA, which is inversely correlated with the decrease in glucose. This effect occurs only in fasted subjects and is presumed to be due to the epinephrine-induced hormone-sensitive lipase. Because NEFA cannot be oxidized while cells are under the influence of ET, they are re-esterified in the liver and released into the blood packaged as very low density lipid cholesterol (VLDL). When nicotinic acid, an inhibitor of lipolysis, is administered with ET, both NEFA and triglycerides (TG) are significantly decreased (Reaven *et al.* 1988). In contrast to the acute effects of ET on lipid metabolism, the chronic studies with repeat dosing schedules cause decreases in cholesterol and TG levels while NEFA remain unchanged. The cause of this hypolipidemic effect is partly due to an increase in lipoprotein lipase activity in the

heart and liver, which causes an increase in clearance of triglycerides from plasma (Agius and Alberti 1985; Rogers 1987). ET also causes an increase in intracellular hepatic and cardiac triglyceride content (Abdel-aleem and el-Merzabani 1997; Koundakjian *et al.* 1984; Schmitz *et al.* 1995; Spurway *et al.* 1997; Yotsumoto *et al.* 2000).

The biochemical effects associated with ET are directly associated with the inhibition of FAO. Blockage of CPT-1 leads to the following intracellular biochemical alterations: decrease in acetyl-CoA and NADH/NAD ratio, and an increase in the long-chain fatty acyl-CoA/long-chain acylcarnitine ratio (LCFA-CoA/LCFA-carn). The combination of decreased acetyl-CoA and NADH/NAD ratio cause inhibition of PDK, which allows full activation of PDH, thus increasing flux through glycolysis. Decreased acetyl-CoA also deactivates pyruvate carboxylase, a key enzyme in gluconeogenesis; and decreases gluconeogenesis, ketogenesis and cholesterolgenesis by way of substrate shortage. Subsequent to the reduced level of acetyl-CoA, the level of citrate also decreases causing a disinhibition of phosphofructokinase-1 followed by an increase glycolytic flux. FAO provides the large amount of ATP necessary to drive the energy-expensive gluconeogenic process. Therefore, the inhibition of FAO causes a shortage of ATP making it energetically unfavorable for the production of glucose. Blocking the entry of LCFA-CoA into the mitochondrial matrix causes the LCFA-CoA/LCFA-carn ratio to increase in the cytosol. This tends to increase the rate of triglyceride esterification and phospholipid synthesis,

but also causes feedback inhibition of lipolysis and fatty acid synthesis (Spurway *et al.* 1997; Wolf 1992).

There is some evidence that high and low concentrations of ET may have opposite effects on lipid metabolism in hepatocytes. According to Spurway, et al. 1997, low concentrations of ET increase NEFA esterification and TG secretion, and inhibit TG depletion by inhibition of FAO. High concentrations of ET inhibit lipolysis, esterification and TG secretion (Spurway *et al.* 1997). The inhibitory effects of ET on fatty acyl esterification and TG secretion may be attributable to activation of PPARα and the associated increase in peroxisomal fatty acid oxidation, but this was not addressed in these studies.

ET and other CPT-1 inhibitors are reported to increase peroxisomal FAO, both directly and indirectly, via the peroxisome proliferator activated-receptor α (PPARα) (Forman *et al.* 1997; Intrasuksri *et al.* 1998; Kaikaus *et al.* 1993; Portilla *et al.* 2000; Skorin *et al.* 1992). Upon activation by one of several ligands, PPARα can heterodimerize with the retinoid X receptor, bind to the peroxisome proliferator response element (PPRE) and initiate transcription of numerous lipid metabolizing genes. The latter include those genes concerned with mitochondrial and peroxisomal β-oxidation, cholesterol synthesis and fatty acid transport proteins (Gonzalez *et al.* 1998). Using a ligand-induced complex (LIC) formation assay, Forman et al (1997) determined that CPT-1 inhibitors directly bind and activate PPARα, while at the same time, increase the concentration of NEFA

which then act as ligands to further activate PPARα. The following genes contain PPREs and serve as markers of PPARα activation by their up regulation: acyl-CoA oxidase (AOX), acyl-CoA synthetase, cytochrome P450 4A family (CYP4A), multifunctional protein, 3-ketoacyl-CoA thiolase (3KACT), CPT-1, HMG-CoA synthase (HMGCS), fatty acid binding protein, malic enzyme, acyl-CoA dehydrogenases, phosphoenolpyruvate carboxykinase (PEP-CK), and steroyl-CoA desaturase (SCD). Other genes with PPREs down regulated by PPARα include fatty acid synthase (FAS), apolipoprotein AI, and apolipoprotein CIII (Latruffe and Vamecq 1997; Yu *et al.* 1998). Obviously, PPARα controls a large portion of the lipid metabolism pathways. The administration of ET and other CPT-1 inhibitors to rodents has been associated with gene expression changes similar to those described above (Anderson 1998; Asins *et al.* 1994; Djouadi *et al.* 1998; Hegardt *et al.* 1995; Ouali *et al.* 2000; Portilla *et al.* 2000).

The administration of ET is associated with hypertrophy of both the liver and the heart in rodents (Anderson 1998; Djouadi *et al.* 1999; Koundakjian *et al.* 1984; Rupp *et al.* 1992; Rupp and Jacob 1992; Wolf 1992; Yotsumoto *et al.* 2000). In a study by Koundakjian and coworkers, ethyl 2-[5-(4-chlorophenyl)pentyl]oxirane-2-carboxylate (POCA), structurally similar to ET, dosed for 12 weeks caused an increase in liver weight and lipid content of up to 17% and 15%, respectively (Koundakjian *et al.* 1984). Feeding rats a 0.02% POCA diet for 4 weeks has been reported to cause a 3-fold increase in the number of peroxisomes and in the activity of peroxisomal β-oxidation (Bone *et al.* 1982). It is unclear whether or not

the hepatic hypertrophy is secondary to the activation of PPARα, oxidative stress, accumulation of intrahepatocellular lipid or another etiology.

Cardiac hypertrophy has been both the bane and the possible boon for CPT-1 inhibitors. In studies where CPT-1 inhibitors were administered to normal, aortic constricted and diabetic rats, there was a statistically significant increase in heart weight (Bressler *et al.* 1989; Kato *et al.* 1999; Rupp *et al.* 1992; Rupp and Jacob 1992; Turcani and Rupp 1997). TDGA, POCA, oxfenicine and ET are reported to cause cardiac hypertrophy in rodents secondary to the inhibition of CPT-1. This link was elucidated in a study by Rupp and associates (1995). Medium-chain fatty acids (MCFA) do not require CPT-1 to enter the mitochondrion, therefore, FAO can continue at a high level despite CPT-1 inhibition. In the study by Rupp, feeding a (MCFA) diet abrogated cardiac hypertrophy caused by ET-induced CPT-1 inhibition. Early in the development of CPT-1 inhibitors, their intended use was in the treatment of hyperglycemia in diabetic patients. However, after determining that these compounds could cause significant cardiac hypertrophy, most clinical researchers were unwilling to risk this adverse effect, especially in patients with chronic and severe Type II diabetes. The incidence of heart disease in diabetic patients is higher than that of non-diabetic controls, which dictates caution when designing therapeutic regimens (Anderson 1998). In contrast, in animals with hypertension, myocardial infarction or diabetes-induced cardiac dysfunction, inhibition of CPT-1 has improved cardiac function (Kato *et al.* 1999; Turcani and Rupp 1997; Zarain-Herzberg and Rupp 1999). Similar findings are

reported in humans with chronic heart failure (Schmidt-Schweda and Holubarsch 2000). Etomoxir is currently in Phase 2 clinical trials for use as a therapeutic entity for congestive heart failure (MediGene^{TM} website: http://www.medigene.com/englisch/projekte.php).

Although the association between ET and hypertrophy of both the heart and liver are well documented in the literature, the specific changes underlying the respective hypertrophies have not been elucidated. Several theories have been forwarded but none have clearly and indisputably explained the pathogenesis of ET-induced changes. Because ET is known to be a weak to moderate peroxisome proliferator (Cabrero *et al.* 1999; Forman *et al.* 1997; Mascaro *et al.* 1998; Portilla *et al.* 2000), the hepatic hypertrophy may be directly related to PPARα related alterations in cell proliferation control. Other possible theories to explain the pathogenesis of ET-induced hepatic hypertrophy include: 1) the shift from fatty-acid oxidation to glycolysis, mimicking the fetal phenotype, 2) accumulation of some substrate of CPT-1, engaging a cell proliferation script, or 3) inhibition of the mevalonate pathway, possibly exerting cell proliferation control (Johnson and Ledwith 2001).

Reactive oxygen species (ROS) are implicated in the development of numerous pathological conditions including inflammatory disease, cancer, ischemia-reperfusion injury, and metabolic diseases such as diabetes mellitus. Etomoxir

has been shown to reduce hyperglycemia in diabetic humans and animals (Wolf 1990), and hyperglycemia has been shown to increase oxidative stress (Rosen *et al.* 2001); therefore, etomoxir might theoretically decrease oxidative stress. A CPT-1 inhibitor, tolbutamide, was found to up regulate oxidative stress gene transcripts *GSR* and *SOD2* in HepG2 cells (Morgan *et al.* 2002). Cabrero and associates determined that ET caused oxidative stress in C2C12 skeletal muscle cells (Cabrero *et al.* 2002). A PPARα-agonist, Wy-14,643, has been shown to stimulate the production of superoxide in Kupffer cells via a protein kinase C pathway. The overproduction of superoxide is linked with the activation of NFκB and TNFα which play a role in cell proliferation (Rose *et al.* 1999). If ET truly causes oxidative stress, what role might this oxidative stress play in the pathogenesis of the hepatic and/or cardiac hypertrophy?

The purpose of the present research was to better understand the toxic mechanisms associated with the administration of ET by examining the transcriptional and biochemical alterations and to elucidate specific modulation of homeostatic gene expression. To this end, two hypotheses were put forth 1) Oxidative stress is generated in hepatocytes dosed with ET and this oxidative stress plays a role in the toxicity of ET; and 2) ET-induced hepatic hypertrophy is associated with a unique, PPARα-related and/or oxidative stress-related modulation of gene expression in the rat. The hypotheses were tested in a two part study: Part I assessed the potential of ET to induce oxidative stress in a human hepatocellular carcinoma cell line (HepG2 cells); and Part II correlated

ET-induced hepatic hypertrophy in the rat with liver gene expression profiles spanning a 12 week period. Part I manuscript has been published in Toxicological Sciences, Vol. 68, 93-101 (2002).

References

Abdel-aleem, S., and el-Merzabani, M. M. (1997). Acute and Chronic effects of adriamycin on fatty acid oxidation in isolated cardiac myocytes. *J. Mol. Cell. Cardiol.* **29**, 789-97.

Agius, L., and Alberti, K. G. (1985). Regulation of flux through pyruvate dehydrogenase and pyruvate carboxylase in rat hepatocytes. Effects of fatty acids and glucagon. *Eur. J. Biochem.* **152**, 699-707.

Anderson, R. C. (1998). Carnitine Palmitoyltransferase: A Viable Target for the Treatment of NIDDM? *Curr. Pharm. Design* **4**, 1-16.

Asins, G., Serra, D., and Hegardt, F. G. (1994). The effect of etomoxir on the mRNA levels of enzymes involved in ketogenesis and cholesterogenesis in rat liver. *Biochem. Pharmacol.* **47**, 1373-9.

Bone, A. J., Sherratt, H. S., Turnbull, D. M., and Osmundsen, H. (1982). Increased activity of peroxisomal beta-oxidation in rat liver caused by ethyl 2(5(4-chlorophenyl)pentyl)-oxiran-2-carboxylate: an inhibitor of mitochondrial beta-oxidation. *Biochem. Biophys. Res.Commun.* **104**, 708-12.

Brandt, J., Djouadi, F., and Kelly, D. (1998). Fatty acids activate transcription of the muscle carnitine palmitoyltransferase I gene in cardiac myocytes via

the peroxisome proliferator-activated receptor alpha. *J. Biol. Chem.* **273**, 23786-92.

Bressler, R., Gay, R., Copeland, J. G., Bahl, J. J., Bedotto, J., and Goldman, S. (1989). Chronic inhibition of fatty acid oxidation: new model of diastolic dysfunction. *Life Sciences* **44**, 1897-906.

Cabrero, A., Alegret, M., Sanchez, R., Adzet, T., Laguna, J., and Vazquez, M. (1999). Etomoxir, sodium 2-[6-(4-chlorphenoxy)hexyl]oxirane-2-carboxylate, up-regulates uncoupling protein-3 mRNA levels in primary culture of rat adipocytes. *Biochem. Biophys. Res.Commun.* **263**, 87-93.

Cabrero, A., Alegret, M., Sanchez, R. M., Adzet, T., Laguna, J. C., and Carrera, M. V. (2002). Increased reactive oxygen species production down-regulates peroxisome proliferator-activated alpha pathway in C2C12 skeletal muscle cells. *J. Biol. Chem.* **277**, 10100-7.

Declercq, P. E., Falck, J. R., Kuwajima, M., Tyminski, H., Foster, D. W., and McGarry, J. D. (1987). Characterization of the mitochondrial carnitine palmitoyltransferase enzyme system. I. Use of inhibitors. *J. Biol. Chem.* **262**, 9812-21.

Djouadi, F., Brandt, J. M., Weinheimer, C. J., Leone, T. C., Gonzalez, F. J., and Kelly, D. P. (1999). The role of peroxisome proliferator-activated receptor alpha (PPARa) in the control of cardiac lipid metabolism. *Prostaglandins Leukot. Essent. Fatty* **60**, 339-343.

Djouadi, F., Weinheimer, C. J., Saffitz, J. E., Pitchford, C., Bastin, J., Gonzalez, F. J., and Kelly, D. P. (1998). A gender-related defect in lipid metabolism and glucose homeostasis in peroxisome proliferator- activated receptor alpha- deficient mice. *Journal of Clinical Investigation* **102**, 1083-91.

Eistetter, K., and Wolf, H. (1986). Etomoxir. *Drug Fut.* **11**, 1034-1036.

Forman, B. M., Chen, J., and Evans, R. M. (1997). Hypolipidemic drugs, polyunsaturated fatty acids, and eicosanoids are ligands for peroxisome proliferator-activated receptors alpha and delta. *Proc. Natl. Acad. Sci. U.S.A.* **94**, 4312-7.

Gonzalez, F. J., Peters, J. M., and Cattley, R. C. (1998). Mechanism of action of the nongenotoxic peroxisome proliferators: role of the peroxisome proliferator-activator receptor alpha. *Journal of the National Cancer Institute* **90**, 1702-9.

Hegardt, F. G., Serra, D., and Asins, G. (1995). Influence of etomoxir on the expression of several genes in liver, testis and heart. *Gen. Pharmacol.* **26**, 897-904.

Intrasuksri, U., Rangwala, S. M., O'Brien, M., Noonan, D. J., and Feller, D. R. (1998). Mechanisms of peroxisome proliferation by perfluorooctanoic acid and endogenous fatty acids. *Gen. Pharmacol.* **31**, 187-97.

Johnson, T. E., and Ledwith, B. J. (2001). Peroxisome proliferators and fatty acids negatively regulate liver X receptor-mediated activity and sterol

biosynthesis. *Journal of Steroid Biochemistry & Molecular Biology* **77**, 59-71.

Kaikaus, R. M., Sui, Z., Lysenko, N., Wu, N. Y., Ortiz de Montellano, P. R., Ockner, R. K., and Bass, N. M. (1993). Regulation of pathways of extramitochondrial fatty acid oxidation and liver fatty acid-binding protein by long-chain monocarboxylic fatty acids in hepatocytes. Effect of inhibition of carnitine palmitoyltransferase I. *J. Biol. Chem.* **268**, 26866-71.

Kashfi, K., and Cook, G. A. (1999). Topology of hepatic mitochondrial carnitine palmitoyltransferase 1. *Adv. Exp. Med. Biol.* **466**, 27-42.

Kato, K., Chapman, D. C., Rupp, H., Lucas, A., and Dhalla, N. S. (1999). Alterations of heart function and Na+-K+-ATPase activity by etomoxir in diabetic rats. *J. Appl. Physiol.* **86**, 812-8.

Koundakjian, P. P., Turnbull, D. M., Bone, A. J., Rogers, M. P., Younan, S. I., and Sherratt, H. S. (1984). Metabolic changes in fed rats caused by chronic administration of ethyl 2[5(4-chlorophenyl)pentyl]oxirane-2-carboxylate, a new hypoglycaemic compound. *Biochem. Pharmacol.* **33**, 465-73.

Latruffe, N., and Vamecq, J. (1997). Peroxisome proliferators and peroxisome proliferator activated receptors (PPARs) as regulators of lipid metabolism. *Biochimie* **79**, 81-94.

Mascaro, C., Acosta, E., Ortiz, J. A., Marrero, P. F., Hegardt, F. G., and Haro, D. (1998). Control of human muscle-type carnitine palmitoyltransferase I gene transcription by peroxisome proliferator-activated receptor. *J. Biol. Chem.* **273**, 8560-3.

Moran, L. A., and Scrimgeour, K. G., eds. (1994). *Biochemistry*. Prentiss-Hall, Inc., Upper Saddle River, NJ.

Morgan, K., Ni, H., Brown, R., Yoon, L., Qualls, C., Crosby, L., Reynolds, R., Gaskill, B., Anderson, S., Kepler, T., Brainard, T., Liv, N., Easton, M., Merrill, C., Creech, D., Sprenger, D., Conner, G., Johnson, P., Fox, T., Tyler, R., Sartor, M., Richard, E., Kuruvilla, S., Casey, W., and Benavides, G. (2002). Mechanism of action combined with cDNA microarray technology to select genes for a real time RT-PCR-based screen for oxidative stress in HepG2 cells. *Toxicol. Pathol.* **30**, 435-51.

Morillas, M., Clotet, J., Rubi, B., Serra, D., Arino, J., Hegardt, F. G., and Asins, G. (2000). Inhibition by etomoxir of rat liver carnitine octanoyltransferase is produced through the co-ordinate interaction with two histidine residues. *Biochem. J.* **351**, 495-502.

Murray, R. K., Granner, D. K., Mayes, P. A., and Rodwell, V. W. (2000). *Harper's Biochemistry*. Appleton & Lange, Stamford, CT.

Murthy, M. S., and Pande, S. V. (1990). Characterization of a solubilized malonyl-CoA-sensitive carnitine palmitoyltransferase from the

mitochondrial outer membrane as a protein distinct from the malonyl-CoA-insensitive carnitine palmitoyltransferase of the inner membrane. *Biochem. J.* **268**, 599-604.

Ouali, F., Djouadi, F., Merlet-Benichou, C., Riveau, B., and Bastin, J. (2000). Regulation of fatty acid transport protein and mitochondrial and peroxisomal beta-oxidation gene expression by fatty acids in developing rats. *Pediatric Research* **48**, 691-6.

Park, E. A., Mynatt, R. L., Cook, G. A., and Kashfi, K. (1995). Insulin regulates enzyme activity, malonyl-CoA sensitivity and mRNA abundance of hepatic carnitine palmitoyltransferase-I. *Biochem. J.* **310**, 853-8.

Portilla, D., Dai, G., Peters, J. M., Gonzalez, F. J., Crew, M. D., and Proia, A. D. (2000). Etomoxir-induced PPARalpha-modulated enzymes protect during acute renal failure. *American Journal of Physiology - Renal Fluid and Electrolyte Physiology* **278**, F667-F75.

Reaven, G. M., Chang, H., and Hoffman, B. B. (1988). Additive hypoglycemic effects of drugs that modify free-fatty acid metabolism by different mechanisms in rats with streptozocin-induced diabetes. *Diabetes* **37**, 28-32.

Rogers, M. P. (1987). Effects of 2[5(4-chlorophenyl)pentyl]oxirane-2-carboxylate on lipoprotein lipase, adipose tissue lipolysis and glycerol phosphate acyltransferase in rats. *Biochem. Pharmacol.* **36**, 971-2.

Rose, M. L., Rivera, C. A., Bradford, B. U., Graves, L. M., Cattley, R. C., Schoonhoven, R., Swenberg, J. A., and Thurman, R. G. (1999). Kupffer cell oxidant production is central to the mechanism of peroxisome proliferators. *Carcinogenesis.* **20**, 27-33.

Rosen, P., Nawroth, P. P., King, G., Moller, W., Tritschler, H. J., and Packer, L. (2001). The role of oxidative stress in the onset and progression of diabetes and its complications: a summary of a Congress Series sponsored by UNESCO-MCBN, the American Diabetes Association and the German Diabetes Association. *Diabetes Metab. Res. Rev.* **17**, 189-212.

Rupp, H., Elimban, V., and Dhalla, N. S. (1992). Modification of subcellular organelles in pressure-overloaded heart by etomoxir, a carnitine palmitoyltransferase I inhibitor. *FASEB J.* **6**, 2349-53.

Rupp, H., and Jacob, R. (1992). Metabolically-modulated growth and phenotype of the rat heart. *Eur. Heart J.* **13**, 56-61.

Rupp, H., Schulze, W., and Vetter, R. (1995). Dietary medium-chain triglycerides can prevent changes in myosin and SR due to CPT-1 inhibition by etomoxir. *American Journal of Physiology* **269**, R630-40.

Schmidt-Schweda, S., and Holubarsch, C. (2000). First clinical trial with etomoxir in patients with chronic congestive heart failure. *Clinical Science* **99**, 27-35.

Schmitz, F. J., Rosen, P., and Reinauer, H. (1995). Improvement of myocardial function and metabolism in diabetic rats by the carnitine palmitoyltransferase inhibitor Etomoxir. *Horm. Metab. Res.* **27**, 515-22.

Schudt, C., and Simon, A. (1984). Effects of sodium 2-[5-(4-chlorophenyl)pentyl]-oxirane-2-carboxylate (POCA) on carbohydrate and fatty acid metabolism in liver and muscle. *Biochem. Pharmacol.* **33**, 3357-62.

Skorin, C., Necochea, C., Johow, V., Soto, U., Grau, A. M., Bremer, J., and Leighton, F. (1992). Peroxisomal fatty acid oxidation and inhibitors of the mitochondrial carnitine palmitoyltransferase-1 in isolated rat hepatocytes. *Biochem. J.* **281**, 561-7.

Spurway, T. D., Pogson, C. I., Sherratt, H. S., and Agius, L. (1997). Etomoxir, sodium 2-[6-(4-chlorphenoxy)hexyl]oxirane-2-carboxylate, inhibits triacylglyerol depletion in hepatocytes and lipolysis in adipocytes. *FEBS Lett.* **404**, 111-4.

Turcani, M., and Rupp, H. (1997). Etomoxir improves left ventricular performance of pressure-overloaded rat heart. *Circulation* **96**, 3681-6.

Vetter, R., Kott, M., and Rupp, H. (1995). Differential influences of carnitine palmitoyltransferase-1 inhibition and hyperthyroidism on cardiac growth and sarcoplasmic reticulum phosphorylation. *Eur. Heart J.* **16**, 15-9.

Watson, R. T., and Pessin, J. E. (2001). Subcellular compartmentalization and trafficking of the insulin-responsive glucose transporter, GLUT4. *Experimental Cell Research* **271**, 75-83.

Wolf, H. P. (1990). Aryl-substituted 2-oxirane Carboxylic Acids: A New Group of Antidiabetic Drugs. In *New Antidiabetic Drugs* (C. Baily and P. Flatt, eds.), pp. 217-229. Smith-Gordon, London.

Wolf, H. P. (1992). Possible new therapeutic approach to diabetes mellitus by inhibition of carnitine palmitoyltransferase 1 (CPT1). *Horm. Metab. Res.* **Suppl.26**, 62-7.

Yotsumoto, T., Naitoh, T., Kitahara, M., and Tsuruzoe, N. (2000). Effects of carnitine palmitoyltransferase I inhibitors on hepatic hypertrophy. *Eur. J. Pharmacol.* **398**, 297-302.

Yu, G. S., Lu, Y. C., and Gulick, T. (1998). Co-regulation of tissue-specific alternative human carnitine palmitoyltransferase Ibeta gene promoters by fatty acid enzyme substrate. *J. Biol. Chem.* **273**, 32901-9.

Zarain-Herzberg, A., and Rupp, H. (1999). Transcriptional modulators targeted at fuel metabolism of hypertrophied heart. *Am. J. Cardiol.* **83**, 31H-37H.

Manuscript I

Etomoxir-induced Oxidative Stress in HepG2 Cells Detected by Differential Gene Expression is Confirmed Biochemically

Christine L. Merrill [1,2], Hong Ni [2], Lawrence W. Yoon [2], Mark A. Tirmenstein[3], Padma Narayanan[3], Gina R. Benavides [2], Marilyn J. Easton [2], Donald R. Creech [2], Catherine X. Hu[3], David C. McFarland[3], Laura M. Hahn[3], Heath C.Thomas[3] and Kevin T. Morgan [4]

1. Safety Assessment, GlaxoSmithKline, RTP, NC 27709
2. Toxicogenomic Mechanisms US, GlaxoSmithKline, RTP, NC, 27709
3. Cellular Pathology, GlaxoSmithKline, King of Prussia, PA, 19406
4. Department of Safety Evaluation, Aventis, Bridgewater, NJ 08807

Abbreviated Title:

ETOMOXIR-INDUCED OXIDATIVE STRESS IN HEPG2 CELLS

Corresponding author:

Christine L. Merrill

Five Moore Drive

RTP, NC 27709

clm70753@gsk.com

Tel. 919-483-9336

Fax 919-315-8391

Abstract

Although known to be effective antidiabetic agents, little is published about the toxic effects of carnitine palmitoyltransferase-1 (CPT-1) inhibitors, such as etomoxir (ET). These compounds inhibit mitochondrial fatty acid β-oxidation by irreversibly binding to CPT-1 and preventing entry of long chain fatty acids into the mitochondrial matrix. Treatment of HepG2 cells with 1 mM etomoxir for 6 h caused significant modulations in the expression of several redox-related and cell cycle mRNAs as measured by microarray analysis. Upregulated mRNAs included heme oxygenase 1 (*HO1*), 8-oxoguanine DNA glycosylase 1 *(OGG1*), glutathione reductase (*GSR*), cyclin-dependent kinase inhibitor 1A (*CDKN1* [$p21^{waf1}$]) and Mn+ superoxide dismutase precursor (*SOD2*); while cytochrome P450 1A1 (C*YP1A1*) and heat shock 70kD protein 1 (*HSPA1A*) were downregulated. Real time quantitative PCR (RT-PCR) confirmed the significant changes in 4 of 4 mRNAs assayed (*CYP1A1, HO1, GSR, CDKN1*), and identified 3 additional mRNA increases; 2 redox-related genes, γ-glutamate-cysteine ligase modifier subunit (*GCLM*) and thioredoxin reductase (*TXNRD1*) and 1 DNA replication gene, topoisomerase IIα (*TOP2A*). Temporal changes in selected mRNA levels were examined by RT-PCR over eleven time points from 15 mins to 24 h post-dosing. *CYP1A1* exhibited a 38 fold decrease by 4 h which rebounded to a 39 fold increase by 20 h. *GCLM* and *TXNRD1* exhibited 13 and 9 fold increases, respectively at 24 h. Etomoxir-induced oxidative stress and impaired mitochondrial energy metabolism were confirmed by a significant decrease in reduced glutathione (GSH), reduced/oxidized glutathione ratio (GSH/GSSG),

mitochondrial membrane potential (MMP), and ATP levels, and by concurrent increase in oxidized glutathione (GSSG) and superoxide generation. This is the first report of oxidative stress caused by etomoxir.

Key words: Etomoxir; toxicity; oxirane-carboxylates; oxidative stress; gene expression

Introduction

Etomoxir is a member of a family of substituted 2-oxirane-carboxylic acids that inhibit mitochondrial long-chain fatty acid β-oxidation (FAO), ketogenesis and gluconeogenesis (Wolf, 1992). Once converted to its CoA ester, etomoxir irreversibly binds to the CPT-1 catalytic site and prevents long chain fatty acids from entering the mitochondrion. Along with this inhibition of FAO, etomoxir causes a shift in energy substrate utilization from fatty acids to glucose, leading to systemic hypoglycemia, hypoketonemia, and hypotriglyceridemia (Wolf, 1992). These effects make etomoxir potentially useful in the treatment of non-insulin-dependent diabetes mellitus (NIDDM). However, the compound has been shown to induce cardiac and hepatic hypertrophy in animals and therefore has not been fully developed as an antidiabetic agent to date (Rupp and Jacob, 1992; Vetter *et al.*, 1995; Yotsumoto *et al.*, 2000). The mechanism(s) of the respective hypertrophies have not yet been worked out, but are shown to be different from those involved in hyperthyroidism and hypertension (Rupp *et al.*, 1992; Vetter *et al.*, 1995).

Reactive oxygen species (ROS) are implicated in the development of numerous pathological conditions including inflammatory disease, cancer, ischemia-reperfusion injury, and metabolic diseases such as diabetes mellitus. Emerging evidence links the presence of free radicals to the progression of diabetes and its complications. There is much evidence that hyperglycemia and advanced glycation end products (AGE) promote the formation of ROS in the diabetic patient and several markers of oxidative stress, such as 8-hydroxydeoxyguanosine, hydroperoxide and oxidized lipoprotein (oxLDL), are increased in these patients (Rosen *et al.*, 2001).

In one study, hyperglycemia was shown to induce mitochondrial superoxide overproduction which in turn activated the hexosamine pathway, thought to be a major factor in the pathogenesis of diabetic complications (Du *et al.*, 2000). Lipid peroxidation and antioxidant depletion, which strongly contribute to the development of atherosclerosis, are both present in diabetes mellitus (Cominacini *et al.*, 1994; Dimitriadis *et al.*, 1995; Leonhardt *et al.*, 1996; Schoen and Cotran, 1999; Srinivasan *et al.*, 1997). In addition to vascular dysfunction, oxidative stress is involved in the pathogenesis of diabetic polyneuropathy, retinopathy and the expansion of extracellular matrix components, type IV and VI collagen, fibronectin, and laminin (Rosen *et al.*, 2001). Diabetes appears to be associated with increased levels of oxidative stress. It would be best, therefore, if a drug designed to treat this metabolic disease did not contribute to such stress.

Etomoxir has been shown to reduce hyperglycemia in diabetic humans and animals (Wolf, 1990), and hyperglycemia has been shown to increase oxidative stress (Rosen *et al.*, 2001); therefore, etomoxir might theoretically decrease oxidative stress. Morgan, et al., however, determined that another CPT-1 inhibitor, tolbutamide, caused upregulation of the oxidative stress gene transcripts *GSR* and *SOD2* in HepG2 cells (Morgan *et al.*, 2002).

The purpose of this study was to evaluate mRNA expression to determine ET-induced mechanisms of toxicity in HepG2 cells, with special emphasis on oxidative stress. Gene expression strongly suggestive of oxidative stress was observed and supported by decreased levels of reduced glutathione, reduced/oxidized glutathione ratio (GSH/GSSG), concurrent increase in oxidized glutathione (GSSG) and superoxide generation. Impairment of mitochondrial energy metabolism was implicated by a significant decrease in mitochondrial membrane potential and ATP levels. Other gene expression findings suggested activation of p53, DNA repair and cell cycle arrest. This is the first report of oxidative stress caused by etomoxir.

Materials and Methods

Chemicals

Etomoxir was obtained from Research Pharmaceuticals, Allensbach, Germany and other chemicals were obtained from Clontech Laboratories, Research Genetics and Ambion.

Cell Culture

Human hepatocellular carcinoma (HepG2) cells (ATCC 1998, CRL-10741, Homo sapiens, HepG2/C3A,Rockville, MD) were maintained in Dulbecco's Modified Eagle Medium (DMEM) with Glutamax and 10% fetal bovine serum (FBS), under standard cell culture conditions (37°C, humidified, 5% CO_2) without antibiotics. For this experiment, time zero ($T_{0)}$ represents the time at which treatment was first begun. At time -48 h, HepG2 cells were seeded at a density of $1x10^7$ in 3 control and 3 treated collagen coated (Vitrogen-100, Cohesion, Palo Alto, CA) 150 mm diameter cell culture dishes (Nontreated, Non-Pyrogenic, Polystyrene, Corning, Inc., NY) with 26 ml medium. A sterile, numbered, collagen-coated glass coverslip was placed in the bottom of each dish for use in the light microscopic determination of cell morphology. Cells were fed at -24 h and re-fed at 0 h with either untreated media (control) or 1 mM etomoxir in media (treated). Treatment duration in the first experiment was 6 hours. In the second experiment, multiple time points were used (0.25 h, 0.5 h, 1 h, 2 h, 4 h, 6 h, 8 h, 12 h, 16 h, 20 h, 24 h) in order to track mRNA expression changes chronologically (timecourse study).

Selection of Exposure Concentration

As previously described (Morgan *et al.*, 2002), ET exposure concentration was selected to be that which caused 50% reduction in MTS assay (Cell Titer 96® AQ_{ueous} Non-radioactive Cell Proliferation Assay, Promega) in HepG2 cells at

24h. MTS is bioreduced by dehydrogenase enzymes in cells into a formazan that is soluble in cell culture medium. The quantity of formazan product as measured by 490 nm absorbance is directly proportional to the number of living cells in culture (Cory *et al.*, 1991; Marshall *et al.*, 1995). HepG2 cells were cultured in 96 well plates with 20,000 cells and 50 μL of DMEM+10% FBS per well. ET was added in fresh medium at serial 10 fold dilutions (6 replicates per dilution). Following exposure for 24 h, 10 μL of MTS reagent were added to each well, the plate was incubated for 1 h at 37°C and the spectrophotometric absorbance read at 490 nm. A 1mM exposure concentration was selected and confirmed in six 150mm plates seeded with $1x10^7$ cells (per RNA collection protocol) and MTS assay was run on media collected from plates. Light microscopy was used to confirm the toxic responses in the cells as measured by the MTS assay.

Cell Morphology and Viability

Coverslips were removed from plates at 6 h time point or at timecourse timepoints (listed above) and fixed in ethanol. Coverslips were hematoxylin and eosin (H&E) stained and evaluated by light microscopy. Using standard cell counting procedures, cell counts were performed at 5 reproducible sites on each 6 h and 24 h timecourse coverslip (control and 1mM ET) (n=3). Utilizing an Olympus 25 grid reticle (total area 25 $mm^{2)}$, cell nuclei within each of the 5 sites were counted for total cell counts. Mitotic figures and apoptotic/necrotic cells within the same sites comprised the mitotic index or apoptotic/necrotic index (number of affected cells/1000 cells counted). Apoptotic cells were characterized

by cell shrinkage, chromatin condensation, formation of cytoplasmic blebs and phagocytosis by adjacent healthy cells. Necrotic cells exhibited loss of nuclear integrity, increased eosinophilia, +/- cell swelling. It was frequently difficult to distinguish these two forms of cell death, therefore apoptotic and necrotic cells were lumped together during cell counts. Release of lactate dehydrogenase (LDH) enzyme activity was used as a measure of cell viability. LDH activity was determined by monitoring the enzymatic formation of NADH from NAD+ in the presence of L-lactic acid. At the indicated time points, media samples were withdrawn and centrifuged to remove viable cells. Post-centrifugation supernatants were diluted five times with phosphate buffered saline (PBS), pH 7.4. An aliquot of 100 µl diluted sample was mixed with 100 µl reagent to give a final concentration of 3.75 mM NAD+ and 25 mM L-lactic acid in 125 mM Tris-HCl buffer, pH 8.9 in a 96 well plate. The increase in absorbance at 340 nm was immediately monitored at room temperature using a SPECTRAmax 250 microplate spectrophotometer (Molecular Devices, Sunnydale, CA). The percent LDH leakage was calculated by comparing values with total LDH activity. Total LDH activity was measured from untreated HepG2 cells lysed with a final concentration of 0.2% Triton X-100 in phosphate buffered saline (PBS).

Gene expression arrays:

Cultured cells, after removal of overlying media, were lysed with Trizol Reagent™ and lysate was frozen at -80°C until use. Total RNA was isolated by a chloroform/isopropanol/ethanol extraction and RNA quality and quantity were

assessed using agarose gel electrophoresis and spectrophotometric 260/280 nm absorbance. ^{33}P-labelled cDNA probes were prepared using a modification of the Clontech™ (Palo Alto, CA) protocol and hybridized to Clontech Atlas™ Human Stress Toxicology cDNA Arrays (234 genes). Denaturation (4 µl) was carried out at 70°C for 10 min using 6 µg total mRNA and 1 µl CDS Atlas™ specific primers (0.2 µM each). The annealing and extension reactions (22 µl, 35 min at 49°C) contained 0.5 mM each dATP, dGTP, dTTP, 50 mM Tris-HCl pH 8.3, 75 mM KCl, 3 mM $MgCl_2$, 4.5 mM, 100µCi ^{33}P-α-dCTP (3000 Ci/mmol, 10 µCi/µl, NEN) and 200 units Super Script II™ reverse transcriptase (Gibco-BRL, MD). Extension was terminated by heating to 94°C for 5 min. Unincorporated ^{33}P-α-dCTP was removed using G-50 MicroSpin columns (Pharmacia Biotech, NJ). Hybridization was carried out at 64°C for 16 h, in 6.5 ml MicroHybe™, 3.25 µl poly-dA (1 µg/µl, Research Genetics, AL) and 6.5 µl Human Cot-1 DNA (1 µg/µl, Clontech, CA) and heat denatured ^{33}P-cDNA . Arrays were washed at 64°C following manufacturer's instructions. Phosphor imaging screens were exposed to the arrays for 24-48 h and the optical density was acquired using OptiQuant and a Cyclone scanner (Packard BioScience Co, CT). Image files generated from phosphorimager scans were analyzed using Clontech AtlasImage Software™.

After background subtraction, non-normalized data were analyzed statistically using Normalization and Local Regression (NLR) software (Tom Kepler, Sante Fe Institute) which is downloadable from the internet at

ftp://ftp.santafe.edu/pub/kepler/. NLR was used to compare control with treated groups (n=3/group), generate p-values, mean log intensity (MLI) to provide an indication of signal strength, and ratio of differences between groups.

Quantitative Real Time PCR:

Total RNA prepared above from 3 control and 3 ET-treated samples was DNAase-treated (Ambion DNAase I) according to the manufacturer's protocol. RNA was quantified using the Molecular Probes Ribogreen™ assay and a Cytofluor 2350 fluorometer. Samples were diluted to 10 ng/µL prior to Taqman™ analysis (Perkin Elmer ABI Prism 7700 Sequence Detection system). A 7-gene plate, described by Morgan, et al. was used to quantitate the mRNA expression of the following genes*: HO1, CYP1A1, TOP2A, CDKN1, GSR, GCLM*, and *TXNRD1 (Morgan et al., 2002)*. The plate was arranged with one row allotted for each gene to be assayed and one row of water blanks, and duplicate columns assigned to each treated or control sample. Primers were designed with Perkin Elmer Primer Express™ software. Forward and reverse primers and probes were diluted to the appropriate concentrations to make the probe/primer master mix. The master mix was prepared according to the manufacturer's protocol (without probes and primers) and 30 µL of master mix, 5 µL of RNA and 15 µL of probe/primer mix were aliquotted per well into the seven-gene plate. The plate was sealed with Optical Adhesive Covers (PE Biosystems™), centrifuged at 3000xg for 10 secs and the reaction was incubated at 48°C for 30 min (reverse transcriptase (RT) step), denatured at 95°C for 10 min (Amplitaq activation and

RT denaturation), and then subjected to 40 PCR cycles of 94°C for 15 sec and 60°C for 1 min. Values of fold change in expression were graphed for comparison purposes. Statistical significance was determined for control *versus* treated groups using a t-test (two-tailed, pooled, assuming normal distribution and variances equal) and significance selected at $p<0.05$.

Oxidative stress assays: *GSH and GSSG* levels were assayed by HPLC according to the method of Martin and White (1991). *Superoxide radical*: Hydroethidine (HE), a sodium borohydride-reduced form of ethidium bromide (EB) was used to evaluate generation of superoxide ($O_2^{-\bullet}$) upon exposure to etomoxir in HepG2 cells. HE, a specific and sensitive indicator of $O_2^{-\bullet}$ (Rothe and Valet, 1990) is cell permeable and can be directly oxidized to EB by $O_2^{-\bullet}$ produced by the cell (Carter *et al.*, 1994). Intracellular EB tightly binds DNA, and is fluorescent (610 nm) on excitation with the 488 nm line of a FACSCalibur (Becton-Dickinson, San Jose, CA). Ten μM HE was added to the cell suspension for dye-loading. Fifteen minutes after incubation at 37°C with HE, HepG2 cells were incubated for an additional 6 h in the presence or absence of ET (500 and 1000 μM) after which sample collection was started immediately on the FACSCalibur bench-top flow cytometer (Becton-Dickinson, San Jose, CA).

Mitochondrial energy metabolism assays: *ATP*: Cellular ATP levels were measured with an ATP Bioluminescent Somatic Cell Assay Kit obtained from Sigma (St. Louis, MO) according to the manufacturer's instructions with slight

modifications. HepG2 cells plated on a 96-well plate were incubated with 500 μM etomoxir in media with serum. After 24 h, the media was removed and cells were lysed by adding 100 μl of ATP releasing reagent and 100 μl of water. Aliquots of 100 μl were transferred to white 96 well assay plates. Luminescence was monitored on a Gemini XS SPECTRAmax dual scanning microplate spectrofluorometer (Molecular Devices, Sunnyvale, CA) in the luminescence mode following the addition of 100 μl luciferin and luciferase. *Mitochondrial membrane potential (MMP):* Disruptions in MMP can be measured using cationic lipophilic fluorochromes such as Mitotracker Red (Chloromethyl-X-Rosamine, MR). These probes diffuse passively across the plasma membrane and accumulate in the negatively charged mitochondrial matrix. The extent of dye uptake depends on the potential difference ($\Delta\psi$); dissipation of MMP results in a decrease in cell-associated fluorescence that can be detected by flow cytometry. To determine changes in MMP, 1 x 10^6 cells were incubated with 100 nM Mitotracker Red for 15 min at 37°C in the dark and then treated with ET (250, 500 and 1000 μM) for 1 h at 37°C. Samples were analyzed immediately by flow cytometry on a FACSCalibur.

Results

Morphology and cell viability: Examination of HepG2 cells treated with 1 mM ET for 6 and 24 h revealed clear morphologic changes (Figure 1.1) including loss of large cytoplasmic vacuoles, and cell shrinkage and rounding-up. Statistically

significant increases in apoptotic/necrotic cells and a marked decrease in mitotic figures were present only at the 24 h timepoint (Table 1.1). Many cells exhibited concurrent mitotic spindles and necrosis. In cell count assays at 24 h, the number of cells was reduced 34% relative to the time-matched controls; mitotic figures dropped from 21.6/1000 cells to 0/1000 cells and apoptotic/necrotic cells were increased ~1200%. LDH enzyme activity was used as a measure of cell viability at 6 and 24 h with significance determined by Dunnett's Test (n=3). Of the 3 concentrations evaluated (0.25, 0.5 and 1 mM), only the 24 h, 1 mM combination caused significant cell death (21%, $p < 0.05$).

Clontech Human Stress arrays: Statistically significant ($p<0.05$) changes (Table 1.2) in mRNA levels relative to controls were induced by treatment of HepG2 cells with 1mM ET for 6h. Redox-related genes: *HO1, GSR, OGG1* and *SOD2* were upregulated and *CYP1A1* was downregulated. Cell cycle/apoptosis genes: growth arrest- and DNA damage-inducible gene 153 (*GADD153*), growth arrest- and DNA damage-inducible gene 45 (*GADD45*), *CDKN1,* mouse double minute 2 homolog (*MDM2)*, ubiquitin and ubiquitin protein ligase were upregulated, while proliferating cell nuclear antigen (*PCNA*), extracellular signal-regulated kinase 1 (*ERK1*) and mitogen-activated protein kinase P38 (aka MAP kinase 14, MAPK14) were downregulated. Heat shock proteins: heat shock protein 40 homolog (HSP40 homolog) and heat shock 70kD protein 5 (*HSPA5,* aka 75-kD glucose-regulated protein) were upregulated. DNA synthesis and repair: excision repair cross-complementing rodent repair deficiency,

complementation group 2 (*ERCC2*, aka xeroderma pigmentosum group D complementing protein) and UV excision repair protein (RAD23A) were upregulated. *Peroxisome proliferator activated receptor (PPAR) genes*: PPAR-alpha mRNA was decreased.

Quantitative Real Time-PCR: RT-PCR was used to confirm selected mRNA expression changes identified by microarray analysis. The following RT-PCR (fold expression) changes in the 6 h, 1mM ET experiment indicate oxidative stress and cell cycle modulation: *CYP1A1* (-9.6)*, HO1* (+1.5)*, TOP2A* (-1.6), *GSR* (+1.3)*, CDKN1* (+2.6)*, GCLM* (+3.4) and *TXNRD1* (+2.7) (Figure 1.2, Table 1.2). Direction of change and statistical significance ($p<0.05$) of the expression of 4 mRNA transcripts (*HO1, CDKN1*, and *GSR* upregulated, and *CYP1A1* downregulated) present on the Clontech Human Stress Array™ were confirmed by RT-PCR. The mRNA expression of TOP2A was downregulated on both platforms (RT-PCR and microarray), but only exhibited statistical significance on RT-PCR. The two genes not present on the arrays (*GCLM* and *TXNRD1*) were both significantly ($p<0.05$) upregulated at 6 h.

The ET timecourse study followed expression of these 7 genes over 11 eleven timepoints from 0.25 h to 24 h (Figure 1.3). Note the severe swing of *CYP1A1* from a decrease of 38 fold at 4 h to an increase of 39 fold at 20 h. *GCLM* and *TXNRD1* proved to be good indicators of oxidative stress as they were

significantly increased above controls at 6 h and continued to rise through the 24 h timepoint to 13 and 9 fold increases, respectively.

Oxidative stress assays: *GSH and GSH:GSSG ratio:* Intracellular reduced glutathione (GSH) levels decreased relative to time-matched controls upon treatment with ET (Figure 1.4). At 6 h, only the 1 mM dose group was significantly decreased; control 53.7±6.4 nmol/mg protein and 1mM ET group 40.1±11.1 nmol/mg protein (-25%). The GSH depletion was more pronounced at the 24 h timepoint with significant reduction in the 0.5 and 1 mM groups; control 55.0±13.5 nmol/mg protein, 0.5 mM ET 24.6±2.8 nmol/mg protein (-55%) and 1 mM ET 24.3±3.9 nmol/mg protein (-56%). There was a significant increase in GSH at 24 h with 0.25mM ET. The ratio of GSH:GSSG, an accepted measure of oxidative stress (Armstrong, 1998), mirrored GSH changes with significant declines at 6 h 1 mM (-56%), and at 24 h 0.5mM ET (-93%) and 1mM ET (-84%). *Superoxide radical:* At 6 h, superoxide radical generation was increased in 0.5 mM ET-treated cells by ~350% *vs* untreated controls (Figure 1.5).

Mitochondrial energy metabolism assays: *ATP:* Treatment of HepG2 cells for 24 h with 0.5 mM ET was associated with an 84% decrease in ATP levels (Figure 1.6). This dose was chosen because it was the highest non-toxic dose (0.5 mM) of ET as measured by lactate dehydrogenase activity. *Mitochondrial membrane potential:* At the 0.5 mM and 1 mM ET concentrations, MMP is reduced by 16

and 28%, respectively (Figure 1.7). The 0.25 mM ET concentration does not change MMP relative to the untreated control.

Discussion

Etomoxir, an effective hypoglycemic, hypotriglyceridemic and hypocholesterolemic compound, has not been fully developed as an antidiabetic drug due to its toxic effects on the liver and heart of some animal species (Anderson, 1998). Hypertrophy of both the heart and liver have been reported with supraclinical doses of etomoxir, but the pathophysiological mechanisms are unclear (Rupp and Jacob, 1992; Yotsumoto *et al.*, 2000). In this study, gene expression patterns were profiled to identify potential toxic pathways associated with the treatment of HepG2 cells with etomoxir. Patterns consistent with oxidative stress, cell cycle arrest, apoptosis and DNA and protein damage were identified by microarray and RT-PCR assays, and confirmed morphologically and biochemically. In addition, the decreases in ATP concentration and mitochondrial membrane potential are indicative of dysregulation of mitochondrial energy metabolism.

Several genes associated with redox imbalance were significantly altered, including *HO1, SOD2, GSR, OGG1,* and *CYP1A1. HO1* is the rate-limiting enzyme in heme degradation, catalyzing the cleavage of the heme ring to form ferrous iron, carbon monoxide and biliverdin. HO1, biliverdin and carbon monoxide have been shown to have protective effects during oxidative stress

(Duckers *et al.*, 2001). *SOD2* is an intramitochondrial free radical scavenging enzyme that serves as the first line of defense against superoxide produced during oxidative phosphorylation. This enzyme catalyzes the dismutation of 2 superoxide anions to hydrogen peroxide. During redox imbalance, excess H_2O_2 produced in HepG2 cells is most likely converted to H_2O by glutathione peroxidase, as there is little measurable catalase in the mitochondria (Bai and Cederbaum, 2000). In the presence of glutathione peroxidase and H_2O_2, 2 molecules of reduced glutathione react to form a molecule of glutathione disulfide (GSSG) causing the concurrent reduction of H_2O_2 to H_2O. The glutathione disulfide molecule is converted back to 2 molecules of reduced glutathione by glutathione reductase and NADPH + H^+. In our study, glutathione reductase mRNA was increased 1.6 fold ($p<0.012$) while glutathione peroxidase and catalase were not significantly altered with ET-treatment. A major mutagenic base lesion in DNA caused by exposure to reactive oxygen species is 8-oxoguanine. This damaged base is excised by *OGG1* (Lu *et al.*, 1997). Although we have no direct evidence of DNA damage in this study, upregulation of OGG1 and direct evidence of oxidative stress gives us strong hypothetical evidence that there is oxidative damage to DNA secondary to ET treatment. *CYP1A1,* a P450 enzyme known to generate reactive oxygen species (Morel *et al.*, 2000; Morel *et al.*, 1999), was markedly downregulated in the first 6 hours. This P450 monooxygenase has recently been shown to exhibit negative autoregulation, when the reactive oxygen species (ROS) generated by action of the enzyme repress the CYP1A1 gene promoter (Morel *et al.*, 1999). Taken together, the

altered gene expression pattern of the above-mentioned five genes is highly suggestive of oxidative stress.

Because microarray technology remains somewhat untested, selected significantly altered stress gene transcripts were quantitated by RT-PCR using the 7-gene plate described by Morgan et.al and compared to the results of the microarray gene expression analysis (Morgan *et al.*, 2002). Dysregulation of three redox-sensitive genes described above (*HO1, GSH* and *CYP1A1*) and a cell cycle gene (*CDKN1*) were confirmed by RT-PCR analysis of the 6 h single time point experiment. *TOP2A,* downregulated, though not significantly according to microarray analysis, was significantly decreased as measured by RT-PCR. The expression levels of *GCLM* and *TXNRD1,* redox-sensitive genes not present on the Clontech Atlas™ Human Stress Array, were also upregulated via RT-PCR analysis.

The time course experiment was performed to track the expression of the 7 genes mentioned above over a 24 h period by RT-PCR. By following the gene expression changes over time, we not only provide a more complete gene expression profile but we also prevent inaccurate conclusions based on a single "snapshot"-type experiment. The timecourse RT-PCR data confirmed the gene expression changes noted in the 6 h microarray and RT-PCR assays, however, the chronology of these transcript changes did not always correlate well between experiments. For example, *GSR* transcripts did not reach values significantly

increased above controls until 8 h in the timecourse experiment but obtained significance at 6 h in the single time point experiment. Given the dynamic nature of gene transcript expression, multiple timepoints are recommended.

Changes in transcription cannot be equated to changes in functional pathways because transcripts have to be translated, and proteins may require post-translational modification in order to become functional. Because the above-mentioned changes in mRNA do not necessarily represent actual changes in the protein profile of the cell, the premise of ET-induced oxidative stress identified by gene expression profiling, needed the support of functional biochemical assays before it could be accepted. At 6 h and 1mM [ET], depletion of intracellular GSH, accumulation of GSSG, and decreased GSH/GSSG ratio confirmed the uncompensated redox imbalance first suggested by analysis of the oxidative stress gene expression. This allows the potential detection of toxic endpoints by evaluation of gene expression prior to morphologic changes in the cells. The 0.5mM [ET], which failed to cause significant cell death at 24 h, caused oxidative stress detectable by decreased GSH, increased GSSG and decreased GSH:GSSG ratio. In contrast to the higher concentrations, 0.25mM [ET] at 24 h gave a significant increase in GSH. This result might be explained by ability of ET to induce GCLM, the rate-limiting step in GSH synthesis, causing an increase in intracellular GSH with [ET] insufficient to deplete GSH.

Decrease in ATP levels may be due to oxidative stress-associated protein cross-linking within the electron transport chain complexes and subsequent decrease in oxidative phosphorylation due to a decrease in mitochondrial membrane potential. Alternatively, the decrease in ATP levels and mitochondrial membrane potential might be due to an ET-induced intracellular increase in acyl-CoA esters which have been shown to be potent inhibitors of the mitochondrial adenine nucleotide translocase (ANT) (Shrago *et al.*, 1995). ANT exchanges mitochondrial ATP for cytosolic ADP, considered to be the overall rate limiting step in energy metabolism (Lemasters and Sowers, 1979). The inability to bring ADP into the mitochondrion would halt the activity of Complex-V, allowing the proton gradient across the inner mitochondrial membrane to increase to dangerous levels. Uncoupling protein-3, known to be upregulated by ET-treatment (Cabrero *et al.*, 1999, 2001), would dissipate the proton gradient and decrease the mitochondrial membrane potential. We know that oxidative stress is present in the ET-treated HepG2 cells, but we don't know if the ATP depletion or decrease in mitochondrial membrane potential is directly related to oxidative stress or if these changes are ET-specific.

Modulation of additional stress gene transcripts was also observed secondary to ET-treatment. *GADD153, GADD45, CDKN1, and MDM2* were upregulated, suggesting that there was DNA damage and p53-activation (Friedberg *et al.*, 1995; Lewin, 2000; Walsh *et al.*, 1995). Ubiquitin and ubiquitin protein ligase were also upregulated suggesting increased turnover of proteins, which may be

secondary to increased cytosolic protein volume or to misfolded or damaged proteins. Downregulated genes included PCNA, ERK1 and MAP kinase p38. Both ERK1 and p38 MAP kinase are responsive to oxidative stress (Ogura and Kitamura, 1998) and MAP kinase p38 is negatively regulated by thioredoxin (Hashimoto *et al.*, 1999) . ET-treated (1mM) HepG2 cells exhibited a significant increase in cell death at 24 h with concurrent reduction in mitotic figures and increase in apoptotic/necrotic cells. All of these morphologic changes in the cells correlate well with downregulation of PCNA, ERK1 and MAP kinase p38. All of these changes in gene expression might be attributable to oxidative stress leading to DNA damage and protein cross-linking with subsequent cell cycle arrest and apoptosis and necrosis, however more work should to be done to confirm these speculative conclusions.

Etomoxir and other CPT-1 inhibitors are known activators of peroxisome proliferator-activated receptor α (PPARα)(Brandt *et al.*, 1998; Djouadi *et al.*, 1999; Forman *et al.*, 1997; Portilla *et al.*, 2000). The cytoplasmic accumulation of long-chain fatty acids secondary to inhibition of CPT-1 serves as a trigger for PPARα activation (Brandt *et al.*, 1998; Forman *et al.*, 1997). In addition, several CPT-1 inhibitors are structural analogs of long chain fatty acids, and therefore can bind directly to and activate PPARα (Forman *et al.*, 1997). Skorin et al. (1992) showed that 2-tetradecylglycidic acid (TDGA) and etomoxir enhance production of H_2O_2 in peroxisome- proliferated rat primary hepatocytes when fatty acids of 12 carbons or more were utilized as substrate. The increase in PPARα

activity and subsequent H_2O_2 generation might be expected to induce oxidative stress in cells treated with CPT-1 inhibitors like etomoxir. It is unclear what role, if any, PPARα plays in generating oxidative stress secondary to ET-treatment of HepG2 cells, but the possible contribution of PPARα cannot be ignored.

In summary, the results of the current study demonstrate etomoxir-induced oxidative stress in a human liver cell line, first identified by analysis of stress gene transcript expression and then confirmed by multiple biochemical oxidative stress/mitochondrial function assays. Alterations in the expression of genes related to cell cycle arrest and apoptosis are also observed and supported by morphological evidence. This is the first report of oxidative stress secondary to etomoxir administration, while the contribution of this oxidative stress to known toxic endpoints remains to be evaluated. This study illustrates the potential for gene expression profiling to serve as a tool to identify toxic mechanisms and pathways.

References

Anderson, R. C. (1998). Carnitine Palmitoyltransferase: A Viable Target for the Treatment of NIDDM? *Curr. Pharm. Design* **4**, 1-15.

Armstrong, D. (1998). *Free Radical and Antioxidant Protocols*.

Bai, J., and Cederbaum, A. I. (2000). Overexpression of catalase in the mitochondrial or cytosolic compartment increases sensitivity of HepG2 cells to tumor necrosis factor-a-induced apoptosis. *J. Biol. Chem.* **275**, 19241-19249.

Brandt, J., Djouadi, F., and Kelly, D. (1998). Fatty acids activate transcription of the muscle carnitine palmitoyltransferase I gene in cardiac myocytes via the peroxisome proliferator-activated receptor alpha. *J. Biol. Chem.* **273**, 23786-92.

Cabrero, A., Alegret, M., Sanchez, R., Adzet, T., Laguna, J., and Vazquez, M. (1999). Etomoxir, sodium 2-[6-(4-chlorphenoxy)hexyl]oxirane-2-carboxylate, up-regulates uncoupling protein-3 mRNA levels in primary culture of rat adipocytes. *Biochem. Biophys. Res.Commun.* **263**, 87-93.

Cabrero, A., Alegret, M., Sanchez, R., Adzet, T., Laguna, J., and Vazquez, M. (2001). Uncoupling protein-3 mRNA up-regulation in C2C12 myotubes after etomoxir treatment. *Biochim. Biophys. Acta.* **1532**, 195-202.

Carter, W., Narayanan, P., and Robinson, J. (1994). Intracellular hydrogen peroxide and superoxide anion detection in endothelial cells. *J. Leukoc. Biol.* **55**, 253-258.

Cominacini, L., Garbin, U., Pastorino, A., and et.al. (1994). Increased susceptibility of LDL to *in vitro* oxidation in patients with insulin dependent diabetes mellitus. *Diabetes Res.* **26**, 173-184.

Cory, A. H., Owen, T. C., Barltrop, J. A., and Cory, J. G. (1991). Use of an aqueous soluble tetrazolium/formazan assay for cell growth assays in culture. *Cancer Commun.* **3**, 207-212.

Dimitriadis, E., Griffin, M., Owens, D., Johnson, A., Collin, P., and Tomkin, G. (1995). Oxidation of low-density lipoprotein in NIDDM: its relationship to fatty acid composition. *Diabetologia* **38**, 1300-1306.

Djouadi, F., Brandt, J., Weinheimer, C., Leone, T., Gonzalez, F., and Kelly, D. (1999). The role of peroxisome proliferator-activated receptor alpha (PPARa) in the control of cardiac lipid metabolism. *Prostaglandins, leukotrienes and essential fatty acids* **60**, 339-342.

Du, X.-L., Edelstein, D., Rossetti, L., Fantus, I., Goldberg, H., Ziyadeh, F., Wu, J., and Brownlee, M. (2000). Hyperglycemia-induced mitochondrial superoxide overproduction activates the hexosamine pathway and induces plasminogen activator inhibitor-1 expression by increasing Sp1 glycosylation. *Procedings of the National Academy of Sciences, USA* **97**, 12222-26.

Duckers, H., Boehm, M., True, A., Yet, S.-F., San, H., and al, e. (2001). Heme oxygenase-1 protects against vascular constriction and proliferation. *Nat. Med.* **7**, 693-98.

Forman, B., Chen, J., and Evans, R. (1997). Hypolipidemic drugs, polyunsaturated fatty acids, and eicosanoids are ligands for peroxisome proliferator-activated receptors alpha and delta. *Procedings of the national academy of sciences* **94**, 4312-4317.

Friedberg, E. C., Walker, G. C., and Siede, W. (1995). *DNA Repair and Mutagenesis*. ASM Press, Washington, DC.

Hashimoto, S., Matsumoto, K., Gon, Y., and et.al. (1999). Thioredoxin negatively regulates p38 MAP kinase activation and IL-6 production by tumor necrosis factor-alpha. *Biochem. Biophys. Res.Commun.* **258**, 443-7.

Lemasters, J., and Sowers, A. (1979). Phosphate dependence and atractyloside inhibition of mitochondrial oxidative phosphorylation. The ADP-ATP carrier is rate-limiting. *J. Biol. Chem.* **254**, 1248-51.

Leonhardt, W., Hahnefeld, M., and Muller, G. (1996). Impact of concentrations of glycated hemoglobin, alpha-tocopherol, copper and manganese on oxidation of low-density lipoproteins in patients with type I diabetes, type II diabetes and control subjects. *Clin. Chim. Acta* **254**, 173-186.

Lewin, B. (2000). *Genes*. Oxford University Press, New York.

Lu, R., Nash, H., and Verdine, G. (1997). A mammalian DNA repair enzyme that excises oxidatively damaged guanines maps to a locus frequently lost in lung cancer. *Curr. Biol.* **7**, 397-407.

Marshall, N., Goodwin, C., and Holt, S. (1995). A critical assessment of the use of microculture tetrazolium assays to measure cell growth and function. *Growth Regul.* **5**, 69-84.

Martin, J., and White, I. (1991). Fluorimetric determination of oxidized and reduced glutathione in cells and tissues by high-performance liquid chromatography following derivatization with dansyl chloride. *J. Chromatogr.* **568**, 219-225.

Morel, Y., De Waziers, I., and Barouki, R. (2000). A repressive cross-regulation between catalytic and promoter activites of the CYP1A1 and CYP2E1 genes: Role of H2O2. *Mol. Pharmacol.* **57**, 1158-1164.

Morel, Y., Mermod, N., and Barouki, R. (1999). An autoregulatory loop controlling CYP1A1 gene expression: Role of H2O2 and NFI. *Mol. Cell. Biol.* **19**, 6825-6832.

Morgan, K., Ni, H., Brown, R., Yoon, L., Qualls, C., Crosby, L., Reynolds, R., Gaskill, B., Anderson, S., Kepler, T., Brainard, T., Liv, N., Easton, M., Merrill, C., Creech, D., Sprenger, D., Conner, G., Johnson, P., Fox, T., Tyler, R., Sartor, M., Richard, E., Kuruvilla, S., Casey, W., and Benavides, G. (2002). Mechanism of action combined with cDNA microarray technology to select genes for a real time RT-PCR-based screen for oxidative stress in HepG2 cells. *Toxicol. Pathol.* **30**, 435-451.

Ogura, M., and Kitamura, M. (1998). Oxidant stress incites spreading of macrophages via extracellular signal-regulated kinases and p38 mitogen-activated protein kinase. *J. Immun.* **161**, 3569-74.

Portilla, D., Dai, G., Peters, J., Gonzalez, F., Crew, M., and Proia, A. (2000). Etomoxir-induced PPARa-modulated enzymes protect during acute renal failure. *Am. J. Physiol.* **278**, F667-F675.

Rosen, P., Nawroth, P., King, G., Moller, W., Tritschler, H.-J., and Packer, L. (2001). The role of oxidative stress in the onset and progression of diabetes and its complications: a summary of the a Congress Series sponsored by UNESCO-MCBN, the American Diabetes Association and the German Diabetes Association. *Diabetes Metab. Res. Rev.* **17**, 189-212.

Rothe, G., and Valet, G. (1990). Flow cytometric analysis of respiratory burst activity in phagocytes with hydroethidine and 2',7'-dichlorofluorescin. *J. Leukoc. Biol.* **47**, 440-8.

Rupp, H., Elimban, V., and Dhalla, N. (1992). Modification of subcellualr organelles in pressure-overloaded heart by etomoxir, a carnitine palmitoyltransferase I inhibitor. *FASEB J.* **6**, 2349-53.

Rupp, H., and Jacob, R. (1992). Metabolically-modulated growth and phenotype of the rat heart. *Eur. Heart J.* **13**, 56-61.

Schoen, F., and Cotran, R., eds. (1999). *Atherosclerosis*. W.B. Saunders Co., Philadelphia, PA.

Shrago, E., Woldegiorgis, G., Ruoho, A., and DiRusso, C. (1995). Fatty acyl CoA esters as regulators of cell metabolism. *Prostaglandins Leukot. Essent. Fatty* **52**, 163-166.

Srinivasan, K., Pugalendi, K., Sambandam, G., Rao, M., and Menon, P. (1997). Diabetes mellitus, lipid peroxidation and antioxidant status in rural patients. *Clin. Chim. Acta* **259**, 183-186.

Vetter, R., Kott, M., and Rupp, H. (1995). Differential influences of carnitine palmitoyltransferase-1 inhibition and hyperthyroidism on cardiac growth and sarcoplasmic reticulum phosphorylation. *Eur. Heart J.* **16**, 15-19.

Walsh, A. C., Michaud, S. G., Malossi, J. A., and Lawrence, D. A. (1995). Glutathione depletion in human T lymphocytes: analysis of activation-associated gene expression and the stress response. *Toxicology and Applied Pharmacology* **133**, 249-261.

Wolf, H. (1992). Possible new therapeutic approach to diabetes mellitus by inhibition of carnitine palmitoyltransferase 1 (CPT1). *Hormone & metabolic research supplement* **26**, 62-67.

Wolf, H. P. O. (1990). Aryl-substituted 2-oxirane Carboxylic Acids: A New Group of Antidiabetic Drugs. In *New Antidiabetic Drugs* (C. Baily and P. Flatt, eds.), pp. 217-229. Smith-Gordon, London.

Yotsumoto, T., Naitoh, T., Kitahara, M., and Tzuruzoe, N. (2000). Effects of carnitine palmitoyltransferase I inhibitors on hepatic hypertrophy. *Eur. J. Pharmacol.* **398**, 297-302.

24 h HepG2	Control Mean ± SD	1 mM Etomoxir Mean ± SD	p-value
Cell count	972 ± 29.4	639 ± 37.5	3.22E-04
Mitotic index (mitotic figures/ 1000 cells)	21.6 ± 2.2	0 ± 0.0	1.73E-07
Apoptotic/ necrotic index (per 1000 cells)	3.4 ± 0.7	41.7 ± 3.6	8.56E-06

Table 1.1: HepG2 Cell Counts, Mitotic Index, Apoptotic/Necrotic Index, after 24 h of 1 mM ET Treatment.

Redox and related genes	**MicroArray (Fold change)**	**p-value**	**TaqMan™ (Fold change)**	**p-value**
HO1	**+2.19**	**<0.0001**	**+1.5**	**<0.038**
GSR	**+1.61**	**<0.0128**	**+1.3**	**<0.0214**
SOD2	**+1.62**	**<0.0048**		
OGG1	**+1.61**	**<0.0155**		
CYP1A1	**-2.24**	**<0.0002**	**-9.6**	**<<0.0001**
TOP2A	**-1.12**	**0.5**	**-1.6**	**<0.0134**
GCLM			**+3.4**	**<0.0018**
TXNRD1			**+2.7**	**<0.0019**
Cell cycle/ Apoptosis				
GADD153	**+26.9**	**<<<0.0001**		
GADD45	**+2.59**	**<<0.0001**		
CDKN1	**+2.74**	**<<0.0001**	**+2.6**	**<<0.0001**
MDM2	**+2.69**	**<<0.0001**		
ubiquitin	**+2.25**	**<<0.0001**		
ubiquitin protein ligase	**+1.65**	**<0.0086**		
PCNA	**-2.34**	**<<0.0001**		
ERK1	**-1.95**	**<0.0004**		
MAP kinase p38	**-1.64**	**<0.009**		
Heat shock				
HSP40 homolog	**+4.76**	**<<<0.0001**		
HSP1A1	**+1.58**	**<0.0043**		
DNA synthesis & repair				
XP gp D complementing protein	**+2.2**	**<0.0001**		
RAD23A	**+1.99**	**<<0.0001**		
PPAR				
PPAR α	**-1.56**	**<0.0337**		

Table 1.2: 6 h, 1 mM ET-induced mRNA expression (ratio treated/control)

Figure 1.1: Morphologic changes in control vs 1 mM ET-treated HepG2 cells at 6 h**: (A)** Control HepG2 cells are large, polygonal cells with numerous variably-sized clear vacuoles, mitotic figures and few apoptotic bodies. **(B)** 1mM etomoxir-treated HepG2 cells have a loss of cytoplasmic vacuoles, cell shrinkage and rounding-up, marked decrease in mitotic figures and increased numbers of apoptotic bodies (arrow). H&E 400X.

Figure 1.2: Gene expression changes identified by microarray platform are confirmed by RT-PCR. mRNA isolated from HepG2 cells treated with 1mM ET for 6 h are quantitated both by RT-PCR and microarray platforms. Results are expressed as a ratio of treated/control. Note the good correlation between the two methods. This pattern is indicative of oxidative stress in HepG2 cells (Morgan *et al.*, 2002). Microarray data are NLR-normalized means of 3 separate hybridizations and RT-PCR data are means of 3 separate experiments. All changes are statistically significant except the TOP2A microarray value.

Figure 1.3: RT-PCR analysis of 7 stress genes in timecourse study demonstrate dynamic nature of mRNA expression secondary to toxic insult and confirm microarray 6 h data. Gene expression of HepG2 cells dosed with 1 mM ET are compared to time-matched controls (n=3/timepoint) at 11 separate time points. (A) *TOP2A, HO1, CDKN1, GCLM, GSR, and TXNRD1* and (B) *CYP1A1* .

Figure 1.4: Depletion of GSH, decrease in GSH:GSSG ratio and increase in GSSG are observed with ET treatment of HepG2 cells. Both time and dose enhance these effects. Data are means of 3 separate experiments.

Figure 1.5: 0.5 mM ET for 6 h causes a marked induction in superoxide radical generation as measured by the oxidation of hydroethidine to ethidium bromide with subsequent fluorescence (610 nm) on excitation (confocal microscopic image).

Figure 1.6: HepG2 cells administered a non-toxic dose of 0.5 mM ET exhibit an 84% reduction in ATP at 24 h. Data are the means of 5 separate experiments as measured by an ATP Bioluminescent Somatic Cell Assay Kit obtained from Sigma (St. Louis, MO). Data are the mean of 2 experiments.

Figure 1.7: ET-treated HepG2 cells exhibit a dose dependent reduction in mitochondrial membrane potential. 1 x 10^6 cells were incubated with 100 nM Mitotracker Red for 15 min at 37°C in the dark and then treated with ET (250, 500 and 1000 μM) for 1 h at 37°C. Samples were analyzed immediately by flow cytometry on a FACSCalibur (Becton-Dickinson, San Jose, CA). (n=2 replicates per concentration)

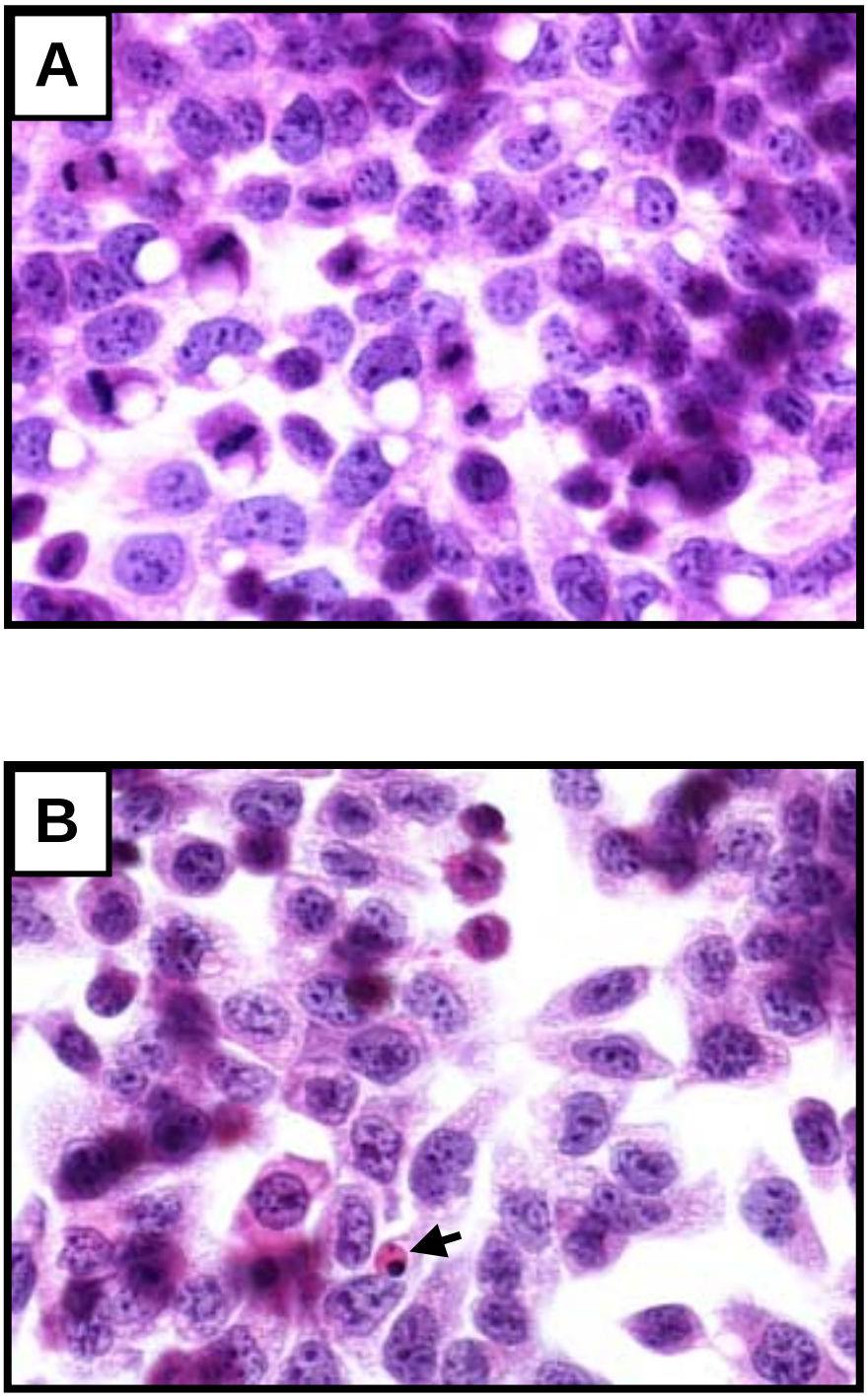

Figure 1.1:

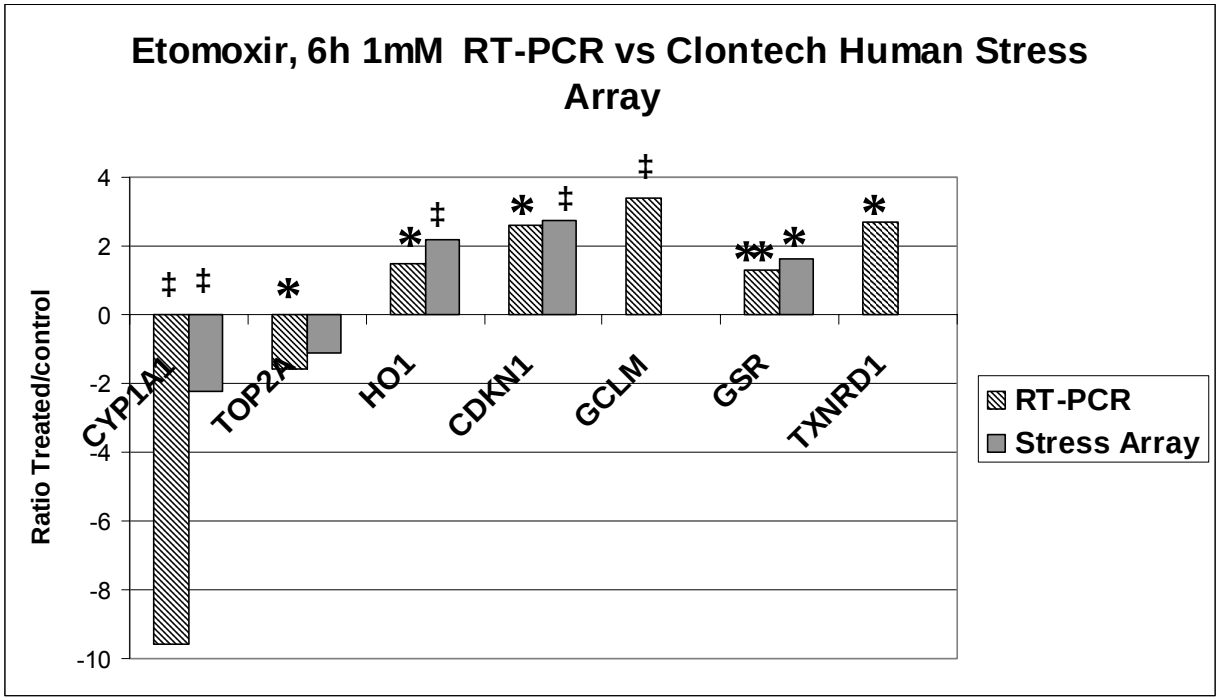

***** $p<0.05$ ****** $p<0.005$ ‡ $p<0.0005$

Figure 1.2:

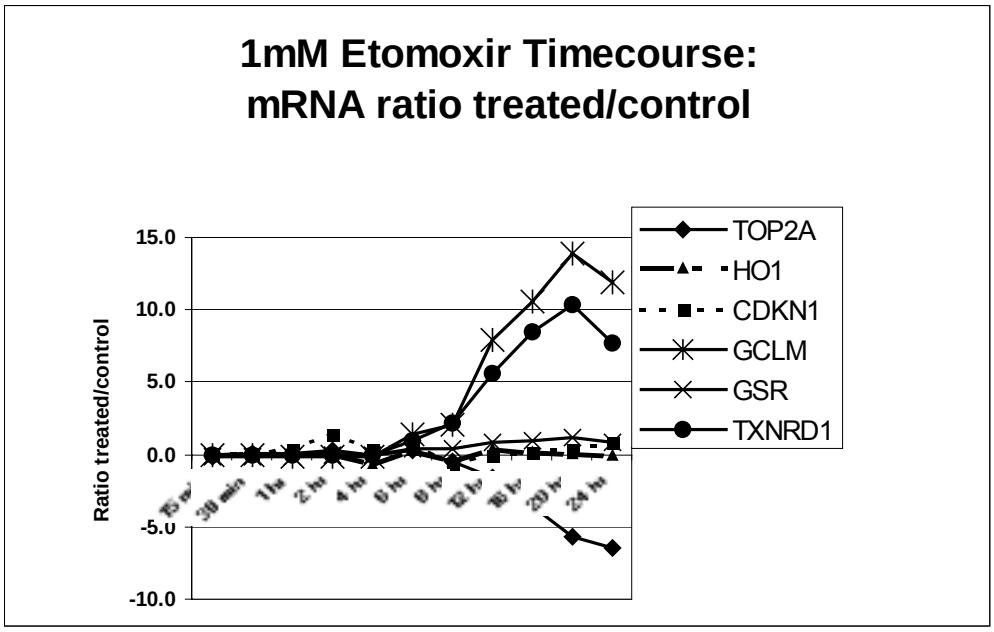

Figure 1.3: A.

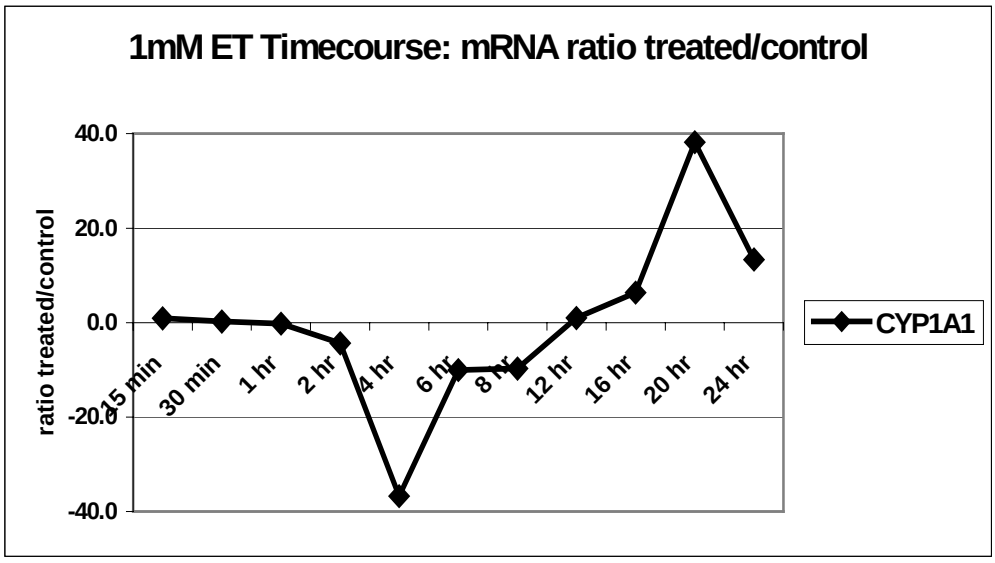

Figure 1.3: B.

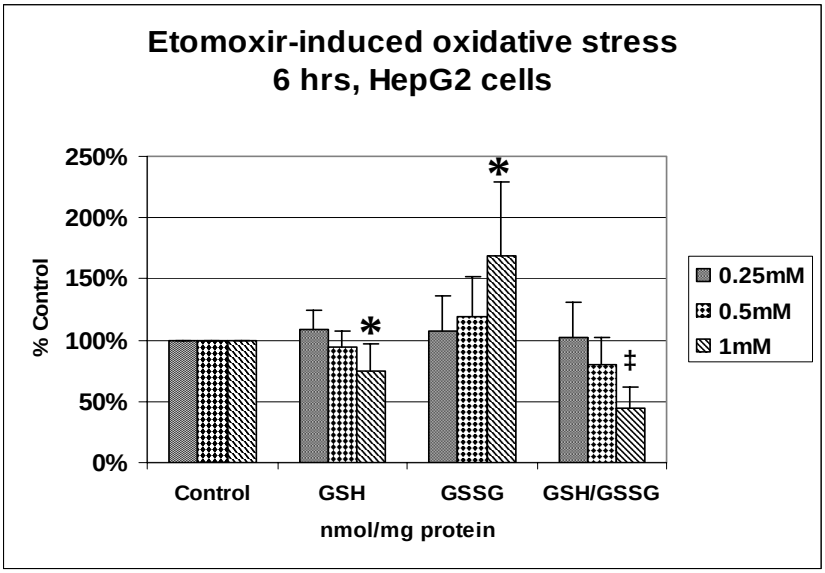

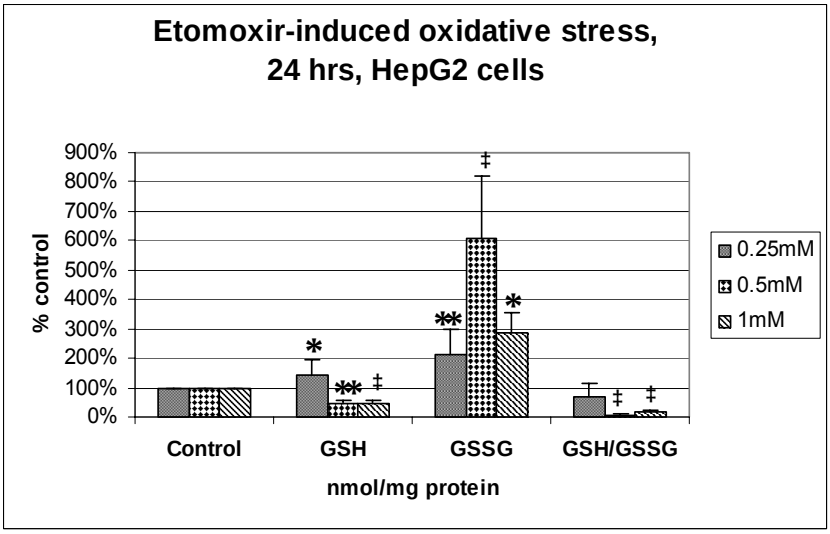

* $p<0.05$ ** $p<0.005$ ‡ $p<0.0005$

Figure 1.4:

Image A: Untreated HepG2 cells

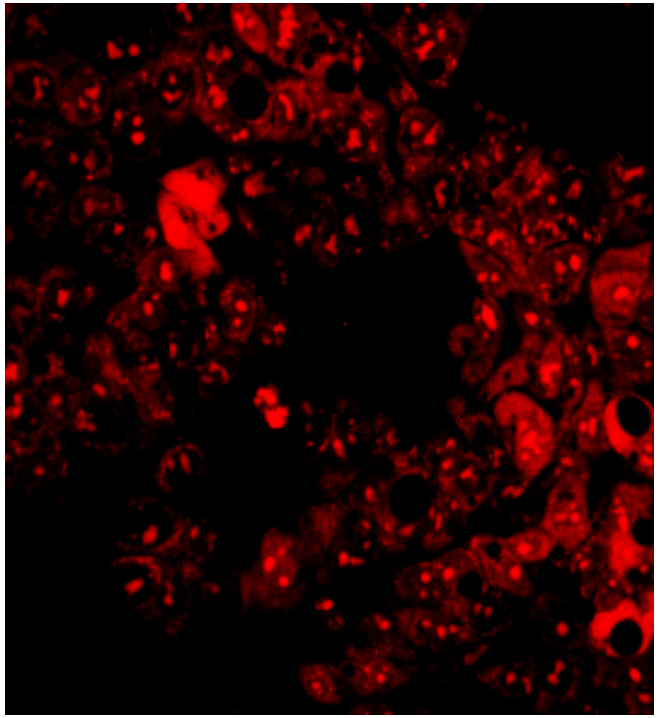

Image B: 0.5mM ET

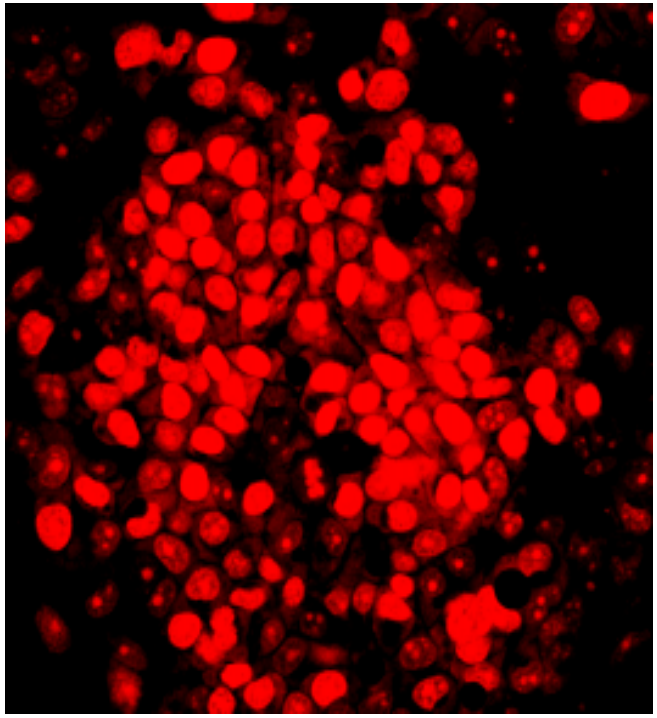

Figure 1.5:

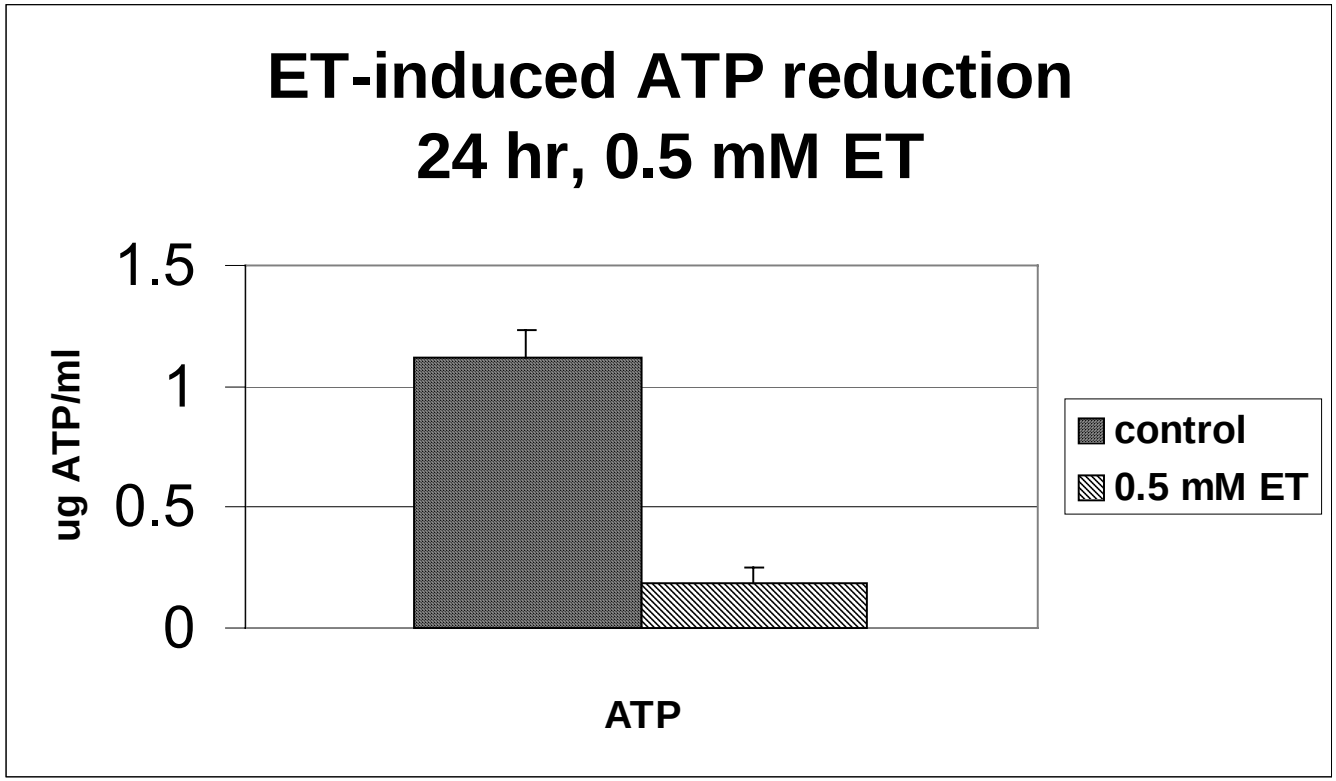
ET-induced ATP reduction
24 hr, 0.5 mM ET
1.5
1
0.5
0
ug ATP/ml
ATP
control
0.5 mM ET

Figure 1.6:

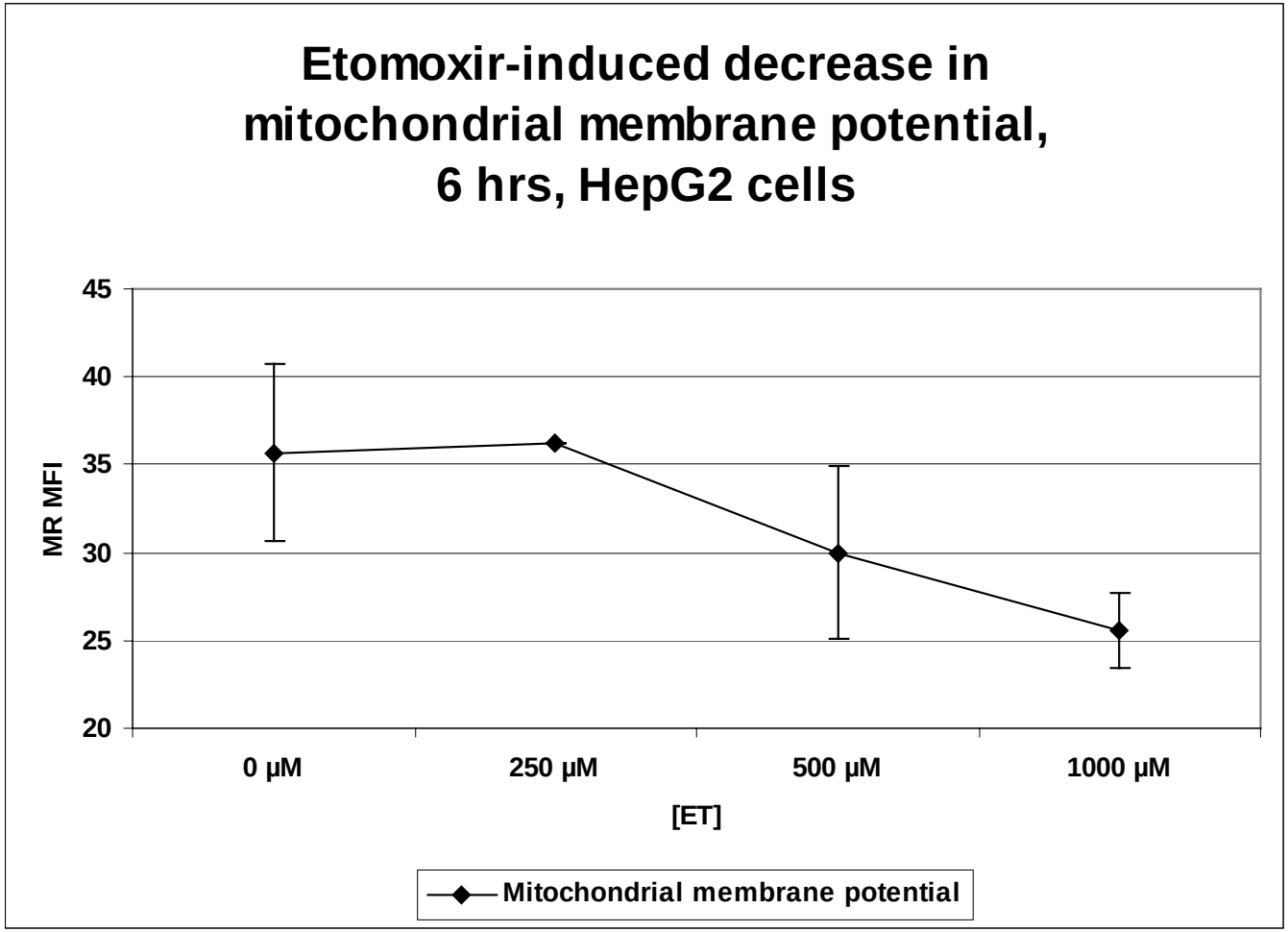
Etomoxir-induced decrease in mitochondrial membrane potential, 6 hrs, HepG2 cells
MR MFI
45
40
35
30
25
20
0 µM
250 µM
500 µM
1000 µM
[ET]
Mitochondrial membrane potential

Figure 1.7:

Manuscript II

Etomoxir-induced Hepatic Hypertrophy in the Rat is Associated with Early Alteration in Cell Proliferation Gene Profile

Christine L. Merrill [1], Hong Ni [2], Lawrence W. Yoon [2], Vicky Satterfield[2], Holly Jordan[1], Jeffrey Ambroso[1] and Kevin T. Morgan [3]

1. Safety Assessment, GlaxoSmithKline, RTP, NC 27709
2. Toxicogenomic Mechanisms US, GlaxoSmithKline, RTP, NC 27709
3. Department of Safety Evaluation, Aventis, Bridgewater, NJ 08807

Corresponding author:

Christine L. Merrill

Five Moore Drive

RTP, NC 27709

Christine.L..Merrill@gsk.com

Tel. 919-483-9336

Fax 919-315-8391

Abstract

Etomoxir (ET), a carnitine palmitoyltransferase -1 (CPT-1) inhibitor, causes hypertrophy of the liver via an undetermined pathogenic mechanism. This compound is a member of the 2-substituted oxirane carboxylate family, which irreversibly binds the ligand-binding domain of CPT-1 and inhibits the entry of long-chain fatty acids into mitochondria. It is well established that ET activates the peroxisome proliferator activated receptor-alpha (PPARα) and that PPARα activation can cause both oxidative stress and dysregulation of the cell cycle control gene program. To better understand the mechanisms associated with ET-induced hepatic hypertrophy, temporal alterations in hepatocyte gene expression, histopathology, clinical chemistry and hematology, and electron microscopy were examined to elucidate the potential role of cell growth dysregulation and/or oxidative stress. Han Wistar rats were dosed with 6, 12 or 25 mg/kg ET daily for 1, 10, 42 and 84 days. On study Day 2 (the first day of dosing is designated as Day 1), a marked, dose-responsive mitogenic response was observed in hepatocytes. This response was characterized by increases in mitotic figures of approximately 3.5-fold, 27-fold, and 38-fold, respectively, for the 6, 12, and 25 mg/kg/day dose groups ($p<0.05$). Cell proliferation/growth-related gene expression changes predominated at Day 2, including up-regulation of growth inducing genes CDC20, CDK2B, IGF1R, GHRH and GHRHR, and down regulation of growth inhibiting genes CDKN1A, WEE1, TGFB1, GMFB and GADD45. Mean liver weight transiently increased 25% above time-matched controls by Day 43 and returned to control liver weights at Day 85. Along with the

hepatic hypertrophy, there was a concurrent increase in PPARα mRNA, peroxisome proliferation, and transitory normalization of previously decreased serum triglycerides. A gene expression profile suggestive of oxidative stress was not observed in livers of ET-dosed rats at any dose or time point examined. A transient increase in lipid synthesis gene expression was present concurrent with the hepatic hypertrophy. In summary, ET induced a strong mitogenic response that was consistent with that generated by other peroxisome proliferators, in the livers of rats 24 h after administration of one 25 mg/kg dose. This finding was coincident with a predominance of cell proliferation/growth-related gene expression alterations. Oxidative stress genes were down regulated; suggesting that this is not a viable etiologic mechanism for induction of ET-induced hepatic hypertrophy. PPARα appears to play a role in ET-induced hepatic hypertrophy, as shown by the early cell proliferation followed by increased level of PPARA mRNA, peroxisome proliferation and increase of some PPARα-related genes.

Introduction

Etomoxir is a member of a family of substituted 2-oxirane-carboxylic acids that inhibit mitochondrial long-chain fatty acid β-oxidation (FAO), ketogenesis and gluconeogenesis (Wolf 1992). Once converted to its CoA ester, etomoxir irreversibly binds to the CPT-1 catalytic site and prevents long chain fatty acids from entering mitochondria. Along with this inhibition of FAO, etomoxir causes a shift in energy substrate utilization from fatty acids to glucose, leading to systemic hypoglycemia, hypoketonemia, and hypotriglyceridemia (Wolf 1992).

These effects make etomoxir potentially useful in the treatment of non-insulin-dependent diabetes mellitus (NIDDM). However, the compound has been shown to induce cardiac and hepatic hypertrophy in rodents and therefore has not been fully developed as an antidiabetic agent to date (Rupp and Jacob 1992; Vetter *et al.* 1995; Yotsumoto *et al.* 2000). The mechanism(s) of the respective hypertrophies have not yet been worked out, but are shown to be different from those involved in hyperthyroidism and hypertension (Rupp and Jacob 1992; Vetter *et al.* 1995).

CPT1 inhibitors, including ET, have been reported to be PPARα-agonists (Forman *et al.* 1997; Intrasuksri *et al.* 1998; Kaikaus *et al.* 1993; Portilla *et al.* 2000; Skorin *et al.* 1992) and to cause hepatomegaly. PPARα-agonists are known to cause hepatomegaly and peroxisome proliferation (Belury *et al.* 1998; Cattley and Roberts 2000). No direct link has yet been established to show that ET-induced PPARα activation is involved in the previously observed hepatomegaly. Djouadi, et al. (1998) examined the effect of ET (50 mg/kg for 5 days) on PPARα knockout mice, and found that individual hepatocytes accumulated large quantities of lipid, but no mention was made regarding the presence or absence of hepatic hypertrophy.

Peroxisome proliferators are associated with changes in both lipid metabolism and cell proliferation genes, and they can generate oxidative stress (Gonzalez *et al.* 1998). (N.B. Cell proliferation is defined in this manuscript as multiplication of

cells and growth is defined as an increase in tissue or organ volume or weight secondary to increased cell number and/or cell volume). In a previous study, Merrill et al. (2002) showed that ET induced oxidative stress and cytotoxicity in a human hepatocyte cell line (HepG2 cells). The etiology of the ET-induced oxidative stress was not known. PPARα-induced peroxisome proliferation and increased peroxisomal fatty acid oxidation have been reported to cause oxidative stress in hepatocytes secondary to increased generation of H_2O_2 and insufficient catalase production (Conway *et al.* 1989; Reddy and Rao 1989). More recently, Rose et al. (1999) showed that Wy-14,643-treated Kupffer cells overproduced superoxide via a protein kinase C pathway. Superoxide is associated with activation of NFκB and TNFα, which play a role in increased cell proliferation.

The purpose of this study was to better understand the mechanisms involved in the development of hepatic hypertrophy in the ET-treated rat. ET induced acute hepatocellular mitogenesis associated with significant changes in cell proliferation/growth gene expression. A transient increase in lipid synthesis gene expression was present concurrent with the hepatic hypertrophy. PPARα appears to play a role in ET-induced hepatic hypertrophy, as shown by the increased level of PPARA mRNA, peroxisome proliferation and increase of some PPARα-related genes.

Materials and Methods

Animals

Male Han Wistar rats were obtained from Charles River Laboratories (Raleigh, NC) at approximately 8 weeks of age, acclimated for at least 7 days prior to initiation of the study. Reverse osmosis-treated water and commercially available rodent diet were provided ad libitum. Rats were kept 3 to a cage in polycarbonate, solid bottom cages with Bed-O'Cobs^{R} bedding (The Andersons, Maumee, OH). Room temperature was maintained between 64-79°F, relative humidity was 30-70% and lighting was fluorescent with 12-hour light/dark cycle. The Institutional Animal Care and Use Committee of GlaxoSmithKline approved all conditions and animal use.

Chemicals

Etomoxir (racemate, sodium salt) was obtained from Research Pharmaceuticals, Allensbach, Germany.

Experimental Design

Etomoxir was diluted to 10mg/ml in reverse osmosis treated water to make a stock solution which was stable for 8 days at 4°C. The control group (Group 1), was dosed with reverse osmosis treated water. ET-treated groups were designated as Groups 2, 3 and 4 and were administered 6 mg/kg, 12 mg/kg and 25 mg/kg, respectively, once daily. The route of administration was oral gavage at 10ml/kg and was performed between 7:00am and 9:00am each morning.

There were four dose durations: 1, 10, 42 and 84 days (referred to as Day 2, Day 11, Day 43 and Day 85). At each time point, 4 rats per dose group were anesthetized with isofluorane, weighed and the caudal vena cava was surgically exposed. Blood samples were collected from the caudal vena cava for clinical chemistry and hematology analysis. After exsanguination via the caudal vena cava, a thorough macroscopic examination was conducted and the following tissues were collected in 10% buffered formalin for histopathological examination: adrenal glands, brown and white adipose tissue, brain, heart, kidneys, liver, lungs, pancreas, pituitary gland, skeletal muscle (gastrocnemius and soleus, representing glycolytic and oxidative muscles, respectively), and thyroid gland. Organ weights were recorded for the brain and liver. Liver samples from the left lateral lobe were collected, flash frozen for gene expression analysis and were collected in Trumps fixative for electron microscopy.

Clinical Chemistry and Hematology

Hematology parameters measured/calculated included hematocrit, hemoglobin, red blood cell (RBC) count, mean RBC volume, mean RBC hemoglobin, mean RBC hemoglobin concentration, white blood cell (WBC) count, differential WBC count and percent for neutrophils, lymphocytes, monocytes, eosinophils, and basophils; platelet count, RBC distribution width, reticulocyte count and percent. Hematology assays were performed on an Advia 120 hematology analyzer. Clinical chemistry parameters measured/calculated included alanine aminotransferase, albumin, albumin/globulin ratio, alkaline phosphatase,

aspartate aminotransferase, blood urea nitrogen, total bilirubin, calcium, cholesterol, chloride, creatine kinase, creatinine, globulin, glucose, hemolysis, insulin, lactate, lactate dehydrogenase, non-esterified fatty acids, phosphorus, potassium, sodium, total protein, and triglycerides (TG). Chemistry assays were performed on a Roche/Hitachi 911 analyzer.

Histopathology

Tissues, listed in study design section above, were fixed in 10% phosphate-buffered formalin (pH 7.4), dehydrated in ethanol and embedded in paraffin using standard procedures. Sections, 5 μM thick, were cut and stained with hematoxylin and eosin. Additional kidney sections from some rats were stained using Ziehl-Neelson and Oil Red O methods for identification of early lipofuscin and lipid, and Schmorl's method for late lipofuscin. Mitotic figures present in right lateral and left median liver lobe sections were counted, total liver area was measured using Image Pro Plus 4.1 software, and mitotic counts were expressed as number of mitotic figures per 100mm^2 liver area.

Electron Microscopy

Liver tissue samples were immediately immersed in cold Trump's fixative and cut into pieces no more than 1 mm^3. Routine methods, as previously described (Dykstra 1993), for preparation of tissue for, and performance of electron microscopy were followed.

mRNA Expression Analysis

Liver samples, previously flash frozen and maintained at -80°C, were lysed with Trizol™ Reagent (Invitrogen, Carlsbad, CA). Total RNA was isolated by a chloroform/isopropanol/ethanol extraction and RNA quality and quantity were assessed using agarose gel electrophoresis and spectrophotometric 260/280 nm absorbance. RNA within each group was pooled and was then prepared for gene expression analysis by Clontech™ Atlas Rat 1.2 cDNA Array (1176 genes, Palo Alto, CA), Affymetrix™ Rat Genome U34A GeneChip protocol or RT-PCR.

Clontech™: ^{33}P-labelled cDNA probes were prepared using a modification of the Clontech™ protocol and hybridized to Clontech Atlas™ Rat 1.2 cDNA Array. Denaturation (4 µl) was carried out at 70°C for 10 min using 6 µg total mRNA and 1 µl CDS Atlas™ specific primers (0.2 µM each). The annealing and extension reactions (22 µl, 35 min at 49°C) contained 0.5 mM each dCTP, dGTP, dTTP, 50 mM Tris-HCl pH 8.3, 75 mM KCl, 3 mM $MgCl_2$, 4.5 mM, 100µCi ^{33}P-α-dATP (10 mCi/ml, >2500 Ci/mM, Amersham) and 200 units Super Script II™ reverse transcriptase (Gibco-BRL, MD). Extension was terminated by heating to 94°C for 5 min. Unincorporated ^{33}P-α-dATP was removed using G-50 MicroSpin columns (Pharmacia Biotech, NJ). Hybridization was carried out at 64°C for 16 h, in 6.5 ml MicroHybe™, 3.25 µl poly-dA (1 µg/µl, Research Genetics, AL) and 6.5 µl Human Cot-1 DNA (1 µg/µl, Clontech™, CA) and heat denatured ^{33}P-cDNA . Arrays were washed at 64°C following manufacturer's instructions. Phosphor imaging screens were exposed to the arrays for 24-48 h and the

optical density was acquired using OptiQuant software and a Cyclone scanner (Packard BioScience Co, CT). Image files generated from phosphorimager scans were analyzed using Clontech™ AtlasImage Software™.

Affymetrix™: Total RNA was purified using a silica gel-based membrane (Qiagen, Valencia, CA), and samples were hybridized to Rat Genome U34A GeneChip (Affymetrix™, Santa Clara, CA) high-density oligonucleotide arrays as previously described (Lockhart *et al.* 1996; Wodicka *et al.* 1997) using the antibody amplification staining protocol. For each time point, 10 μg of total RNA was used as starting material. Primary image analysis of the arrays was performed using the Genechip 5 software package (Affymetrix™) and images were scaled to an average hybridization intensity of 150.

RT-PCR (TaqMan™): Unpooled total RNA was DNAase-treated (Ambion DNAase I) according to the manufacturer's protocol. RNA was quantified using the Molecular Probes Ribogreen™ assay and a Cytofluor 2350 fluorometer. Samples were diluted to 10 ng/μL prior to Taqman™ analysis (Perkin Elmer ABI Prism 7700 Sequence Detection system). Cell proliferation/growth-related genes were selected for RT-PCR analysis because of: 1) good agreement between the Clontech™ and Affymetrix™ platforms (cell division cycle 20 homolog (*CDC20*, *synonym* p55cdc), early growth response 1 (*EGR1*), tumor necrosis factor alpha (*TNFA*), wee1 (*WEE1*), cyclin dependent kinase inhibitor 1 (*CDKN1A*, *synonyms* p21 and waf1), insulin-like growth factor 1 receptor (*IGF1R*) and growth arrest and DNA-inducible gene 45 (*GADD45*)); or 2) large positive or negative changes

in mRNA expression relative to the control (glia maturation factor beta (*GMFB*), insulin-like growth factor binding protein 1 (*IGFBP1*), and nuclear receptor subfamily 1, group D, member 1 (*NR1D1*, *synonyms* Rev-ErbA-alpha and thyroid hormone receptor)). A 7-gene plate, described by Morgan et al.*(2002)*, was used to quantitate the mRNA expression of the following oxidative stress genes in Group 1 and 4 rats at all four time points*:* heme oxygenase 1 *(HO1),* cytochrome P450 1A1 *(CYP1A1)*, topoisomerase IIα *(TOP2A)*, cyclin-dependent kinase inhibitor 1A *(CDKN1A* $p21^{waf1}$*]),* glutathione reductase *(GSR),* γ-glutamate-cysteine ligase modifier subunit *(GCLM*) and thioredoxin reductase *(TXNRD1).* PPARα mRNA concentration in Day 2 rats, Groups 1 and 4 was also examined. Primers were designed with Perkin Elmer Primer Express™ software. Forward and reverse primers and probes were diluted to the appropriate concentrations to make the probe/primer master mix. The master mix was prepared according to the manufacturer's protocol (without probes and primers) and 30 µL of master mix, 5 µL of RNA and 15 µL of probe/primer mix were aliquotted per well. The plate was sealed with Optical Adhesive Covers (PE Biosystems™), centrifuged at 3000xg for 10 secs and the reaction was incubated at 48°C for 30 min (reverse transcriptase (RT) step), denatured at 95°C for 10 min (Amplitaq activation and RT denaturation), and then subjected to 40 PCR cycles of 94°C for 15 sec and 60°C for 1 min. Values of fold change in expression were graphed for comparison purposes. Statistical significance was determined for control *versus* treated groups using a t-test (two-tailed, pooled, assuming normal distribution and variances equal) and significance selected at $p<0.05$.

Results

Clinical Pathology

With the exception of TG and lactate dehydrogenase, clinical chemistry values for untreated control rats at all time points examined exhibited small standard deviations and means fell within clinically normal ranges. TG values from control rats showed significant variability with the means ranging from 128 to 193 mg/dl, mean 157 mg/dl and standard deviation 49 mg/dl. Lactate dehydrogenase values were also variable, ranging from 282 – 516 U/L, mean 432 U/L and standard deviation 142 U/L.

Serum triglycerides from ET-treated rats exhibited an oscillating pattern over the duration of the study across all dose groups (Figure 2.1). For example, TG in the 25 mg/kg dose group decreased to 70% ($p=0.13$) and 39% ($p=0.01$) of time-matched control values at Day 2 and Day 11, respectively. However, at Day 43 TG rebounded to 94% ($p=0.63$), followed by decreases to 57% ($p=0.07$) and 47% ($p=0.11$) of controls at Days 51 and 85. Utilizing ANOVA, TG levels at each study time point, except Day 43, were significantly lower than that of respective controls ($p<0.1$). Serum glucose concentrations decreased slightly (10%) but significantly ($p<0.1$) below controls at Days 43 and 85 only in the 25 mg/kg dose groups. Chloride levels in treated animals were slightly elevated at days 11 through 85. Creatinine concentrations were slightly decreased and phosphorus levels were slightly increased in most treated animals at most time points. These

trends were of small magnitude and were not consistently dose-dependent. Other changes in mean chemistry values were not considered significant because they were limited to one time point; were of small magnitude; or were confounded by inter-animal variation. No toxicologically significant treatment-related effects were observed in the hematologic profile.

Organ Weights/Body Weight

Control rats ranged from 250-300 grams in body weight upon entry into this study and they gained a mean 53% in total body weight over the duration of the 12 week period. Mean body weights did not change significantly from the time-matched controls. The largest body weight difference was observed at Day 43 in Group 4 with a 12% increase in body weight relative to time-matched controls. ET-treated, Day 43 liver weights (both absolute weights and as a ratio to brain weight) were significantly increased above time-matched controls at the 12 and 25 mg/kg doses (11% and 25%, respectively, $p<0.05$). The liver weights at Days 2, 11 and 85 were not significantly different from the controls.

Gross Observations/Histopathology

There were no significant external or internal gross lesions observed in the control or treated rats. All rats were in good body condition and had smooth, shiny hair coats. The most significant microscopic finding in the ET-treated rats was a large, dose-dependent increase in mitotic figures (hepatocellular proliferation) observed on Day 2 after a single dose of ET (Figures 2.2 and 2.3).

The number of mitotic figures counted in the liver sections increased significantly by approximately 3.5-fold, 27-fold, and 38-fold, respectively, for the 6, 12, and 25 mg/kg/day dose groups ($p<0.05$). A concurrent increase in apoptosis in the liver was not observed by microscopic examination of H&E stained sections. Intracytoplasmic golden-brown pigment, present in tubular epithelial cells of the cortex and corticomedullary junction in Groups 3 and 4 rats at Day 85, failed to stain with Ziehl-Neelson, Schmorl's, and oil red O stains (early and late lipofuscin and lipid, respectively). A low incidence of multifocal aggregates of foamy macrophages were observed in the alveolar air sacs of the lungs of Day 43-25 mg/kg rats, and Day 85- 6, 12, and 25 mg/kg rats. No significant, treatment-related microscopic lesions were observed in adrenal glands, brown and white adipose tissue, brain, heart, pancreas, skeletal muscle, pituitary gland and thyroid gland.

Electron Microscopy

Peroxisome counts were performed on electron micrographs of the liver (total magnification of 9750X). Peroxisomes in two randomly selected, ultrathin liver sections from Day 2 Control and Group 4 (25 mg/kg ET) rats were counted and there was no significant difference between control and treated values (mean Control peroxisomes 9.0+/-1.41, mean 25 mg/kg ET 6.5+/-2.12). At Day 43, peroxisomes were counted in 5 randomly selected, replicate areas of Control and Group 4 rat ultrathin liver sections. There was approximately a 2 fold, statistically significant increase in the number of peroxisomes (mean control peroxisomes

10.5+/-1.73, mean 25 mg/kg ET 19.5+/-3.87, $p < 0.005$). Intrahepatocytic lipid globules were mildly increased in number and size in Day 43, 25 mg/kg rats versus untreated controls. This increase in lipid was not detectable upon light microscopic examination. The quantity of smooth endoplasmic reticulum, lipid and glycogen present in ET-treated hepatocytes was not substantially different than that in time-matched controls. Electron microscopy was not performed on Day 11 and Day 85 liver samples.

mRNA Expression Analysis

Evaluation of hepatic gene expression changes before, during and after ET-induced hepatomegaly gives us a way to identify potential mechanisms/pathways that are altered by ET. However, the use of gene expression microarrays as a quantitative or even semi-quantitative tool in molecular biology is relatively new and requires additional steps to assure that the data is as accurate as possible. In the present study, two separate microarray platforms (Clontech™ Atlas Rat 1.2 cDNA Array and Affymetrix™ Rat GenomeU34A GeneChip) were used to allow comparison and contrast of the ET-induced gene expression changes. Selected genes were then confirmed by RT-PCR. Analysis of ET-induced gene expression alterations using the Affymetrix™ platform, showed that an average of 17% (approximately 1500/8800) of all genes on the Genechip were altered at least 2 fold up or down relative to the control intensities. Clontech™ exhibited a similar percentage of total gene expression alterations, with 14% (170/1187) of the total number of genes being significantly changed. mRNA samples used for

microarray/gene chip analysis were pooled within groups; therefore statistical analysis of the data was not possible. RT-PCR data was generated from mRNA from individual animals and statistical analysis was performed.

Cell Proliferation/growth-related Genes: Consistent with the large increase in hepatocellular mitotic figures observed in the 25 mg/kg dose group at Day 2, the expression of several proliferation/growth-related genes, as detected by Clontech™ Rat Atlas 1.2 and/or Affymetrix™ Rat Genome U34A GeneChip were significantly altered (Table 2.1, Figure 2.4). These genes can be subdivided into the following categories: growth regulatory, cell division control, carcinogenesis "gatekeeper"/tumor suppressor, apoptosis regulatory and signal transduction. ***Growth regulatory*** genes that were up regulated included: early growth response protein 1 (*EGR1*), transforming growth factor-beta 2 receptor (*TGFBR2*), insulin-like growth factor binding protein 1 (*IGFBP1*), insulin-like growth factor 1 receptor (*IGF1R*), nuclear receptor subfamily 1, group D, member 1 (*NR1D1*, *synonym* rev-erbA-alpha or thyroid hormone receptor 1-alpha), growth hormone releasing hormone (*GHRH*), and growth hormone releasing hormone receptor (*GHRHR*). Genes that were down regulated in the **growth regulatory** category included: tumor necrosis factor-alpha (TNFA), c-myc (MYC), glia maturation factor beta (GMFB), and transforming growth factor-alpha (TGFA). Some of the genes up regulated in ***cell division control*** included: cell division control protein 20 (*CDC20*, *synonym* p55cdc), cyclin dependent kinase-2 beta (*CDK2B*), and cyclin dependent kinase 1 (*CDK1*). Down regulated ***cell division control*** genes included cyclin E (CCNE), p21 (CDKN1A), wee-1

(WEE1), and cdc25B (CDC25B). The expression of a small number of ***carcinogenesis "gatekeeper"/tumor suppressor*** genes was altered; neurofibromatosis 2 (*NF2*) being up regulated and p53 (TP53), and growth arrest and DNA damage inducible gene 45 (GADD45) being down regulated. Plasminogen activator inhibitor 2 type A (*PAI2A*), an ***apoptosis-regulatory*** gene, was up regulated and GTPase activating protein (*GAP*), a ***signal transduction*** gene was also up regulated.

Ten genes were selected from the large list above to confirm with RT-PCR (Figure 2.5). Seven of the above-listed genes, CDC20, EGR1, GADD45, WEE1, CDKN1A, TNFA, andIGF1R, were chosen because of their importance as cell proliferation-related genes and for their agreement between Clontech™ and Affymetrix™. Four genes, GMFB, IGFBP1, NR1D1 and TNFA, were chosen for RT-PCR because of a large expression change observed in at least one microarray platform. None of the large expression changes noted in these 3 genes were present on RT-PCR. In fact, RT-PCR quantitated TNFA mRNA as virtually the same as the control, while GMFB and IGFBP1 were both changed in the same direction as that measured by Affymetrix™ but the fold change was much smaller.

By Day 11, a second set of cell division control/growth promoting genes (CCND1, HBEGF and CDK1) and growth-inhibitory genes (TGFB1) were invoked (Figure 2.6). If these mRNAs were actually translated into their respective proteins, the

effect was not observed until the next time point, as liver weights did not increase at Day 11. This Day 11 up-regulated gene set, when viewed over the first three time points of the study, tracked similarly with most genes unchanged at Day 2, up-regulated at Day 11, and decreased to control levels or lower at Day 43. Some of the genes that are down regulated at Day 11 inhibit cell growth or induce apoptosis (VHL and CASP7), with an end result of increasing overall cell numbers. In contrast, CCNB, VEGF3. CL-6 and FGFR1, are promoters of cell proliferation that are decreased at Day 11.

Results for Days 43 and 85 are summarized in Figures 2.7 and 2.8.

Oxidative Stress Genes: The RT-PCR (TaqMan™) plate, first reported by Morgan, et al., (2002) as useful for in vitro screening of compounds for oxidative stress, was employed to assess ET in the present in vivo study. The pattern most often observed in Morgan's report showed CYP1A1 and TOP2A down regulated and HO1, GSR, GCLM and TXNRD1 up regulated in response to oxidative stress. In the present study, this pattern of oxidative stress gene expression was not observed in livers of rats dosed with 25 mg/kg/day ET at any time point (Figure 2.9). CYP1A1 was consistently down regulated at Days 2, 11, 43 and 85 as measured by RT-PCR. However, HO1, GSR, GCLM and TXNRD1, genes that tend to be more directly associated with the redox state of the tissue, were either down regulated or not significantly changed.

PPARα-related Gene Expression: (Figure 2.10) PPARα mRNA level was transiently increased (+63%) relative to the time-matched controls only at Day 43. PPARα-target genes (Desvergne and Wahli 1999; Latruffe and Vamecq 1997) that were up regulated in the livers of the 25 mg/kg/day rats for the duration of the study included: CYP4A1, 3-ketoacyl-CoA thiolase (3KACT), and CPT-1 Liver (CPT1A) (Figure 2.6). Other PPARα-target genes, such as acyl-CoA oxidase (ACO), 3-hydroxymethyl-3-glutaryl CoA synthase (HMGCS), long chain acyl-CoA dehydrogenase (LCAD) and very long chain acyl-CoA dehydrogenase (VLCAD), were not differently expressed relative to time-matched controls throughout the duration of the study. A PPARα-responsive gene, cyclin D1 (CCND1) (Desvergne and Wahli 1999) exhibited an oscillating pattern of expression that was minimally decreased (-43%) below control values at Day 2, significantly increased (+313%) at Day 11, significantly decreased (-323%) at Day 43 and increased again (+51%) at Day 85.

Energy Metabolism Gene Expression: Table 2.2 summarizes the gene expression changes for energy metabolism as measured by the Affymetrix™ platform.

LIPID METABOLISM: In general, there was an increase in peroxisomal FAO gene expression as shown by the increase in 3KACT across all 4-time points and the increase of peroxisomal carnitine octanoyltransferase (COT) at Days 11 and 43. Cholesterol synthesis genes (HMGCR, OSC and SQLE) were down regulated for the first 10-43 days of ET-treatment. The expression of

mitochondrial and peroxisomal fatty acid dehydrogenase enzyme genes (MCAD, LCAD, AOX and VLCAD) was not significantly changed throughout the study. Fatty acid transport protein was down regulated at Day 2, returned to within normal limits for Days 11 and 43, and then was up regulated at Day 85. The expression of CPT1A was minimally increased at all 4 time points, peaking at Day 11. Fatty acid translocase (FAT, *synonym* CD36) was mildly increased at Day 11 and more substantially increased at Day 85. Hormone-responsive lipase (LIPE), which releases FA from adipose tissue, was slightly down-regulated at Day 11 and substantially increased at Day 85. Although hormone-responsive lipase protein is not known to be present in the liver, the down regulation of this gene product in the liver may represent changes present in adipose tissue. Data suggest a trend toward a decrease in saturated FAO early and an increase late in the study. There were changes observed in numerous lipid synthesis-associated genes. Malic enzyme, which provides reducing power for lipogensis and for steroyl-CoA desaturase 2 (SCD2) in the synthesis of unsaturated fatty acids, was unchanged until Days 43 and 85, when mRNA levels increased substantially (+11.5 and +3.5 fold, respectively). SCD2 mRNA expression was lower than controls on Days 2 and 11, higher than controls on Day 43 and significantly lower than controls by Day 85 (-28 fold).

GLUCOSE METABOLISM: Glucose metabolism genes, throughout the study, exhibited a complex and often discordant pattern of expression. There was agreement of gene expression early in the study to indicate increased glucose utilization. Increased expression of gycerol-3-phosphate dehydrogenase (GPD2),

hexokinase 2 (HKII) and pyruvate dehydrogenase kinase isoenzyme 4 (PDK4) suggests that glycolytic flux increased on Day 2. mRNA of enzymes which could convert pyruvate to lactate (lactate dehydrogenase) or to oxaloactetate for gluconeogenesis (pyruvate carboxylase), were not increased at Day 2. Serine pyruvate aminotransferase (SPAT), which converts alanine from the muscle to pyruvate in the liver, was up regulated early in the study. The Glucose-Alanine Cycle is a variant of the Cori Cycle with 2 advantages: 1) nitrogen is transported back to the liver along with the 3 carbon skeleton, and 2) it yields more energy in the glucose-utilizing tissue by sparing the NADH required to convert pyruvate to lactate (Moran and Scrimgeour 1994). Increased expression of SPAT suggests high glucose flux through the glycolytic pathway in muscle at Days 2 and 11, which is abrogated at Day 43 when levels decrease -3.55 fold below controls.

PLATFORM CONCORDANCE: Oxidative stress gene data (described above) derived from Clontech™, RT-PCR and Affymetrix™ were compared (Figure 2.9). In the present study, there was a 35% concurrence (7 of 20) of all three platforms (RT-PCR, Affymetrix™ and Clontech™ microarrays) for these 7 genes. There was a 57% agreement (16 of 28) between RT-PCR and Affymetrix™, a 50% agreement between RT-PCR and Clontech™ (10 of 20), and a 60% agreement between Affymetrix™ and Clontech™ (12 of 20).

DISCUSSION

The purpose of this study was to better understand the mechanisms involved in the development of hepatic hypertrophy in the ET-treated rat. To this end, the temporal alterations in biochemical parameters, microscopic lesions and gene expression profiles associated with the development of hepatic hypertrophy in the ET-treated rat were investigated.

The most striking finding was the marked, dose-dependent increase in the number of hepatocellular mitotic figures after only one day of ET administration. This rapid increase in hepatocellular proliferation is consistent with the liver effects observed in PPARα-treated rats (Eacho *et al.* 1991; Reddy *et al.* 1979), and has not been previously reported in the ET literature to date. The increased mitotic rate and apparent lack of increase in apoptosis present at Day 2, are consistent with the statistically significant increase in liver weights observed at Day 43. It is difficult to explain why liver weights at Day 11 are not increased after the Day 2 hepatocellular proliferation. The prototype PPARα-agonist causes hepatomegaly in rats within the first several days of dosing. ET-treated rats exhibited the early hepatic mitogenic response typical of PPARα-agonists, but a significant amount of time elapsed prior to development of increased liver weights as compared with other PPARα-agonists. It is possible that the early hepatocellular replication was followed by slow growth of individual daughter cells, leading to the Day 43 hepatomegaly without significant increase in liver weights at Day 11.

Gene expression in Day 2 livers was evaluated in order to gain understanding of the pathways/mechanisms involved in the ET-induced mitogenesis. The majority of growth regulatory genes that were up regulated are involved in the inhibition of cell division, and most of those genes that were down regulated are involved in promotion of cell division. This makes sense when viewed in context of the liver morphology on Day 2. Cells were already dividing at a rapid rate; therefore the genes involved in slowing down cell division would be appropriately activated or de-activated to maintain cell number homeostasis. For example, EGR1 gene product directly controls expression of TGFB1, which, in turn inhibits cell replication and promotes differentiation (Liu *et al.* 1999). Growth regulatory signals occur early in the cell division pathways, whereas cell division control proteins act immediately before or during cell division. In the present study, cell division was occurring at a rapid rate and genes involved in this activity would continue to be predominantly up regulated until which time the inhibitory growth regulatory mRNAs, described above, could be translated. Recognizing the numerous feedback loops, agonist-antagonist interplay and allosteric inhibition involved in all biological processes, creates considerable complexity to the interpretation of any gene expression pattern frozen for one minute in time. Further increasing the difficulty of interpretation are the following: mRNA is not necessarily translated into protein; mRNA can become more stable or labile changing the amount of protein translated without affecting the mRNA levels; and post-translational modifications can alter the milieu of the cell without changing

mRNA levels (Lewin 2000). Regardless of the direction of expression change for the growth/proliferation genes, the large number of these genes whose mRNA levels are significantly altered by ET administration indicates that ET is changing the growth pattern of the liver.

This complex transcriptional interaction between cell proliferation inducing and inhibiting genes continues throughout the remainder of the study. Overall, the gene expression pattern agrees with the temporal changes in the liver: weighted toward the promotion of growth during the first two time points (Days 2 and 11), equally weighted at Day 43 and weighted toward growth inhibition by Day 85. To better understand this expression pattern, more studies are needed to increase the number and frequency of gene expression time points examined, to confirm more individual mRNA expression levels by RT-PCR, and to determine the protein profile of the cells using immunohistochemical techniques or Western blots. In this way, we may be able to track the changes of the growth promoting and inhibiting genes that appear to be expressed out of synchrony in the current study.

CPT-1 inhibitors have been reported to be PPARα-agonists (Forman *et al.* 1997; Intrasuksri *et al.* 1998; Kaikaus *et al.* 1993; Portilla *et al.* 2000; Skorin *et al.* 1992). However, these studies were performed for short periods, usually in cultured cells and the potential increase in number of peroxisomes was not evaluated. There is no direct link in the literature between ET-induced hepatic

hypertrophy and PPARα activation, which was one goal of the present study. In the present study, PPARα mRNA was not yet up regulated at Day 2, PPARα-related gene expression was mixed (AOX and VLCAD unchanged; CYP4A1, 3KACT, LCAD, and CPT1A up regulated) and peroxisome proliferation was not observed. However, there was marked hepatocellular proliferation within 24 hours of the first dose of ET, which is consistent with the effects caused by other PPARα-agonists. By Day 43, AOX and VLCAD were still not increased, but PPARα mRNA was up regulated, there was a 2-fold increase in peroxisomes and the mean liver weight was increased 25% above control values. The data suggest that PPARα plays a role in ET-induced hepatic hypertrophy. It is unclear why AOX and VLCAD are not up regulated with the increased transcription of PPARA. In transient transfection assays performed in our laboratories (unpublished data), ET and the PPARα-agonist, Wy-14,643 activated PPARα to a similar extent. Previous studies (Marsman *et al.* 1992), however, show that low dose Wy-14,643 exhibited stronger PPARα effects than did ET in the current study. Wy-14,643 increased liver weights 200% over controls and increased peroxisome proliferation by approximately 3-fold over controls, while ET in the current study increased liver weights 25% and peroxisome proliferation by 2-fold. These data, in addition to the fact that there are no reports of ET-induced carcinogenesis, suggest that ET is not as potent a peroxisome proliferator as Wy-14,643. This difference may help explain why AOX and VLCAD genes are not significantly up regulated in our study.

In a previous study, Merrill, et al. (2002) showed that ET induced cytotoxicity and oxidative stress in cultured hepatocytes. Rose et al. (1999) showed that Wy-14,643-treated Kupffer cells overproduced superoxide via a protein kinase C pathway, and increased superoxide generation has been associated with activation of NFκB and TNFα affecting regulation of cell proliferation. To determine whether or not oxidative stress played a role in the ET-induced hepatic hypertrophy, gene expression associated with redox regulation was evaluated at all four time points. In contrast to the RT-RCR results obtained by Merrill, et al. in ET-treated HepG2 cells, oxidative stress was not a feature of ET administration *in vivo* as determined by gene expression analysis. Based upon histochemical staining, the golden brown intracytoplasmic pigment, observed in the 12 and 25 mg/kg ET-treated rat kidneys, was determined not to be lipofuscin. Lipofuscin is an insoluble pigment that results from lipid peroxidation. The lack of lipofuscin in the renal tubular epithelium suggests that significant oxidative stress was not present in the kidneys. Some possible reasons for the observed difference in the redox potential of ET *in vitro* versus *in vivo* include: 1) hepatocytes in the living animal are provided much more antioxidant protection than cultured cells (serum glutathione, Vitamins E and C, etc.), 2) the *doses in vitro* vs. *in vivo* are not comparable (1mM in vitro vs. 25 mg/kg in vivo), so the concentration reaching the cells in vivo was unknown, and 3) difficulty in comparing a human hepatocellular carcinoma cell line (HepG2) to normal rat hepatocytes. It has been reported that human hepatocytes have a higher sensitivity to inhibition of FAO by ET than do either guinea pig or rat hepatocytes (Agius *et al.* 1991). This

increased sensitivity may contribute to the difference in ET-induced oxidative stress in HepG2 cells as compared to rat hepatocytes.

Energy substrate shift from fatty acids to glucose has been linked to cardiac hypertrophy (Bressler and Goldman 1993; Frey and Olson 2002; Rupp and Jacob 1992). CPT1 inhibitors, including TDGA, oxfenicine and ET, force the shift of primary energy substrate from fatty acids to glucose and cause cardiac hypertrophy (Anderson 1998; Lee *et al.* 1985; Wolf 1992). ET is known to cause hepatic hypertrophy, but speculation in the literature regarding an etiology is nonexistent. In the present study, ET-induced changes in energy metabolism gene expression were reviewed in context with development of hepatic hypertrophy. Lipid synthesis gene expression (both saturated and unsaturated) was decreased at Days 2 and 11, increased at Day 43 and decreased again at Day 85. Serum TG levels followed the same temporal pattern as the lipid synthesis genes, decreasing at the first two time points, increasing at Day 43 and decreasing late in the study. It is unclear if the temporal changes in fatty acid synthesis and serum TG are causally linked to the hepatic hypertrophy. The mild accumulation of lipid in hepatocytes at Day 43 is consistent with the only time point at which GPAM is up regulated because it is the first step in triglyceride synthesis. The data suggest that changes in lipid metabolism may play a role in the ET-induced hepatic hypertrophy.

Cholesterol synthesis gene expression was down regulated throughout the study, most likely due to the decrease in acetyl-CoA from ET-induced inhibition of FAO. Johnson, et al. (2001) showed that PPARα and FA inhibit mevalonate pathway without inhibiting cell cycle progression and cell proliferation. Similar to the findings by Johnson, et al., cholesterol synthesis inhibition (decrease in HMGCR mRNA expression) caused by ET in the current study appears to have no inhibitory effect on cell proliferation.

In summary, ET induced a strong mitogenic response that was consistent with that generated by other peroxisome proliferators in the livers of rats 24 h after administration of one 25 mg/kg dose. This finding was coincident with a predominance of cell proliferation/growth-related gene expression alterations. Oxidative stress genes were down regulated; suggesting that this is not a viable etiologic mechanism for induction of ET-induced hepatic hypertrophy. PPARα appears to play a role in ET-induced hepatic hypertrophy, as shown by the early cell proliferation followed by increased level of PPARA mRNA, peroxisome proliferation and increase of some PPARα-related genes.

References

Agius, L., Peak, M., and Sherratt, S. A. (1991). Differences between human, rat and guinea pig hepatocyte cultures. A comparative study of their rates of beta-oxidation and esterification of palmitate and their sensitivity to R-etomoxir. *Biochem. Pharmacol.* **42**, 1711-5.

Anderson, R. C. (1998). Carnitine Palmitoyltransferase: A Viable Target for the Treatment of NIDDM? *Curr. Pharm. Design* **4**, 1-16.

Belury, M. A., Moya-Camarena, S. Y., Sun, H., Snyder, E., Davis, J. W., Cunningham, M. L., and Vanden Heuvel, J. P. (1998). Comparison of dose-response relationships for induction of lipid metabolizing and growth regulatory genes by peroxisome proliferators in rat liver. *Toxicology & Applied Pharmacology.* **151**, 254-61.

Bressler, R., and Goldman, S. (1993). A role of fatty acid oxidation in cardiac hypertrophy. *Cardioscience.* **4**, 133-42.

Cattley, R. C., and Roberts, R. A. (2000). Peroxisome proliferators and carcinogenesis: editorial perspectives. *Mutation Research.* **448**, 117-9.

Conway, J. G., Tomaszewski, K. E., Olson, M. J., Cattley, R. C., Marsman, D. S., and Popp, J. A. (1989). Relationship of oxidative damage to the hepatocarcinogenicity of the peroxisome proliferators di(2-ethylhexyl)phthalate and Wy-14,643. *Carcinogenesis.* **10**, 513-9.

Desvergne, B., and Wahli, W. (1999). Peroxisome proliferator-activated receptors: nuclear control of metabolism. *Endocrine Reviews.* **20**, 649-88.

Djouadi, F., Weinheimer, C. J., Saffitz, J. E., Pitchford, C., Bastin, J., Gonzalez, F. J., and Kelly, D. P. (1998). A gender-related defect in lipid metabolism and glucose homeostasis in peroxisome proliferator- activated receptor alpha- deficient mice. *Journal of Clinical Investigation* **102**, 1083-91.

Dykstra, M. J. (1993). *A manual of applied techniques for biological electron microscopy*. Plenum Press, New York.

Eacho, P. I., Lanier, T. L., and Brodhecker, C. A. (1991). Hepatocellular DNA synthesis in rats given peroxisome proliferating agents: comparison of WY-14,643 to clofibric acid, nafenopin and LY171883. *Carcinogenesis.* **12**, 1557-61.

Forman, B. M., Chen, J., and Evans, R. M. (1997). Hypolipidemic drugs, polyunsaturated fatty acids, and eicosanoids are ligands for peroxisome proliferator-activated receptors alpha and delta. *Proc. Natl. Acad. Sci. U.S.A.* **94**, 4312-7.

Frey, N., and Olson, E. N. (2002). Modulating cardiac hypertrophy by manipulating myocardial lipid metabolism? [letter; comment.]. *Circulation.* **105**, 1152-4.

Gonzalez, F. J., Peters, J. M., and Cattley, R. C. (1998). Mechanism of action of the nongenotoxic peroxisome proliferators: role of the peroxisome proliferator-activator receptor alpha. *Journal of the National Cancer Institute* **90**, 1702-9.

Intrasuksri, U., Rangwala, S. M., O'Brien, M., Noonan, D. J., and Feller, D. R. (1998). Mechanisms of peroxisome proliferation by perfluorooctanoic acid and endogenous fatty acids. *Gen. Pharmacol.* **31**, 187-97.

Johnson, T. E., and Ledwith, B. J. (2001). Peroxisome proliferators and fatty acids negatively regulate liver X receptor-mediated activity and sterol biosynthesis. *Journal of Steroid Biochemistry & Molecular Biology* **77**, 59-71.

Kaikaus, R. M., Sui, Z., Lysenko, N., Wu, N. Y., Ortiz de Montellano, P. R., Ockner, R. K., and Bass, N. M. (1993). Regulation of pathways of extramitochondrial fatty acid oxidation and liver fatty acid-binding protein by long-chain monocarboxylic fatty acids in hepatocytes. Effect of inhibition of carnitine palmitoyltransferase I. *J. Biol. Chem.* **268**, 26866-71.

Latruffe, N., and Vamecq, J. (1997). Peroxisome proliferators and peroxisome proliferator activated receptors (PPARs) as regulators of lipid metabolism. *Biochimie* **79**, 81-94.

Lee, S. M., Bahl, J. J., and Bressler, R. (1985). Prevention of the metabolic effects of 2-tetradecylglycidate by octanoic acid in the genetically diabetic mouse (db/db). *Biochemical Medicine.* **33**, 104-9.

Lewin, B. (2000). *Genes VII*. Oxford University Press, New York.

Liu, C., Yao, J., de Belle, I., Huang, R.-P., Adamson, E., and Mercola, D. (1999). The transcription factor EGR-1 suppresses transformation of human fibrosarcoma HT1080 cells by coordinated induction of transforming

growth factor-beta-1, fibronectin, and plasminogen activator inhibitor-1. *J. Biol. Chem.* **274**, 4400-11.

Lockhart, D. J., Dong, H., Byrne, M. C., Follettie, M. T., Gallo, M. V., Chee, M. S., Mittmann, M., Wang, C., Kobayashi, M., Horton, H., and Brown, E. L. (1996). Expression monitoring by hybridization to high-density oligonucleotide arrays. *Nature Biotechnology* **14**, 1675-80.

Marsman, D. S., Goldsworthy, T. L., and Popp, J. A. (1992). Contrasting hepatocytic peroxisome proliferation, lipofuscin accumulation and cell turnover for the hepatocarcinogens Wy-14,643 and clofibric acid. *Carcinogenesis.* **13**, 1011-7.

Merrill, C. L., Ni, H., Yoon, L. W., Tirmenstein, M. A., Narayanan, P., Benavides, G. R., Easton, M. J., Creech, D. R., Hu, C. X., McFarland, D. C., Hahn, L. M., Thomas, H. C., and Morgan, K. T. (2002). Etomoxir-induced oxidative stress in HepG2 cells detected by differential gene expression is confirmed biochemically. *Toxicological Sciences* **68**, 93-101.

Moran, L. A., and Scrimgeour, K. G., eds. (1994). *Biochemistry*. Prentiss-Hall, Inc., Upper Saddle River, NJ.

Morgan, K., Ni, H., Brown, R., Yoon, L., Qualls, C., Crosby, L., Reynolds, R., Gaskill, B., Anderson, S., Kepler, T., Brainard, T., Liv, N., Easton, M., Merrill, C., Creech, D., Sprenger, D., Conner, G., Johnson, P., Fox, T., Tyler, R., Sartor, M., Richard, E., Kuruvilla, S., Casey, W., and Benavides, G. (2002). Mechanism of action combined with cDNA microarray

technology to select genes for a real time RT-PCR-based screen for oxidative stress in HepG2 cells. *Toxicol. Pathol.* **30**, 435-51.

Portilla, D., Dai, G., Peters, J. M., Gonzalez, F. J., Crew, M. D., and Proia, A. D. (2000). Etomoxir-induced PPARalpha-modulated enzymes protect during acute renal failure. *American Journal of Physiology - Renal Fluid and Electrolyte Physiology* **278**, F667-F75.

Reddy, J. K., and Rao, M. S. (1989). Oxidative DNA damage caused by persistent peroxisome proliferation: its role in hepatocarcinogenesis. *Mutation Research.* **214**, 63-8.

Reddy, J. K., Rao, M. S., Azarnoff, D. L., and Sell, S. (1979). Mitogenic and carcinogenic effects of a hypolipidemic peroxisome proliferator, [4-chloro-6-(2,3-xylidino)-2-pyrimidinylthio]acetic acid (Wy-14, 643), in rat and mouse liver. *Cancer Research.* **39**, 152-61.

Rose, M. L., Rivera, C. A., Bradford, B. U., Graves, L. M., Cattley, R. C., Schoonhoven, R., Swenberg, J. A., and Thurman, R. G. (1999). Kupffer cell oxidant production is central to the mechanism of peroxisome proliferators. *Carcinogenesis.* **20**, 27-33.

Rupp, H., and Jacob, R. (1992). Metabolically-modulated growth and phenotype of the rat heart. *Eur. Heart J.* **13**, 56-61.

Skorin, C., Necochea, C., Johow, V., Soto, U., Grau, A. M., Bremer, J., and Leighton, F. (1992). Peroxisomal fatty acid oxidation and inhibitors of the mitochondrial carnitine palmitoyltransferase-1 in isolated rat hepatocytes. *Biochem. J.* **281**, 561-7.

Vetter, R., Kott, M., and Rupp, H. (1995). Differential influences of carnitine palmitoyltransferase-1 inhibition and hyperthyroidism on cardiac growth and sarcoplasmic reticulum phosphorylation. *Eur. Heart J.* **16**, 15-9.

Wodicka, L., Dong, H., Mittmann, M., Ho, M. H., and Lockhart, D. J. (1997). Genome-wide expression monitoring in Saccharomyces cerevisiae. *Nature Biotechnology* **15**, 1359-67.

Wolf, H. P. (1992). Possible new therapeutic approach to diabetes mellitus by inhibition of carnitine palmitoyltransferase 1 (CPT1). *Horm. Metab. Res.* **Suppl.26**, 62-7.

Yotsumoto, T., Naitoh, T., Kitahara, M., and Tsuruzoe, N. (2000). Effects of carnitine palmitoyltransferase I inhibitors on hepatic hypertrophy. *Eur. J. Pharmacol.* **398**, 297-302.

Gene name	Clontech™ Ratio treated/control	Affymetrix™ Ratio treated/control	TaqMan™ Ratio treated/control
CDC20	+2.30	+1.52	+2.02
EGR1	+1.68	+1.77	+1.43
TGFBR2	+1.47	-1.06	
TNFA	-5.00	-4.42	+1.04
CCNE	-4.00	-1.43	
GADD45	-2.46	-1.84	-1.87
CDKN1A	-1.93	-5.00	-1.72
WEE1	-1.89	-1.23	-1.70
IGFBP1	-1.20	+17.37	+1.48
NR1D1	N/A	+15.89	+32.74
GHRH	N/A	+10.47	
CDK2B	N/A	+6.82	
BCL2	N/A	+4.39	
CDK1	+1.50	+2.92	
IGF1R	+2.00	+2.84	-1.95
NF2	-1.08	+2.05	
GAP	-1.08	+1.67	
GHRHR	N/A	+1.62	
TP53	-1.70	+1.47	
GMFB	+1.09	-16.61	-1.40
CDC25B	+1.14	-8.44	
MYC	-4.00	-6.32	
TGFA	-2.00	-1.85	

Table 2.1: Day 2 Cell Proliferation Gene Changes
(Expressed as ratio of treated over control)

Lipid Metabolism Genes	Day 2	Day 11	Day 43	Day 85
ADCY	5.22	-0.32	2.02	-1.72
3KACT	2.96	2.10	1.90	2.78
PDE4	1.92	8.14	0.05	-1.55
ECI	1.24	1.39	0.64	0.94
GPAM	-6.37	-5.32	1.42	-1.22
HMGCR	-3.14	-18.47	-7.98	-1.14
SCD2	-1.47	-7.70	6.36	-28.37
FATP	-1.42	0.07	-0.13	1.95
COT	0.19	1.32	0.94	0.56
OSC	-0.88	-5.34	0.98	1.55
ACLY	-0.39	-4.48	0.54	-0.56
FAS	-0.78	-3.88	0.05	-0.60
CPT1A	0.47	0.96	0.55	0.43
SQLE	-0.41	-2.35	-0.47	0.23
ME1	0.45	0.27	11.47	3.47
LIPE	-0.22	-0.96	0.12	2.16
FAT	0.20	0.52	0.23	1.93
VLCAD	0.33	0.24	0.12	0.33
LCAD	0.19	0.30	0.37	0.41
MCAD	0.15	0.27	0.14	0.17
Glucose Metabolism Genes	**Day 2**	**Day 11**	**Day 43**	**Day 85**
GPD2	1.50	-1.08	0.71	0.22
HKII	1.17	0.82	-0.17	-0.56
PFKFB1	0.18	1.60	1.45	-0.64
SPAT	11.96	10.15	-3.55	0.82
PDHP2	-1.42	1.56	-0.95	4.33
PDK4	-1.61	1.27	-1.48	-2.77

Table 2.2: Energy Metabolism Gene Expression
(Fold change of 25 mg/kg ET-treated liver mRNA vs. control)

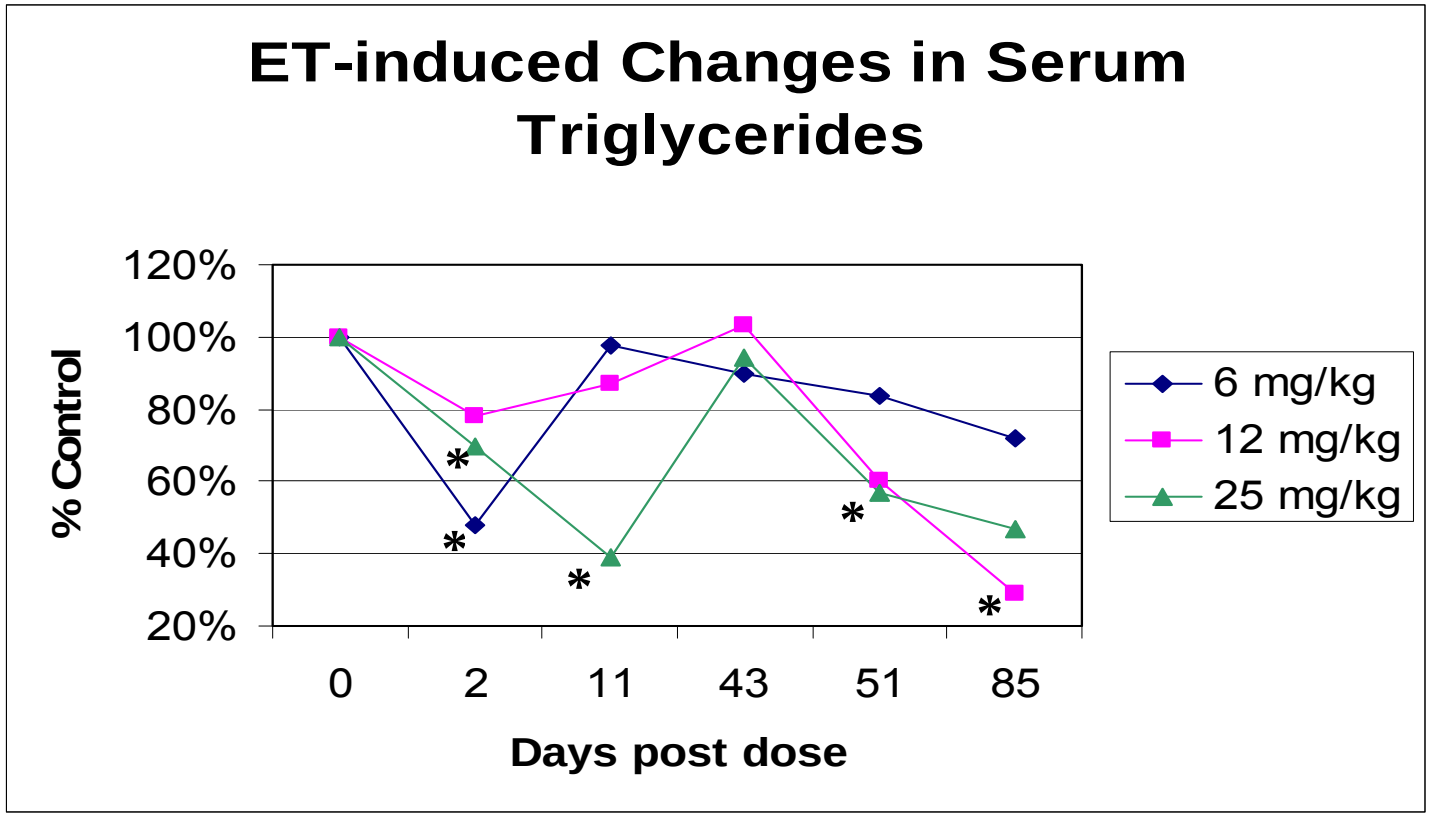

* = p < 0.1

Figure 2.1: Serum triglyceride changes

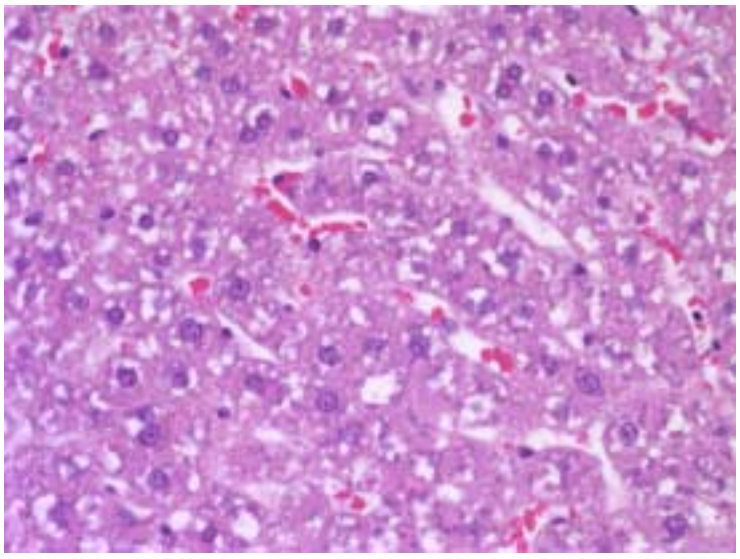

A. Day 2, Control Liver

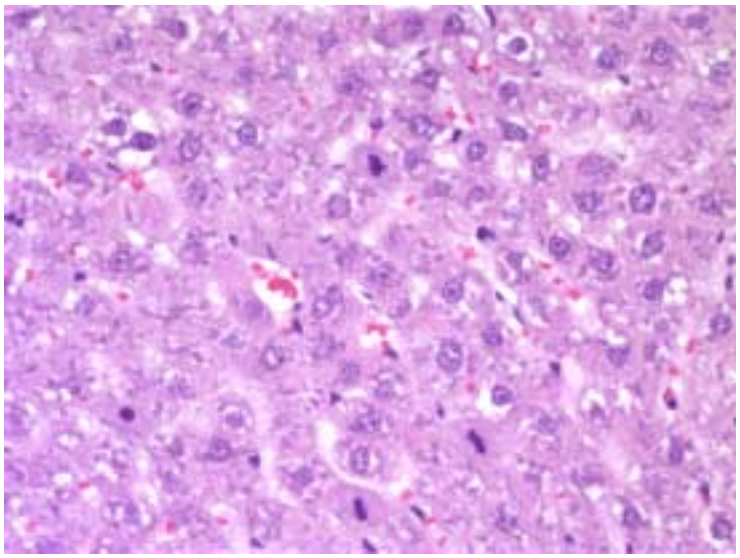

B. Day 2, Group 4 (25 mg/kg) Liver: Note multiple mitotic figures.

Figure 2.2: Increase in hepatocellular mitotic figures (400X)

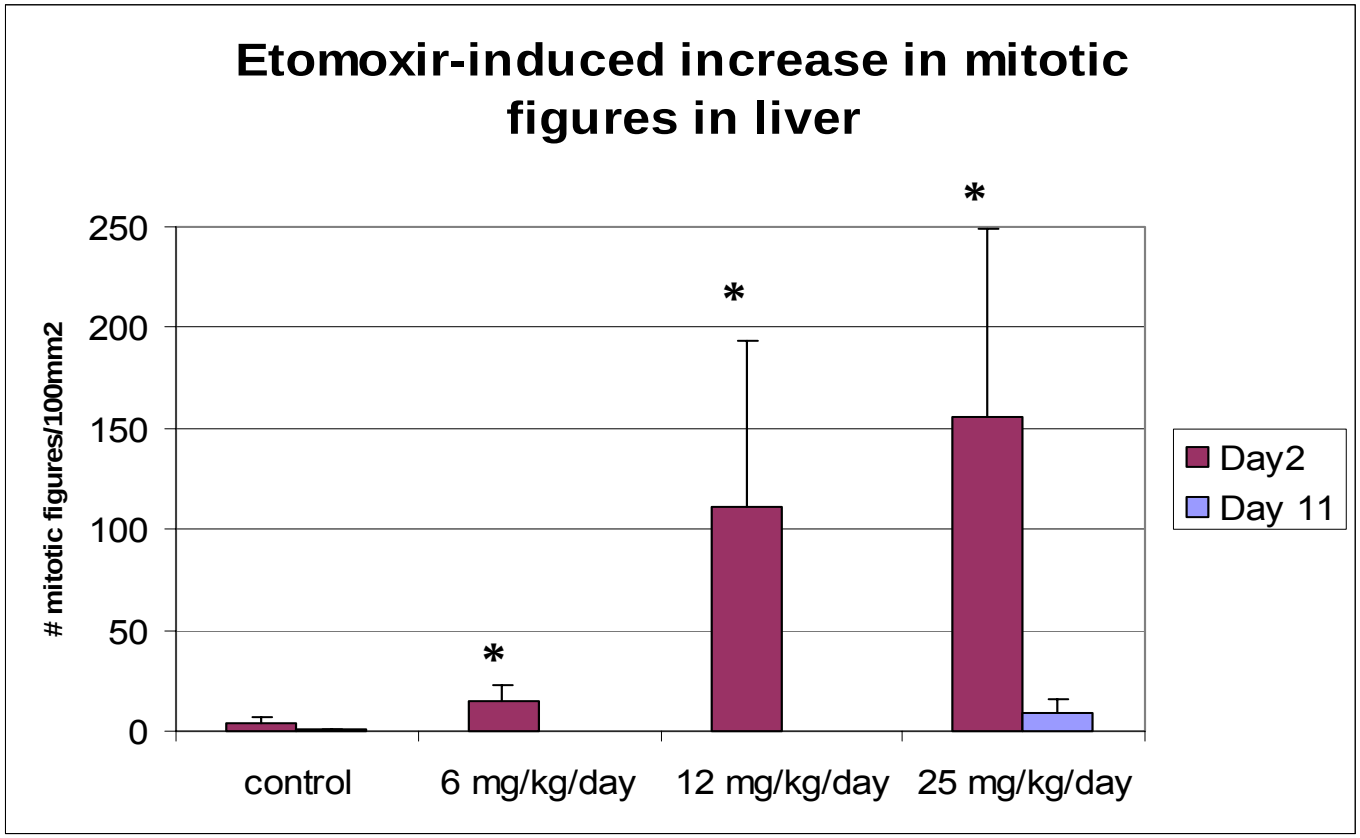

* p < .05

Figure 2.3: Increase in mitotic figures

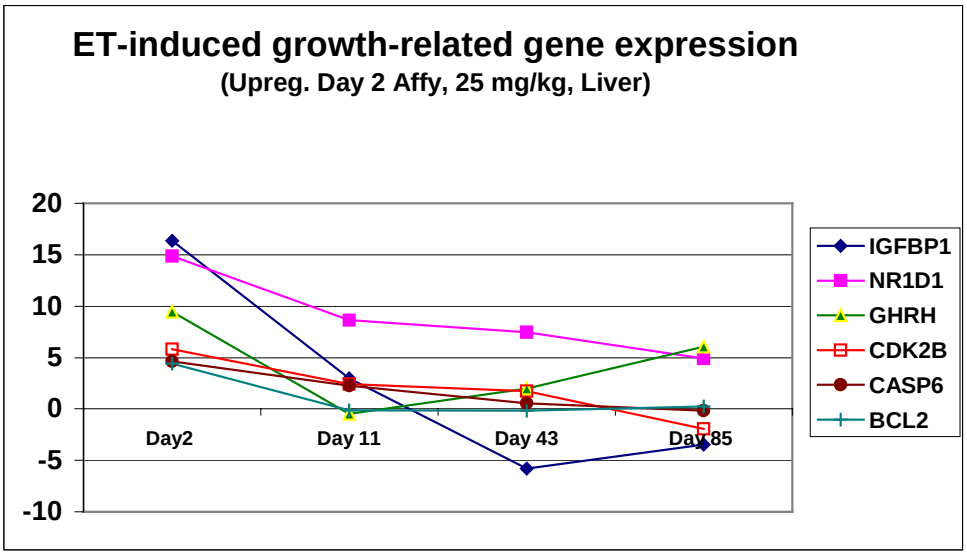

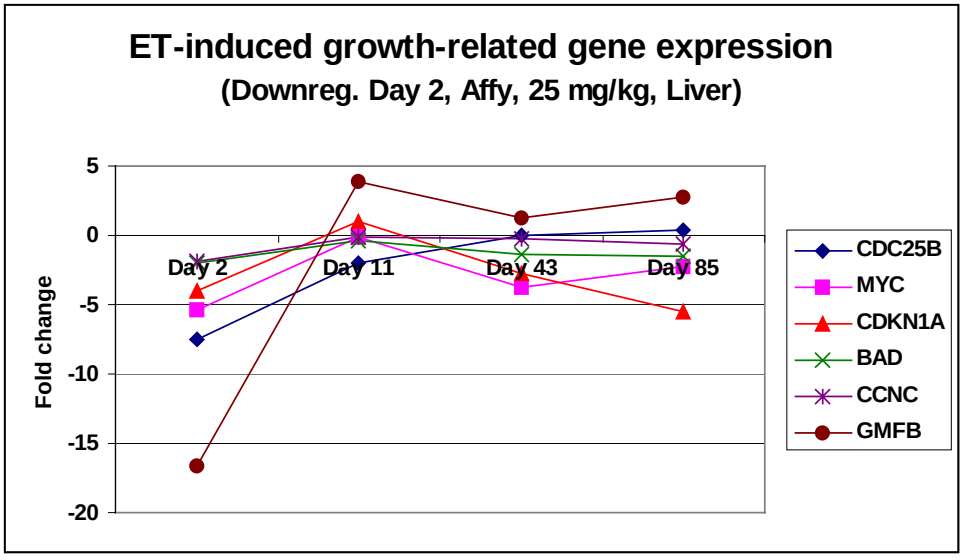

Figure 2.4: Day 2 Growth-related Gene Expression Changes

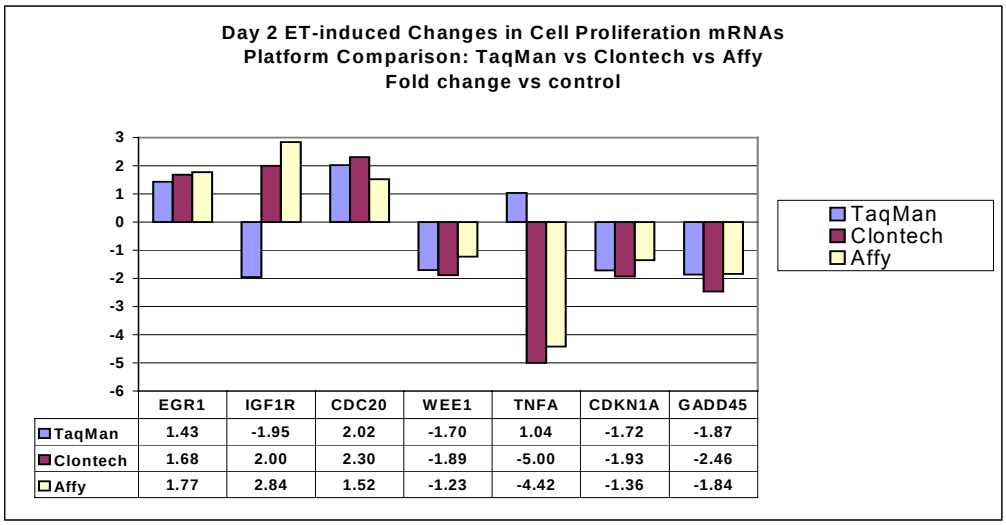

	EGR1	IGF1R	CDC20	WEE1	TNFA	CDKN1A	GADD45
TaqMan	1.43	-1.95	2.02	-1.70	1.04	-1.72	-1.87
Clontech	1.68	2.00	2.30	-1.89	-5.00	-1.93	-2.46
Affy	1.77	2.84	1.52	-1.23	-4.42	-1.36	-1.84

Figure 2.5A

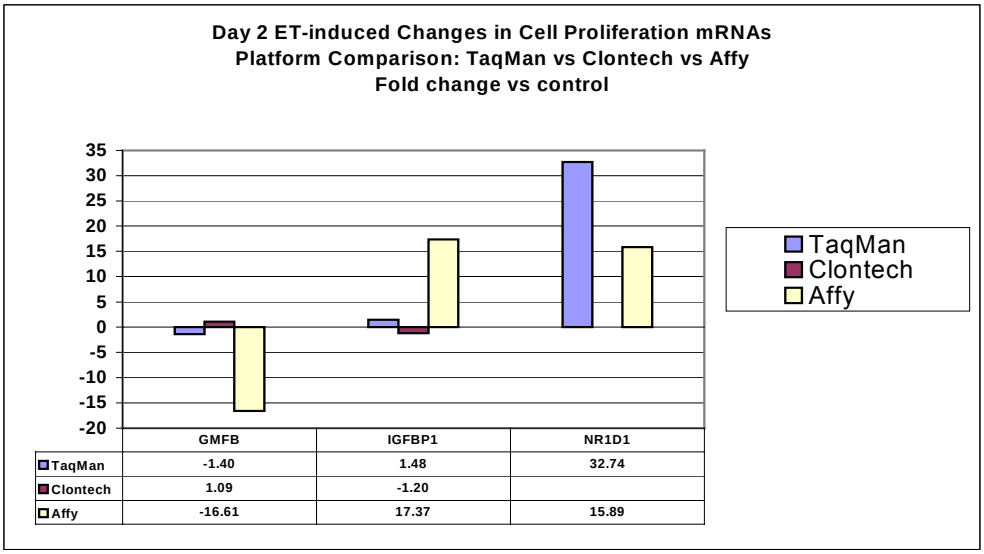

	GMFB	IGFBP1	NR1D1
TaqMan	-1.40	1.48	32.74
Clontech	1.09	-1.20	
Affy	-16.61	17.37	15.89

Figure 2.5B: Day 2 platform comparisons of cell proliferation gene expression changes

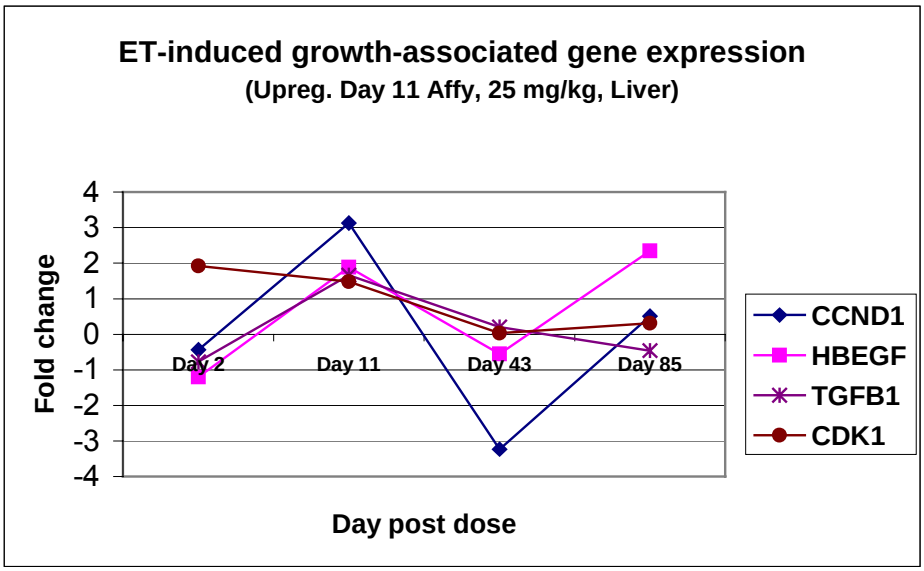

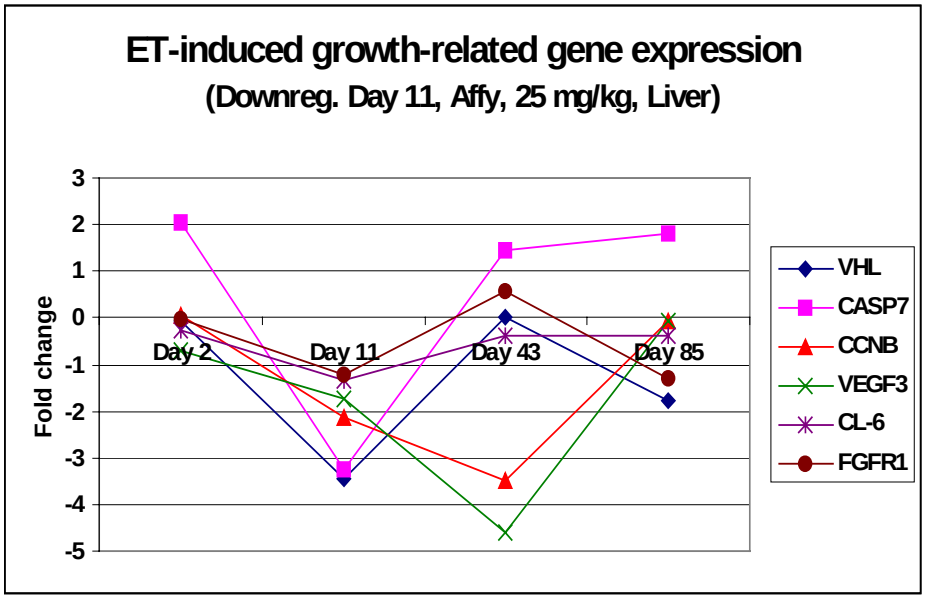

Figure 2.6: Day 11 Growth-related Gene Expression Changes

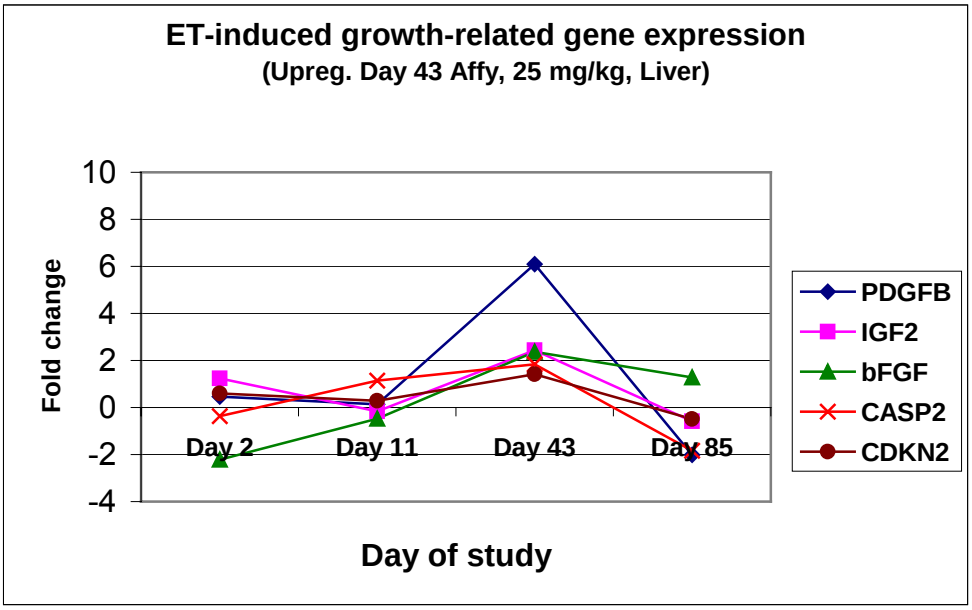

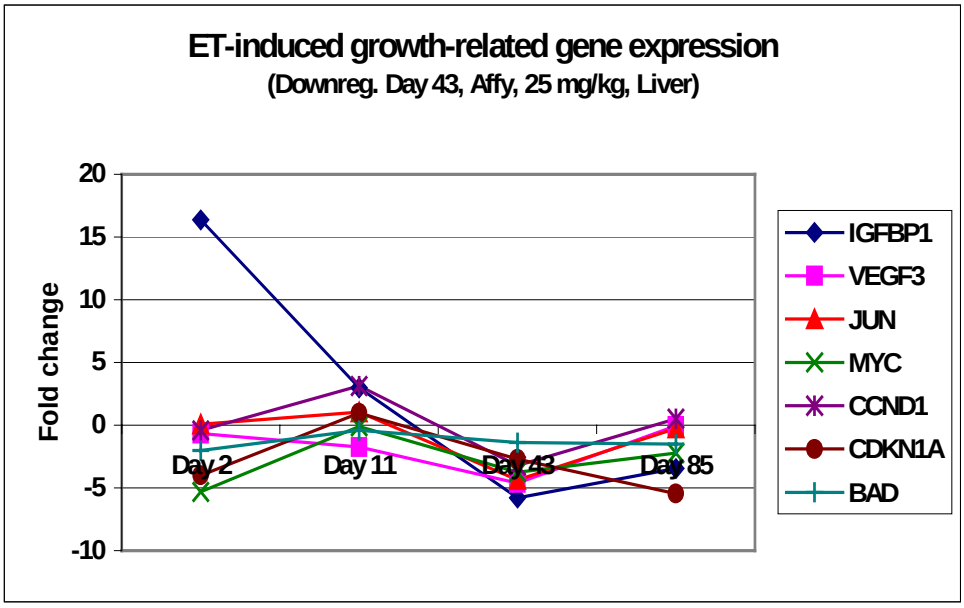

Figure 2.7: Day 43 Growth-related Gene Expression Changes

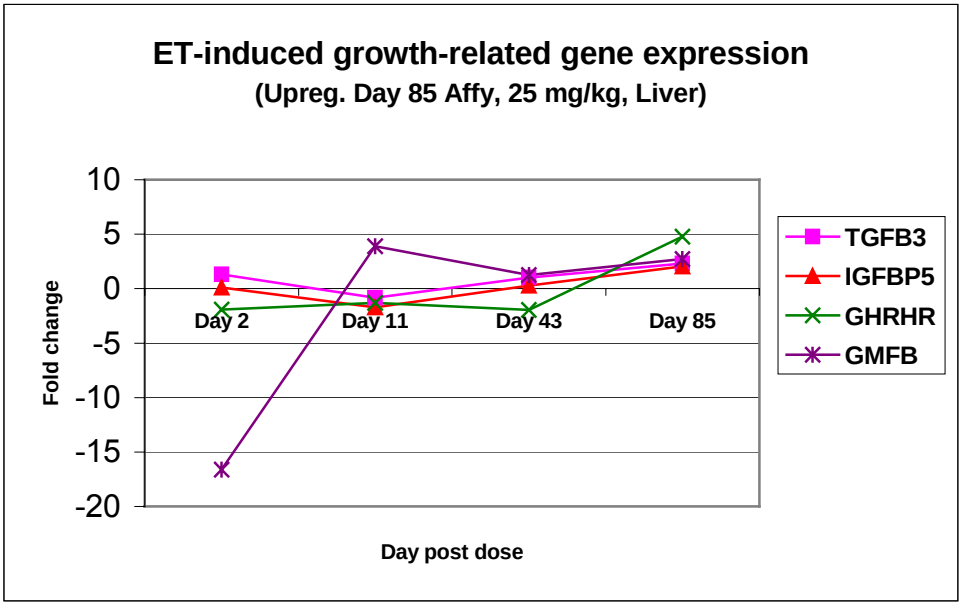

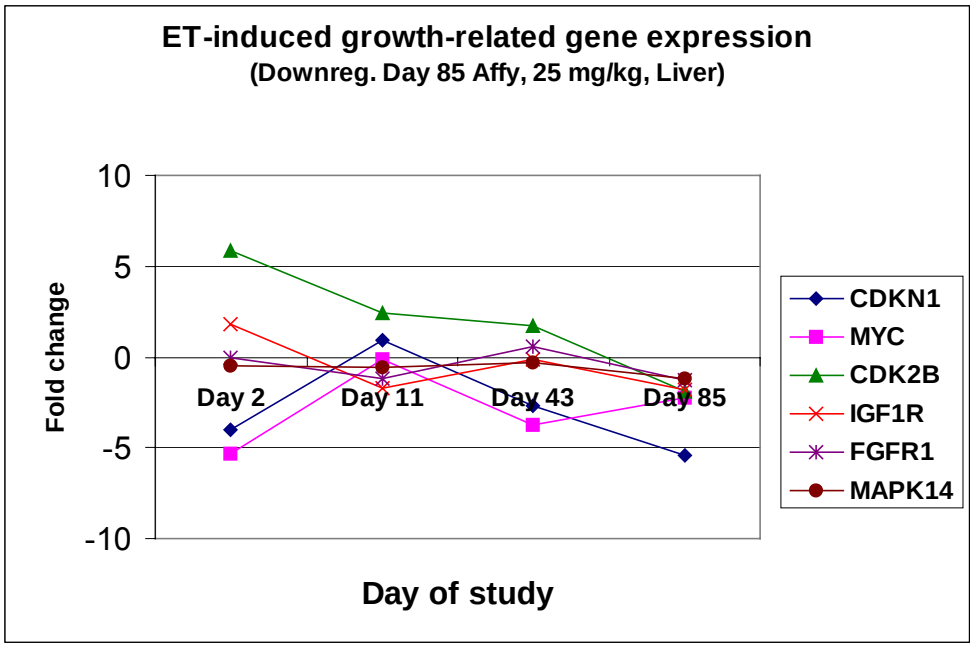

Figure 2.8: Growth-related Gene Expression, Day 85

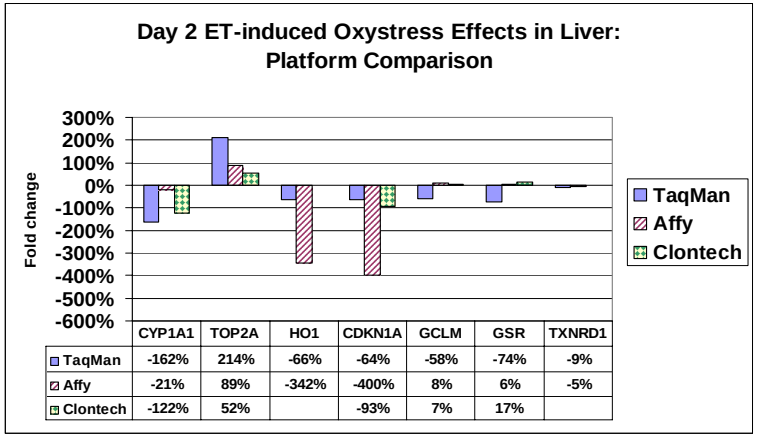

	CYP1A1	TOP2A	HO1	CDKN1A	GCLM	GSR	TXNRD1
TaqMan	-162%	214%	-66%	-64%	-58%	-74%	-9%
Affy	-21%	89%	-342%	-400%	8%	6%	-5%
Clontech	-122%	52%		-93%	7%	17%	

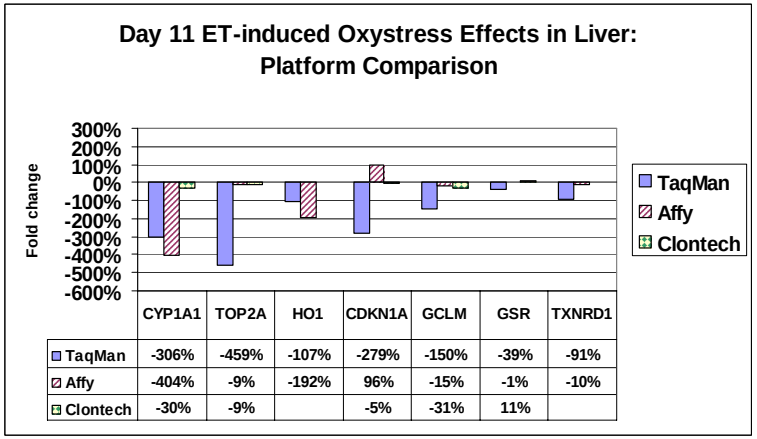

	CYP1A1	TOP2A	HO1	CDKN1A	GCLM	GSR	TXNRD1
TaqMan	-306%	-459%	-107%	-279%	-150%	-39%	-91%
Affy	-404%	-9%	-192%	96%	-15%	-1%	-10%
Clontech	-30%	-9%		-5%	-31%	11%	

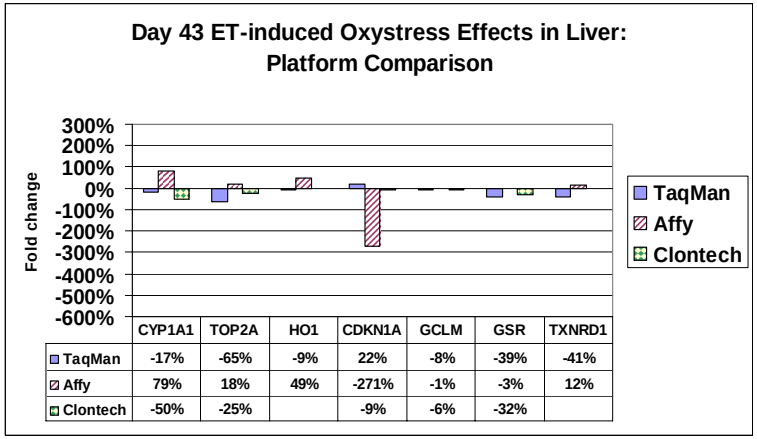

	CYP1A1	TOP2A	HO1	CDKN1A	GCLM	GSR	TXNRD1
TaqMan	-17%	-65%	-9%	22%	-8%	-39%	-41%
Affy	79%	18%	49%	-271%	-1%	-3%	12%
Clontech	-50%	-25%		-9%	-6%	-32%	

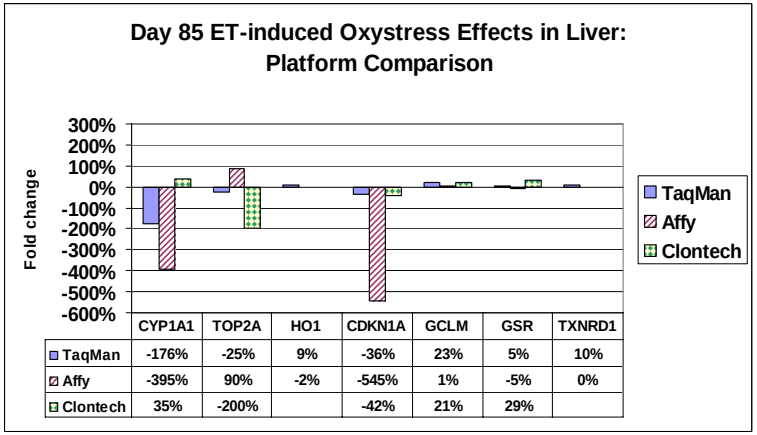

	CYP1A1	TOP2A	HO1	CDKN1A	GCLM	GSR	TXNRD1
TaqMan	-176%	-25%	9%	-36%	23%	5%	10%
Affy	-395%	90%	-2%	-545%	1%	-5%	0%
Clontech	35%	-200%		-42%	21%	29%	

Figure 2.9: Platform Comparison of Oxidative Stress Gene Changes, 25 mg/kg/day ET

% change	Day 2	Day 11	Day 43	Day 85
CYP4A1	164%	203%	126%	132%
ACO	14%	26%	14%	26%
3KACT	296%	210%	190%	278%
PPARA	0%	17%	63%	-11%
CPT1A	47%	96%	55%	43%
HMGCS	3%	19%	3%	3%
VLCAD	33%	24%	12%	33%
LCAD	19%	30%	37%	41%
CCND1	-43%	313%	-323%	51%

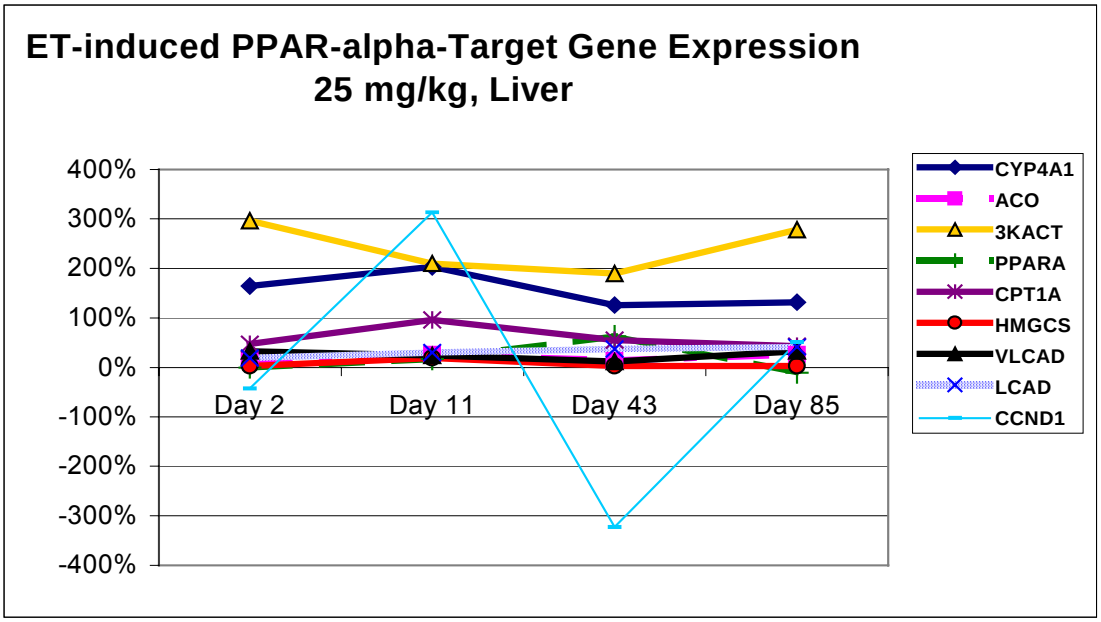

Figure 2.10: PPARa-target gene expression changes

General Summary and Conclusions

The purpose of this research was to gain a better understanding of the toxic mechanisms associated with the administration of etomoxir (ET) to the rat. ET is a 2-oxirane-carboxylate compound that inhibits long-chain fatty acid beta-oxidation by irreversibly binding to the ligand-binding domain of carnitine palmitoyltransferase-1 (CPT-1). CPT-1 is the gatekeeper controlling the entry of long-chain fatty acids into the mitochondrial matrix, thereby controlling rates of mitochondrial FAO. Long-chain fatty acids cannot cross the inner mitochondrial membrane into the matrix without the participation of CPT-1.

ET is known to cause hepatic hypertrophy in rodents but the etiologic mechanism is not yet elucidated. We theorized that because ET is a PPARα-agonist, the hepatic hypertrophy could be secondary to effects initiated by this receptor. PPARα activation is associated with oxidative stress and cell cycle dysregulation, both of which might play a role in ET-induced hepatic hypertrophy. Using gene expression analysis, we screened both a human hepatocellular carcinoma cell line (HepG2 cells) and rat hepatocytes (*in vivo*) dosed with ET for changes potentially attributable to PPARα.

In the first study, HepG2 cells were dosed with 1 mM ET for 6 h, after which a time course experiment was design to track the gene expression trends at 0.25, 0.5, 1, 2, 4, 6, 8, 12, 16, 20 and 24 h. Mitotic index was decreased, apoptosis

was increased and total cell number was decreased relative to the controls. Gene expression strongly suggestive of oxidative stress was observed and supported by decreased levels of reduced glutathione, decreased ratio of reduced/oxidized glutathione (GSH/GSSG), and increased levels of oxidized glutathione (GSSG) and superoxide. A significant decrease in mitochondrial membrane potential and ATP levels implicated impairment of mitochondrial energy metabolism. Because PPARα mRNA levels decreased significantly during the study, it is unlikely that this receptor plays a significant role in the ET-induced generation of oxidative stress. Other gene expression findings suggested activation of p53, DNA repair and cell cycle arrest. This is the first report of oxidative stress caused by etomoxir in a human hepatocyte cell line.

In contrast to the *in vitro* results, gene expression changes associated with oxidative stress were not present in the ET-dosed rat livers. ET administered to rats caused hepatocellular proliferation at 24 h that was followed by a 25% increase in mean liver weight at Day 43 of treatment. This finding was supported by significant changes in cell proliferation/growth gene expression. Along with the hepatic hypertrophy observed at Day 43, PPARα mRNA was increased 63% and there was a 2-fold increase in the number of peroxisomes. Coincident with the hepatic hypertrophy at Day 43, transient increases in lipid synthesis gene expression and transient normalization of previously decreased triglyceride levels were observed. The data suggest that PPARα plays a role in ET-induced hepatic

hypertrophy via alterations in cell division/growth gene expression, but not through the generation of oxidative stress.

Results for the *in vitro* and *in vivo* ET studies were almost diametrically opposed. Hepatocytes from ET-treated rats did not have up regulation of oxidative stress genes, as did the human hepatocellular carcinoma cell line (HepG2 cells). This could be explained by the fact that hepatocytes in the living animal are provided much more antioxidant protection than are cultured cells (serum glutathione, Vitamins E and C, etc.). In addition, the *in vivo* scenario includes constantly changing concentrations of energy substrates, metabolic end products, and oxygen tension due to dynamic interactions between organ systems, hormones, and nutritional status, and these interactions are not present in cultured cell systems. Pharmacokinetic studies were not performed for ET in the rat, so the concentration of ET contacting the hepatocytes in the rats is unknown. Another possible explanation is that human hepatocytes have a higher sensitivity to inhibition of FAO by ET than do rat hepatocytes. This increased sensitivity may contribute to the difference in ET-induced oxidative stress in HepG2 cells as compared to rat hepatocytes.

Rats respond to strong peroxisome proliferators (PP) with hepatocellular peroxisome proliferation and carcinogenesis, neither of which is a significant response in the PP-treated human. Human liver tends to express PPARα at one order of magnitude less than that seen in rodents, and some of the human

PPARα-target genes have mutations within their PPREs, which reduces the binding and transcriptional activation. The failure of the HepG2 cells to proliferate could also be due to the fact that there were no Kupffer cells present in the culture. Previous studies have shown that inhibition of Kupffer cells blocks PPARα-induced cell proliferation.

Gene expression is a useful tool in identification of pathogenic mechanisms and pathways; however, limitations associated with use of this tool should be reiterated. Gene expression does not equate to the protein profile of the cell because it does not take into account the mRNA half-life, translation, and post-translational modification. This tool can be most useful if there are multiple animals per test group and replicate mRNAs are evaluated. This allows for increased confidence in the results by statistical support. Northern blot or RT-PCR assays should be performed to confirm important gene changes. Tissue morphology, biochemical analysis, Western blots and immunohistochemical techniques can be employed to further complement the gene expression analysis. In spite of these limitations, differential gene expression is clearly a valuable investigative tool.

Overall, ET caused mild PPARα effects in rats, which were transient in nature. The oxidative stress caused by ET *in vitro*, was not present *in vivo* as determined

by evaluation of gene expression changes. So, based on the data presented in these studies, ET does not appear to pose a significant health risk to humans.